Exploring the Dynamics of Rapid Urbanization in Megacities using Remotely Sensed Time-Series and Object-Based Graph Structures

Xiangning Fan

Lancaster Environment Centre

This thesis is submitted for the degree of Doctor of Philosophy

Lancaster University

Dec 2024

Abstract

Urbanization has accelerated globally in recent decades, producing dramatic urban land expansion. With cities attracting attention from scientists from different fields, urban growth is a key topic, commonly studied using remotely sensed raster imagery. Urban entities such as cities are more readily thought of as spatial objects. Despite this, object-based methods are rarely applied in research on urban growth. This research utilized newly available remotely sensed annual land cover time-series data coupled with a novel object-based approach involving (i) raster-to-vector conversion, (ii) careful temporal linking of objects, (iii) comprehensive specification of the possible urban growth states (introduction, establishment, coalescence and no change) and (iv) the creation of a spatial graph structure linking neighbouring objects, to study urban growth. The stated object-based graph structure facilitated analysis of the state of urban objects based on previous states of the object and its neighbours, and the spatial-temporal links between them. First, the unprecedented scale of urban expansion between 1992 and 2014 was quantified across 13 regional capitals and their surrounding cities in China. By characterizing urban growth based on urban objects in different buffers at the regional level, the results suggested that core cities doubled or tripled in size, with synchronized growth patterns at specific times potentially driven by national and regional policies. Regional disparities were also observed which highlight the impacts of regional governance and local policy interventions. Second, a conceptual framework characterizing urban growth events was proposed including introduction (including through dispersal), establishment, coalescence and no change. Applying a rule-based approach to identify these events and quantifying their spatial-temporal changes, synchronous temporal trends in growth events in the core and buffer regions at the landscape level were observed. However, a specific logical sequence of these events at the population (or landscape) level was not obvious. The results show concurrent events with shifting dominance of specific

events over time, thus, providing insights into urban growth processes and reflecting the complexity of urban growth processes. Third, a Bayesian linear mixed-effects model was integrated with a spatial-temporal graph of urban objects to model the states of urban objects. It was found that the coalescence state of urban objects is influenced by their prior object states, proximity to neighbouring objects, and the states of neighbouring objects in a defined small buffer. The growth state (i.e., growth or unchanged) is related to its previous state and the dynamics of neighbouring objects. The area of objects that have grown was found to be influenced by the largest interactions with neighbouring objects, with the magnitude of these effects varying by object size. By modelling explicitly the relationships between urban objects on a graph, the developed object-based approach provides valuable insights into the dynamics of urban objects and their relationships within megacities, using cities in China as examples.

This research advances the understanding of urban growth by quantifying spatial-temporal patterns, building spatial-temporal links between urban objects, and explicitly modelling the relationships between objects. It provides a new perspective for studying urban dynamics and may contribute to better urban development, governance strategies and sustainable environment management in future.

Declaration

I declare that the following thesis is the result of my original work and has not been submitted to qualify for another academic degree at any other university. Many of the ideas in this work were the product of discussions with my supervisors, Professor James Duncan Whyatt, Professor George Alan Blackburn, and Professor Peter M. Atkinson at Lancaster University. This thesis does not include any work done in collaboration with others except where have been identified. Chapters 3 to 5 are intended for publication in peer-reviewed journals.

Chapter 3 was submitted to the journal **Applied Geography** (2024) and has been accepted subject to major revision as:

Fan, X., Blackburn, G.A., Whyatt, J.D. and Atkinson, P.M. (2024). Revealing the scale and synchronicity of rapid urban growth in China in the 2000s in response to reform and regional policies by treating provincial capital cities as sets of spatial objects.

Chapter 4 was published in the journal **Geographical Analysis** (2024) as:

Fan, X., Blackburn, G.A., Whyatt, J.D. and Atkinson, P.M. (2024). The Geographical Analysis of Megacities Through Changes in Their Individual Urban Objects. Geographical Analysis, 56: 451-470. https://doi.org/10.1111/gean.12386

Chapter 5 will be submitted to an appropriate journal later this year as:

Fan, X., Whyatt, J.D. and Atkinson, P.M. (2024). Modelling urban objects through Bayesian linear mixed-effects models

Xiangning Fan

2024 December

Acknowledgements

Completing this PhD is such a long journey, but I can still remember the day I first arrived at Lancaster University and met my supervisor. The mixture of excitement and nervousness from that day still stays with me. Lancaster welcomed me with typical autumn weather, with some beautiful sunshine but mostly layers of clouds, just like this extraordinary journey, with moments of happiness and fulfilment, but also many periods of challenges and frustration. It is a valuable experience that I will cherish forever in my life. At this finishing stage, I am deeply grateful to all the people and institutions that supported and encouraged me during this period.

First and most importantly, I want to express my sincere thanks to my supervisors: Professor Peter Atkinson, Professor Duncan Whyatt and Professor Alan Blackburn. Without their guidance and patience, I could not finish my research. I truly appreciate Pete for his insightful guidance, valuable suggestions and constant encouragement during my PhD. His extensive expertise and creativity have inspired this research. He leads me to the field of less commonly used yet highly promising object-based methods in urban studies. His enthusiasm for exploring the unknown, conscientious attitude in research and encouragement when I am a beginner at research and at my low point will benefit not only my research but also my life. It is such an honour to be your PhD student. I am also really grateful to Duncan. He is always careful and patient and can always perceive some hidden details. His valuable feedback has helped to improve the quality of my work. His kind encouragement supports me to go through the difficulties. Lastly, special thanks to Alan. He was kind and responsible, and could always give constructive suggestions from a different perspective. I first met him during the welcome week when he gave a short talk to new students and said that cherish your PhD journey since it is a valuable time of your whole life that you can explore whatever you like with other people supporting you. I always remember these words and now I want to say “Yes you are right! And

I finally make it!”

I would deeply appreciate the Chinese Student Council for funding this research. I am truly honoured to be sponsored for my PhD at Lancaster University. I would also express my thanks to the staff members at Lancaster University, especially at Lancaster Environment Centre for their always kind help whenever needed. I would like to thank all the friends I have made at Lancaster. Some of them have become my friends for life. Their accompany and support have given me so much strength and made me feel at home.

I want to thank my family members for their support and encouragement and for always caring about my study and life abroad. Special thanks to my parents for their unconditional support and love. They always encourage me to do the things I like. Words could not express my love for them. Also, in loving memory of my grandfather. I miss you. Lastly, I would thank Dabao, Ershun and Xiaobao. You are the cutest rabbits. I also thank Agui. You are the best turtle to me.

Lastly, I want to thank myself for not giving up. With so many hard moments during this journey, you finally make it. I also need to thank my boyfriend for his understanding and encouragement. You are always there.

Table of Contents

List of Figures

List of Tables

1 Introduction

Urbanization is one of the most significant processes experienced globally, especially in recent decades (Bloom et al., 2008; Batty, 2020). It promotes economic growth, urban population increase and the transformation of the landscape (Marshall, 2007; Bloom et al., 2008; Clemente, 2021). Take China as an example, whose urbanisation level calculated by urban population increased from 17.9% in 1978 to over 60% by 2018 from Chinese National Statistics Bureau. Such rapid urban growth is usually accompanied by significant urban land expansion, with profound implications for related economic, social, and environmental systems(Chan, 1994; Deng et al., 2010; Dai et al., 2018; Chen et al., 2022). In general, the transformation to urban land cover is irreversible, fundamentally reshaping landscapes and creating new opportunities as well as considerable challenges. While urbanization has provided better lives for people around the world, it has also led to substantial problems such as environmental pollution, social inequalities, and loss of biodiversity(Robinson et al., 2012; Seto, Güneralp, et al., 2012; Li et al., 2023). For example, urban expansion, typically at the expense of agricultural and forest land cover, l leads to soil degradation, habitat loss and climate change (DeFries et al., 2010; d'Amour et al., 2017; Zhu & Yuan, 2023). This effect is not restricted to the region where urbanization occurs but influences global change in the long term which threatens sustainable development worldwide (Entwisle et al., 2008; Meyfroidt et al., 2009). To understand the implications of urbanization and address these emerging issues, the first step is to understand the dynamics of urban growth. This can lead to a better understanding of how it affects other systems and processes which could further contribute to providing management strategies and sustainable urban planning.

1.1 Urban Growth Studies

Urban growth has been measured using a variety of approaches, including the increase in the

transformation of land cover to urban land, migration of population to cities and development of the economy (Anderson & Ge, 2004; Berling-Wolff & Wu, 2004; Marshall, 2007; Ding & Li, 2019; Mahtta et al., 2022). Thus, to learn about urban growth, the first crucial step is to determine how best to represent it. Different representations provide different data that leads to different methods to be utilized to study urban growth. Urban growth studies have developed significantly over the past century, from focusing on quantifying urban growth of an area or its population (Feng et al., 2002; Lin, 2002; Anderson & Ge, 2004) to monitoring spatial urban change and analysing the spatial pattern of urban growth (Cheng & Masser, 2003a; Aguilera et al., 2011; Liu et al., 2016) by analysing urban areas within land cover data generated from remote sensing data and Geographic Information System (GIS) methods; and to further predicting urban growth with the development of computational techniques by incorporating data representing different aspects of cities (Castells, 2010; Meerow et al., 2019; Burghardt et al., 2022). The availability of remote sensing data significantly promotes the development of urban growth studies since they provide consistent, frequent and complete land cover data that are ideally suited to analysis of change in space and time. Meanwhile, urban growth studies have also evolved to incorporate approaches from other disciplines such as economics, social science, landscape ecology and computer science (Aguilera-Benavente et al., 2014; Cottineau et al., 2018; Zhai et al., 2020).

1.1.1 Characterizing urban growth

Early studies on urbanization were largely descriptive and focused on quantifying the growth of cities, identifying drivers of urbanization (Yue et al., 2013; Wu et al., 2019) and understanding the basic patterns of urbanization (Capello & Camagni, 2000; Luo & Wei, 2009; Aguilera et al., 2011) due to data availability and limitation of analysis techniques. Typically, using statistical data such as urban area or urban population, they sought to understand how cities expand over time and investigate the consequences of such growth. Such approaches

were helpful for examining growth rates over time across different cities. Some studies examine urban growth from a different perspective, using concepts from fractal geometry and complexity science (Shen, 2002; Tan et al., 2021). These studies suggest that urban growth exhibits similar characteristics at different levels of magnification, much like the growth patterns observed in the growth of organisms in biological systems. Studies use this concept to characterize growth patterns over time or compare the growth trends in different cities. Similarly, some studies have utilized rank-size methods to analyse how cities grow over time with the assumption that there is a relationship between the rank of the city and its size (Fragkias & Seto, 2009; Huang et al., 2015). This kind of research provides insights into the overall structural change of cities. Other studies have combined demographic, social, and economic data and utilize statistical methods to understand factors and processes that drive urban growth and model the relationship between urban growth and its underlying drivers (Goodkind & West, 2002; Kuang et al., 2016; Wu et al., 2019).

With the availability of fine-resolution remote sensing data in recent decades, urban growth has been intensively studied especially for its spatial-temporal patterns using various spatial metrics. Within this framework, cities have been represented as raster data extracted from remote sensing data. This approach allows for a detailed exploration of the spatial aspect of urban growth, such as how urban growth differs at within city level (Cheng & Masser, 2003b; Li et al., 2013), and how the spatial form and patterns change as urban areas expand (Burger & Meijers, 2012; He et al., 2017). For example, a variety of landscape metrics have been developed to analyse the spatial characteristics of urban land over space and time (Seto & Fragkias, 2005; Aguilera et al., 2011). Based on spatial patterns, various metrics relating to density, compactness and spatial form have also been developed to characterize the detailed inter or intra-city level patterns (Jiao, 2015; Dibble et al., 2017; Luan & Fuller, 2022). These methods provide insights into the spatial-temporal dynamics of urban growth. From studying

how urban spatial structure and morphology change over time, researchers can infer related processes that contribute to observed urban growth patterns.

Some researchers have proposed urban growth theories relating to growth phases (Dietzel, et al., 2005a, 2005b; He et al., 2017). They identified different growth phases including dispersal and coalescence representing the introduction of new urban land into the space and the connection of existing urban land, and suggested that urban growth shifts between dispersal and coalescence (Dietzel, et al., 2005b). This study implies that on the city level, different growth stages could be inferred through the analysis of spatial patterns using landscape metrics. Meanwhile, some studies distinguished different growth types based on the spatial relationships between new and existing urban land (Li et al., 2013; Jiao et al., 2015; Glockmann et al., 2022), such as identifying infilling development, edge expansion and leapfrogging growth at the patch level (Li et al., 2013). When mapped, these different growth types can provide deeper insights into related processes. These studies suggest that urban growth studies, which had previously been more conceptual, became increasingly sophisticated and able to examine the spatial-temporal change in patterns and forms of cities by incorporating spatial patterns analysis. The key contribution is that they provided a perspective to link the pattern change to underlying processes.

1.1.2 Modelling urban growth

However, these are all static methods but cities are essentially dynamic systems that evolve. Urban systems exhibit continuous dynamics both spatially and temporally. This is why the cellular automata (CA) models were introduced into urban studies. CA models can simulate urban growth by representing a landscape as a lattice of grid cells, each of which can be either urban or non-urban. It follows predefined transition rules to determine the states of grid cells, so each cell is updated at every timestep. This method can be used to simulate how urban cells spread over time at the micro level and therefore capture the spatial-temporal evolution of

urban growth. Since it allows for continuous updating of urban cells and non-linear relationships, and incorporates many other aspects, such as population density, economic activities, land availability, infrastructure conditions and interaction between lands, it provides a more flexible way to model urban growth compared to other approaches.

In CA models, cities are often treated as self-organizing systems. They are viewed as complex systems consisting of different aspects interacting with each other and evolving continuously driven by both internal dynamics and external forces. Since in CA models, urban land is represented by cells, one of the major advantages is that it can incorporate spatial interactions between cells in the model. In the transition rules, the state of cells is determined by the state of the cell itself and its neighbours. Therefore, the interaction term is represented in the model which is crucial in geographic processes.

CA models have been intensively studied and widely applied in urban growth modelling due to their simplicity, flexibility, and intuitive representation of spatial dynamics. They have also evolved and been integrated with other methods as well. For example, parcel-based CA models have also been applied to urban growth (Abolhasani et al., 2016; Guan et al., 2023). They represent cities as parcels which overcome the cell-size sensitivity in traditional CA and define a neighbourhood effect based on parcel characters and geometric parameters. With the development of artificial intelligence algorithms, related methods have also been integrated with CA models, such as AI-CA, neural network with CA and machine learning with CA (Shafizadeh-Moghadam et al., 2017; Zhai et al., 2020). These newly developed CA models have contributed to improving the model accuracy and power of simulations.

1.2 Object-based methods

Despite these advancements in urban growth research, there is still a need for a more explicit

representation of urban entities to study their dynamics and the spatial-temporal relationships between them, since cities are not just collections of individual cells but are complex systems of interconnected components that interact with each other over time and space (Benenson & Torrens, 2004; Batty, 2020). In the real world, cities are urban objects with various activities located on them and interacting with each other, which influences the dynamic change of objects. Urban objects also evolve over time by expanding in area and merging with other objects to become new objects which suggests that urban object have their own “lead” objects unless newly introduced into the space. It implies that urban objects have a potential temporal link between them and could be defined through this expansion or merging behaviour. Overall, cities are urban objects interacting with each other through spatial-temporal links.

Object-based approaches, which have emerged from disciplines like landscape ecology and remote sensing, focus on the analysis of land cover as individual "objects"(Cantwell & Forman, 1993; Fall et al., 2007; de la Barra et al., 2022). For example, some researchers have used object-based methods to study the land cover change over time and the dynamics of habitat and its connectivity (Minor & Urban, 2008; Zou et al., 2023). By representing different land cover as objects, these studies explicitly track how land objects evolve. Some researchers have attempted to build spatial and temporal links among objects and study their dynamics with graph-based methods. These prove that object-based methods can be used to explicitly characterise how land objects change over time (Zou et al., 2023) and provide insights into how objects relate to each other both spatially and temporally. However, object-based methods are rarely applied in urban studies and currently, most studies concentrate on characterising the dynamics of land objects. Even though the object-based methods provide a perspective to study the relationship between objects, most studies focus on the network structure and the interactions between objects are not explicitly studied. Therefore, object-based methods are employed to represent urban land to characterize urban growth and explore the relationships

between objects by building spatial-temporal links in this research. At this stage, the object-based data is obtained by extracting objects from remote sensing data. In this research, the object-based data is extracted from land cover products generated by the European Space Agency which have global coverage for multiple years and relatively high accuracy of land cover classes, including the urban class.

1.3 Research Aims and Objectives

This research aims to analyse and model the spatial-temporal patterns and processes of urban growth by treating individual urban patches as geospatial objects and building spatial and temporal links among them.

In this study, traditional concepts of urban growth phase, including dispersal and coalescence, are replaced by four definitive, measurable types of growth event: introduction, establishment, dispersal and coalescence, and a fifth inactivity event, stability. These events are attributable at the object level hence are measurable directly once each individual city is represented as a geospatial object. Spatial links are also constructed between objects to derive spatial-temporal networks that can be used to study spatial-temporal interactions between objects. In this context, the research aim is achieved through addressing the following objectives.

1. Developing an object-based representation of urban areas from a time-series of high-quality land cover data.
2. Characterizing urban growth over space and time from the perspective of urban objects.
3. Expanding traditional concepts of urban growth theory to incorporate additional states for urban objects by linking urban objects through time.
4. Exploring urban growth processes by analysing the spatial-temporal dynamics of the states of urban objects.

5. Exploring spatial-temporal interactions between these objects by building spatial-temporal networks between urban objects.

6. Predicting the dynamics of urban land at the object level.

The specific research questions are listed as follows:

1. What are the temporal trajectories and spatial patterns of urban growth in the study region, especially for the growth characteristics of different-sized objects across cities and what can be inferred from their temporal trajectories and differences between cities?

2. How do urban growth states in different study areas change over time? What underlying urban growth processes can be inferred when accumulating the characters of urban growth states at the city level? Compared to current key urban theories, what evidence and references can be made from the results?

3. What is the relationship between the object states of coalescence, establishment and unchanged and the dynamics of other neighbouring objects and can these states be predicted through Bayesian linear mixed effects models? How do the interactions between objects affect the area of grown objects and how does this effect differ across different-sized objects?

1.4 Thesis structure

This thesis consists of six chapters with an introduction chapter and a literature review chapter; three chapters on analysing and addressing the aims and objectives respectively, and a discussion and conclusion chapter on the overall findings and suggestions for future research. The details for each chapter are as follows:

Chapter 1. Introduction

This chapter first introduces the research background and provides a brief review of urban growth studies. It then explains the importance of urban growth studies and why object-based methods is used to study urban growth. Finally, it introduces the research aims and objectives.

Chapter 2. Literature review

This chapter first reviews the urbanization process in China and how urban spatial patterns change in China. It then introduces related definitions and different measurements of cities in related research. It follows with reviews of urban growth studies including characterising urban growth with landscape metrics, fractal analysis, rank-size analysis and related geostatistical models; models for predicting urban growth; dynamic models including Cellular Automatic models and Agent-Based models used in urban growth study and forecasting in urban growth studies. Finally, it summarises the related gaps in the literature and suggests direction for future study.

Chapter 3. Revealing the scale and synchronicity of rapid urban growth in China in the 2000s in response to reform and regional policies by treating provincial capital cities as sets of spatial objects

This chapter quantifies the temporal trajectories and spatial patterns of urban growth in China post-Reform based on urban objects. It examines how cities of different sizes and across various regions have experienced distinct growth patterns to provide insights into the factors driving urban growth in different regions. This study was submitted to the journal **Applied Geography** (2024) and has been accepted subject to major revision.

Chapter 4. Analysing the Growth of Megacities Using an Object-based Method

This chapter quantifies changes in different growth events based on the urban objects method and makes references to the urbanization processes across different cities. This study was

published in the journal **Geographical Analysis** (2024).

Chapter 5. Modelling urban objects through Bayesian linear mixed effect models

This chapter models the states of urban objects through their relationships with neighbouring objects and predicts their states using Bayesian linear mixed effect models. It also explores the relationships between the area of grown objects and their interactions with neighbouring objects. This study will be submitted to an appropriate journal later this year.

Chapter 6. Discussion and conclusion

This chapter discusses the results and findings of chapters 3 to 5; and makes references to the main contribution of this research, as well as the limitations and suggestions for future research.

2 Literature Review

2.1 Introduction

2.1.1 Research background

More than half of the global population now lives in urban areas (United Nations, Department of Economic and Social Affairs). Population growth and urbanization are projected to continue, especially in developing countries, with more than two thirds of world population projected to live in urban areas by 2050 (United nations, 2022). The rate of urban growth in Africa and Asia is higher than in other regions (United Nations, 2022). Furthermore, medium- and small-sized cities have experienced more urbanisation than large cities or metropolitan areas in recent decades (UNDESA, 2014) with rapid urbanization resulting in increasing numbers of people living in cities. Urban areas influence on the environment and biochemistry process from local to global scales, such as carbon cycle, air quality, and climate change (Kalnay & Ming, 2003; Seto et al., 2010; Li et al., 2023; Tu et al., 2023). The impact of urbanization is not constrained to its surrounding area, and can extend far away from the "source" area through teleconnection (Seto, Reenberg, et al., 2012; Yu et al., 2013). For example, importing construction materials such as wood from other countries directly influences forest patterns in the country of origin with impacts on the local climate and related environmental processes. Furthermore, the dynamics of the urbanized area have a direct and close relationship with the quality of people's lives (Parr, 2007; Huang & Wong, 2016). Different urban forms can lead to different patterns of commuting and transportation of goods and services. Overall, the study of urban growth not only gives us insights into the urban dynamics and contributes to sustainable urban landscape planning and management, but is also essential to understand global change and make strategies and adaptations to these changes.

2.1.2 Urbanization in China

2.1.2.1 Historical period of urbanization in China

The urbanization process in China can be classified into two major periods: the pre-Reform period and the post-Reform period. Urban growth, urban size, and urban spatial form have shown different characteristics before and after the Reform and Opening-up in 1979 (Plan, 2014; Schneider et al., 2015; Wang et al., 2022). China experienced a relatively low rate of urbanization before the Reform, but relatively high rates of urbanization after the Reform, especially in recent years (Gaughan et al., 2016; Wang et al., 2022).

Before the Reform and Opening-up which took place in 1979, state control and planning economics played an important role in the urbanization process (Lin, 2002). During this period, city forms were strongly impacted by planning economics. The state emphasized industrial production in cities while their consumption and commercial sectors were weakened (Chan, 1992). Concentrating on industrial production and planning economics, 'work units' played an important role in shaping urban spatial form. These units were self-contained spaces that provides not only spaces for working, but also people's daily services, such as housing, education, and food for its residents (Schneider et al., 2015). Widely implemented across China, these work units resulted in cities taking on highly standardised, lower density forms during this period (Abramson, 2006).

Migration to cities was under strict control. Before the Reform. The state adopted a 'hukou' system (a national household registration system) to divide residents into two groups: the agricultural population and the non-agricultural population (Chan, 1994; Cheng & Selden, 1994). The state was concerned that a large number of the population migrating to cities might put pressure on the provision of food and urban services. This hukou system widened the urban-

rural gap and contributed to the creation of a dual urban-rural structure at this time (Lin, 2002).

Before the Reform, both the growth of existing cities and the creation of new cities were limited with levels of urbanization increasing from 10.64% in 1949 to 18.96% in 1979 (based on the percentage of urban population in total population) (Chan, 1992). The number of cities increased from 132 to 193 during the same period (Lin, 2002). Geographically, the state focused on a different location in different periods (Abramson, 2006). Initially, the state focused on Northeast and North China where energy and resources were relatively abundant; then, the state concentrated on Southwest and interior China (which is called the Third Front project) in the 1960s and early 1970s due to national security and defence concerns.

During this period, large cities experienced significant growth while the development and growth of small cities were limited (Chan, 1992). Most of these large cities are provincial capitals or special municipalities. They were regarded as important political and critical economic centres which had better infrastructure and more state investment.

After the Reform, the economy gradually shifted to a more market-led economy (Chan, 1994; Lin, 2002; Power, 2018). In the meanwhile, decision-making became more decentralized, giving local government more power. In accordance with the Reform, there were several policies that had significant impacts on urbanization.

First, migration policy was gradually relaxed even though migration (to get a “hukou”) to large cities was maintained (Chan, 1994; Gaughan et al., 2016). A shift in power of decision-making to individual agricultural households significantly boosted agricultural productivity and efficiency resulting in the release of a large amount of the agricultural population (Lin, 2002; Schneider & Mertes, 2014). This change in policy has allowed large numbers of surplus labours in the agricultural population to migrate to nearby small towns and small cities. This in turn helped boost the economic growth of both large and small cities. The amount of urban

population and size of cities has grown tremendously since then.

Second, the housing reforms enacted in 1982. This allowed foreign and domestic capital to build houses in cities which had a direct impact on the urban spatial form and commuting patterns. In addition, urban land use value and the urban land market were introduced in 1987. Since then, urban land value has played an essential role in shaping urban spatial patterns. This has helped to make Chinese cities exhibit spatial gradients based on land rent (Seto & Fragkias, 2005; Yue et al., 2013). Urban land sales and leasing have accounted for a large percentage of local government budgets in recent years. This money has been used to boost economic growth such as infrastructure construction, education, and medical services which in turn has led to more significant urban growth.

Last but not least, after the Reform, several different kinds of development zones were established, with the aim of attracting investment and boosting economic growth. In 1979, four Special Economic Zones were established in Shenzhen which proved successful. In 1984, 14 coastal cities were opened to foreign investment. Economic Technology Development Zones were also built in many open cities. After that, large areas were opened as Coastal Open Economic Zones and these areas were ultimately extended to all coastal provinces. These development zones have successfully boosted economic growth in coastal areas. To balance the development between eastern and western regions, High-Technology Industrial Development Zones were set up in provincial capitals in inland China in 1991. Due to the success of national development zones, local governments started to build provincial-level development zones. These development zones (both national and provincial level) have played a crucial role in the urbanization process (Seto & Fragkias, 2005; Schneider et al., 2015). On the one hand, these areas have made a significant contribution to economic growth in these areas. On the other hand, these areas were established near urban fringes which were mostly

formerly agricultural land or green land and affected the urban spatial pattern. During this period, the development was concentrated in coastal areas which led to a higher urbanization level in coastal areas. Since 2000, the state has set up a series of policies to balance this spatial inequality of urbanization, aiming to stimulate economic growth in interior China. Central governmental investment has played an important role in urban growth in Western China and Foreign Direct Investment (FDI) played an important role in Eastern China (Schneider et al., 2005, 2015).

2.1.2.2 Urban spatial pattern in China

Urban spatial form can also be characterized by two periods: pre-Reform and post-Reform. The spatial form of cities was relatively compact and monocentric before the Reform (Lin, 2002). While after the Reform, cities have witnessed rapid growth in both urban population and urban land use amount (Gaubatz, 1999; Schneider & Mertes, 2014; Montero et al., 2021; He & Zhou, 2024). The relaxation of rural-urban migration policy has contributed to simulating urban growth, especially in small cities and urban fringe areas (Lin, 2002). The rapid growth of small towns or cities especially those near large cities has led to the emergence of polycentric characteristics in large cities (Schneider et al., 2015; Liu & Wang, 2016). There are some other phenomena related to this such as semi-urbanization, suburbanization, and urban clusters. All of these have emphasized the decentralization of urban population and function and the development of surrounding urban areas. However, most research on polycentric cities has been based on urban land data or population or employment data to identify the polycentric morphological characteristics (Burger & Meijers, 2012; Liu & Wang, 2016). Studies on the functional characteristics of polycentric cities, and levels of connectivity between them, are largely limited. In the meantime, large metropolitan areas have formed in some areas, such as Shanghai (the Yangtze River Delta), Beijing, and Guangzhou (the Pearl River Delta). The

housing reform and development zones made a significant contribution to shaping urban form during this rapid urbanization period. The pursuit of land rent has potentially accelerated the transformation of agricultural land close to cities to urban land (Wu et al., 2015). Research has shown the urban edge area to be fragmented at the micro level (Liu, Li, Chen, et al., 2010a). Most development zones are located in urban fringe areas, leading to dispersed urban growth. It is argued that this is often followed by an infill process.

2.2 Definition

2.2.1 Land cover and land use

Land cover and land use are two commonly used terms in geography and other related disciplines such as urban planning and resource management. Land cover and land use have distinct definitions. Land cover describes the physical surface of the earth, such as forest, grassland, river, and concrete. In contrast, land use refers to the purpose the land serves, for example, road, park, and agriculture. Land cover only describes the surface on the ground regardless of its usage. Land use is a function-based concept that indicates how people use the land. The same land cover type can be used for different purposes (uses), for instance, grassland land cover can be used for pasture, leisure, and environmental protection. Conversely, the same land use type can consist of different types of land cover, for example, land for leisure activities could include grassland, water, and forest.

Land cover data can be derived from a variety of different sources, including aerial photography and remote sensing data, which provide data at the pixel level. Land cover data is dependent on the classification and interpretation of raw data. The classification system determines the land cover data extracted from the original data (Schneider et al., 2005). The classification systems are hierarchical since the land cover itself is hierarchical. The classification starts at a broad level and divides each class into more detailed sub-classes. It is

mutually exclusive at each level. In contrast, land use data is usually hierarchically aggregated from land cover data. It is inferred from land cover data based on other related knowledge, such as urban planning and environmental protection documents, and is usually, object-based. Land cover and land use data provide useful information across a variety of fields including ecological conservation, land management, urban planning, and resource management. Land use and land cover data can be analysed to highlight changes over time. Such information is not only useful for governments and agencies, but also for researchers in a variety of fields, including climatologists, ecologists, and urban planners.

2.2.2 Urban area and rural area

Urban land and rural land are land use-based definitions. They describe how people are using this land and potentially whether this land is used for urban-related purposes or non-urban-related purposes. Both urban and rural land can be composed of a variety of different land cover types. For example, in an urban area, asphalt and concrete can be treated as urban land; grass can also be treated as urban land when it is used for leisure and climate mitigation. When defining urban land, it is important to distinguish this from other similar land cover or land use definitions, such as built area, settled area, and impervious area. Built area or built-up area is strongly related to the urban space. The criteria (minimum population or population density) may be slightly different in different countries, but it is usually defined as a well-urbanized area, used for urban functions, such as work, residence, and industrial production, with basic infrastructure (Parr, 2005, 2007). In a monocentric city, the built-up area is usually a large continuous area; while in a polycentric city, the built-up area may be composed of several contiguous areas (Burger & Meijers, 2012). The settled area is another land use-based definition. It refers to land used for settlement. An urban area encompasses not only a settled area. Impervious areas are closely related to human activities. They are defined as artificial

surfaces covered by impenetrable materials such as asphalt and concrete. For instance, pavement, industrial construction, and buildings are regarded as impervious areas.

When studying urban-related topics, researchers with different backgrounds focus on different aspects of cities and use different definitions based on the research topic. Spatially, an urban area can be treated as a physical entity (Parr, 2007). From this perspective, the urban spatial pattern can help to define the city and characterize its features, such as landscape metrics and geostatistical models. However, it is not only a spatial entity, but it is also a centre for economic activities, consumption, employment, and workforce (Parr, 2007; Huang & Wong, 2016; Fang & Yu, 2017). It is not a sum of these activities, rather, it is a hierarchical, dynamic, adaptive system, with all these activities which are the behaviour of individuals and groups interacting with each other (Bettencourt et al., 2007; Batty, 2008; Sultana & Weber, 2014). Scholars emphasize the importance of connections and networks in cities (Vasanen, 2012). Rather than considering the city as a top-down entity (control with policies and planning), it is argued that these interactions and networks directly relate to the nature of cities and urban patterns from the bottom up (Batty & Longley, 1994; Batty, 2012, 2013a). Both physical and social networks connect people in cities and allow the flow of goods, energy, and information. As the node or centre for connection, cities attract more people which leads to more connections and flows, eventually causing the growth of cities. Furthermore, urban land is also connected with other urban areas or different land use types through teleconnection (Seto, Reenberg, et al., 2012; Yu et al., 2013). This teleconnection also has a link to urban pattern change and urban growth. The contemporary world has made this connection even more complex and dynamic. To better understand these interactions and connections, dynamic models have been used to simulate urban systems.

2.2.3 Representations: raster-based and object-based model

Raster-based and object-based models are two ways of representing specific objects or phenomena in geography. Unlike modelling in other disciplines, modelling in geography describes not only the characters of objects or phenomena but also their spatial location (Lloyd et al., 2017). When representing phenomena or objects in space, there are two approaches to modelling them: the entity approach and the continuous field approach. In Geographical Information Systems (GIS), the continuous field approach relates to gridded data or raster data, which equates to a set of pixels (the size is the spatial resolution), with each pixel having an (x,y) value representing its location in space and a value representing the value of specific phenomena (e.g., land cover, elevation) at that location. The entity approach relates to an object or vector data, which consists of a set of points, lines, or polygons with an (x,y) value representing its location and associated attributes held in attribute tables (e.g., name of zone, area of zone)

2.3 Measurement

2.3.1 Remote sensing data

Remote sensing data has been widely used in many aspects, such as urban planning, agriculture management, environmental protection, natural hazards monitoring, and geology (Schneider & Woodcock, 2008; Sexton et al., 2013; Taubenböck et al., 2017; Wu et al., 2019; Zou et al., 2023). It provides long-term, consistent data for large spatial extents and has been used in numerous studies regarding monitoring urban change, including changes of size, shape, location and pattern (urban spatial characteristics) in recent decades (Anderson et al., 1976; Decker et al., 2007; Schneider, 2012). Raw remote sensing data records land surface radiation (reflected radiation or emitted radiation) in different wavebands as grid cells. The size of grid cells or pixels is the resolution of remote sensing data and this can vary from 1km to less than

1m depending on the satellite sensors. Before being used for analysis, raw remote sensing data needs to be pre-processed, for example, to correct for any atmospheric effects, and geometrically registered to a coordinate system. These processes occur before any interpretation of remote sensing data. After image classification, the accuracy of classification is usually checked. The classified product can then be interpreted or analysed accordingly.

Remote sensing data is a major source for quantifying urban change and spatial patterns. After being classified, remote sensing data provide basic land cover or land use information. When used in quantifying urban spatial patterns, it is crucial to take spatial resolution into consideration, to ensure that the resolution is sufficient to capture the dynamics of the land surface under investigation.

2.3.2 Population data and economic data

Population data is frequently used when studying urban-related topics. For example, population is widely used to classify cities (large, medium, or small cities) and calculate levels of urbanization; the spatial distribution of population also provides useful information when studying urban form and spatial structure (DeFries et al., 2010; Hernando et al., 2013; Gaughan et al., 2016). Population data is often obtained from government census data. Since the data collection process is usually based on administration units, population data is often available at aggregate level, e.g., county, city, and province level. When used spatially, this type of population data is usually displayed in vector format with polygons representing administrative boundaries and population data assigned as an attribute of corresponding polygons. However, this level of aggregation can be quite coarse when researching at local scales, especially when used in conjunction with land cover or land use data which is usually available at much finer resolution. Thus, researchers have utilized a variety of approaches to generate raster population data at finer spatial resolution. The Gridded Population of the World (GPW) series is an openly

available gridded global dataset which models the spatial distribution of population on land surfaces with grid-type data. This is now in the fourth version (Doxsey-Whitfield et al., 2015). This data set utilizes an area-weighting method which disaggregates population from administrative units into raster cells. The GPW v4 is available at a resolution of 30 arc-seconds (approximately 1 km) for 2000, 2005, 2010, and 2020. Recently, the WorldPop Project has produced an open-access population dataset at a finer resolution with higher accuracy (Lloyd et al., 2017). This dataset utilised a variety of spatial datasets such as nightlight data, land cover data, Open Street Map, and elevation, to generate gridded population data at 3 arc-second spatial resolution (approximately 100m). These finer-resolution population datasets provide essential support to measure a variety of population-related research topics, for example, urban growth, urban planning, impacts of population growth, and epidemic modelling.

Economic data is another widely used data when studying urban-related topics, especially urban economic activities. Usually, economic data can be obtained from official census data. When studying urban growth, economic data is usually used in combination with other data to measure the growth rate and amount (Bloom et al., 2008).

2.3.3 Other types of data

There are some other ways to measure urban patterns in urban studies. Scholars have used nighttime lights to measure the urban extent and urban growth, which usually refers to the Defence Meteorological Satellite Program/Operational Line-scan System (DMSP/OLS) nighttime stable light (Zhou et al., 2015). Some efforts have been made to use this nighttime light data alone or with data such as population data to measure urban extent nationally or even globally and identify urban clusters (Yu et al., 2014; Gao et al., 2016). In recent years, an increasing number of researchers have used social network data and other types of big data such as mobile phone signal and transportation data to study urban growth and urban activity

patterns(Chen et al., 2022; Dong et al., 2024). This type of data is usually individual as opposed to aggregate, making it useful in modelling urban evolution, the pattern of activities, and connections within a city or among cities (Batty, 2013a; Huang et al., 2016; Huang & Wong, 2016). For example, population flow is considered as a useful tool to study urban growth in recent years since cites are becoming more connected as networks through the flow of goods, technologies and information (Xia et al., 2019; Xu et al., 2021; Xu et al., 2023; Hu et al., 2024).

2.4 Statistical Model: Characterization Model

2.4.1 Landscape metrics analysis, fractal analysis, and rank-size analysis

2.4.1.1 Landscape metrics in analysing urban pattern dynamics

Landscape metrics are effective ways to characterise urban patterns and configurations at multiple scales over time. Landscape metrics can be patch-based (e.g., patch density, patch shape, patch size, and fractal dimension) and pixel-based (e.g., contagion). These metrics can be used to describes the size, complexity, shape, and other aspects of urban areas at different scales (Schneider et al., 2005; Torres et al., 2016; Bosch et al., 2020). For example, frequently used landscape metrics such as patch density, mean patch size, and edge density can be used to measure the continuous fragmentation of urban land whilst the contagion index can be used to measure the heterogeneity of landscape (Luck & Wu, 2002; Von Der Dunk et al., 2011; Fan & Myint, 2014). Landscape metrics can be classified by quantifying the composition or configuration of the landscape (Berling-Wolff & Wu, 2004a; Yu et al., 2014). No single metric can adequately measure or describe complex urban patterns and their changes over time. However, many landscape metrics are correlated. Thus, the metrics selected for research should not be highly correlated and can be used to capture essential and meaningful landscape information. Another critical issue that needs to be considered when using landscape metrics

is scale. Since the landscape itself exhibits different characteristics at different scales of investigation, no single scale can provide full information on the landscape. Therefore, it is essential to calculate metrics at multi-scales.

Scholars have utilized landscape metrics to characterize spatial-temporal urban patterns within a single city, in several cities in a region, or even globally (Berling-Wolff & Wu, 2004a; Schneider & Woodcock, 2008; Schneider et al., 2015). Landscape metrics have been used to calculate changes in urban form within different buffer zones to better understand urban growth both spatially and temporally, indicating that common patterns exist in the size, shape, and growth of urban land across cities in a region and that disconnected urban land converges to a continuous urban fabric (Schneider et al., 2005, 2015). Landscape metrics have also been used to assess policy and planning outcomes, and how policies have driven urban growth, which supports planning and management in the future (Schneider et al., 2005). Another benefit of landscape metrics is that they provide a series of consistent measures which can be applied to different cities to make comparisons across cities. Researchers have used metrics to measure urban growth characteristics and urban form within countries, such as comparison among coastal cities and inland cities in China, and globally, to contribute to understanding of urban sprawl among countries (Schneider & Woodcock, 2008; Gao et al., 2016). Researchers have used landscape metrics to link empirical observations to urban growth theory. For example, a case study in California's Central Valley was used to identify diffusion and coalescence process and link to relating theory (Dietzel, et al., 2005a). In addition to these classical landscape metrics, researchers have introduced new indexes based on landscape pattern characteristics to better quantify landscape pattern dynamics. For instance, the Landscape Expansion Index (LEI) was used to identify different urban growth patterns, i.e., infilling, edge expansion, and outlying (Liu et al., 2014; He & Zhou, 2024). Unlike most landscape metrics that measure characteristics for one period of time, the LEI identify and quantifies urban growth types and characters for

two or more periods of time (Liu, Li, Chen, et al., 2010a) which essentially provides insights into urban growth process at the micro level.

2.4.1.2 Fractal analysis

The concept of fractal refers to spatial objects exhibiting self-similarity, scale-independent, and irregularity characteristics (Falconer, 1986; Batty, 2013b). When a fractal object is subdivided into parts, each part looks similar to the whole object (Frankhauser, 2009). Many natural spatial objects have been found to exhibit fractal characteristics, including coastlines and plants. Many artificial spatial objects have also been shown to exhibit fractal characteristics, including urban areas and transportation infrastructure (Batty & Longley, 1988; Wong & Fotheringham, 1990; Lu & Tang, 2004; Mohajeri et al., 2012; Batty, 2013b). The fractal dimension has been widely used to measure how the detail in the fractal changes with scale. The most commonly used methods for calculating fractal dimension include box-counting analysis (Benguigui et al., 2000; Shen, 2002), area-radius scaling (Chen, 2010), and area-perimeter scaling (Wang et al., 2005). It is suggested that the box-counting approach works best when analysing the spatial distribution of built-up objects, while the area-radius scaling approach works best when analysing the fractal dimension of the urban growth process due to its consistency with urban areas and urban peripheries (Chen, 2013). Since being introduced into geographical research, fractal analysis has been applied to analyses of urban form, urban growth, urban systems, and inner urban structure (e.g., transportation, infrastructure, and population density) (Wong & Fotheringham, 1990; Chen, 2010; Tannier & Thomas, 2013; Chen et al., 2014). Fractal theory provides new perspectives with which to understand cities (Batty, 2013b; Bosch et al., 2020; Lagarias & Prastacos, 2020; Tan et al., 2021).

Using fractal simulation techniques, researchers have explored the fractal dimension of urban form, urban growth, and urban structure for individual or multiple periods in time. For instance,

empirical analysis of the fractal dimension of urban growth in London was consistent with that of urban growth in Cardiff (Batty & Longley, 1994). Extensive research has also been conducted for cities across the world, studying urban form, urban agglomeration, and a specific inner urban characteristics (Wong & Fotheringham, 1990; Chen, 2010; Thomas et al., 2012; Tannier & Thomas, 2013). To better compare the fractal characteristics among different cities, the top 20 cities ranked by population in the US were selected using a box-counting algorithm to calculate their fractal dimension for urbanized areas and examined to determine the statistical relationship between fractal dimension and population density using a log-linear function (Shen, 2002). The results indicated that different urban forms could share similar dimension values, and that cities with the same dimension values and urbanised areas could have very different population sizes. This suggests that the fractal dimension worked as an aggregate measure of the whole urban form rather than its specific configuration, and the fractal dimension alone was not a good indicator of population density. To investigate the reasonable range of fractal dimension value and explore the relationship among various urban fractal indicators, scholars have integrated the scaling analysis, spectral analysis, and spatial correlation analysis to generate a set of fractal parameters linked with each other based on the density-radius scaling method (Chen, 2013). The results revealed that the appropriate range of dimension value is between 1.5 to 2.0. This approach could be applied as a useful tool to understand urban evolution. The morphological similarities of the built-up area have been explored across countries. Researchers utilized fractal indices to calculate the morphological similarities of 97 towns located in 18 European urban agglomerations (Thomas et al., 2012). The results indicated that the morphological characteristics resembled each other more strongly across cities (or countries) than within cities. This research has provided many empirical cases, advanced analysis techniques, and enhanced fractal theories. In addition to that, researchers have also developed a multifractal method to study the spatial form and growth and cities. It is

argued that the monofractal methods lack self-comparability, has limited ability to conduct analysis at a local scale to provide more details, and cannot provide multiple perspectives (Chen & Wang, 2013). Thus, the multifractal method was developed and has been used to study different components of urban systems, such as the spatial distribution of population, the rank-size distribution of cities, and the morphological characters of cities (Haag, 1994; Appleby, 1996; Chen & Zhou, 2004). Based on the box-counting method, the research utilized the multifractal method to study the multifractal characters in Beijing, China (Chen & Wang, 2013). The results indicated that the growth pattern of this city exhibited multifractal characteristics. The high-density city centre area was degenerated due to space over filling and the fringe low-density area exhibited a disordered character. These two areas are where urban problems mainly occur such as traffic congestion, inefficient land use, and high population density. This approach is effective in helping to understand the urban evolution process from a different perspective. Recently, it has also been suggested that fractal analysis could be used to transform the study urban systems from the perspective of complex networks (Zhang et al., 2020) since recent rapid developments in technology and the availability of data make it possible for researchers to conduct more complex analyses from different perspectives.

2.4.1.3 Rank-size analysis

Some research has focused on the intra-city relationship, the spatial distribution, spatial layouts of cities, and the morphology of urban clusters (Brakman et al., 1999; Reed, 2002; Fragkias & Seto, 2009; Xu & Harriss, 2010; Peris et al., 2021; Wang et al., 2024). The rank-size distribution research has explored the distribution of some elements of cities, such as city size, city population, and economic activities (Berry, 1961; Haag, 1994; Guérin-Pace, 1995; Reed, 2002; Fragkias & Seto, 2009). One widely used power law to characterize the distribution is Zipf's law. Zipf discovered that the frequency of some events and their rank were connected

through a power law function. This was later called Zipf's law (Brakman et al., 1999). Zipf's law has been extensively applied to various elements of the urban system, providing much empirical research on the rank-size distribution (Gabaix, 1999; Decker et al., 2007; Marshall, 2007). For example, the rank-size distribution was conducted based on multiple time series remote sensing data to study the urban cluster evolution in a metropolitan area (Fragkias & Seto, 2009). This research revealed the intra-city variation of urban form and the oscillating behaviour in the rank-size distribution. This research also provided an empirical study of the birth-growth-coalescence urban growth process. These laws have also been combined to reveal the overall evolution of urban systems (Xu et al., 2025). Overall, the rank-size analysis could help to understand the distribution of urban clusters at regional or national scales and reflect the evolution process of urban clusters, but it could not adequately capture the spatial pattern of urban areas, especially the multiple scales pattern.

2.4.2 Geostatistical Model in Characterizing

It is recognized that in geostatistics two things need to be considered unlike in traditional statistics. The first one is the sampling framework. The spatial data obtained is the function of the sampling framework and its spatial variation. The sampling framework determines the resolution of spatial data which directly influences the analysis results since the resolution is crucial in capturing the spatial variation (Atkinson, 1999). The second one is that in traditional statistics, data is assumed to be independent. While in geography, the spatial data is spatially dependent and exhibits an auto-dependent behaviour (Tobler, 1979; Overmars et al., 2003). Usually, the closer the two data are located, the more similar the two data are.

Geostatistics is usually applied to spatial variables which exhibit spatially dependent characteristics. It is widely used in remote sensing image analysis (e.g., texture classification and smooth classification) and for characterizing spatial patterns (Woodcock et al., 1988;

Atkinson & Lewis, 2000; Atkinson & Tate, 2000; van der Meer, 2012).

Among these techniques, variogram analysis has been extensively used in remote sensing research, to characterize image structure, estimate image texture, classify texture, map land use and identify spatial patterns and land cover change (Curran, 1988; Garrigues et al., 2007; Millward, 2011; Balaguer-Beser et al., 2013). Variograms could reflect the spatial variation of a specific variable. Its shape and properties could provide information on the spatial pattern of specified elements (Woodcock et al., 1988). For example, semivariogram indices were used to study the spatial distribution and spatial pattern of trees (Balaguer-Beser et al., 2013). This approach considered a limited number of directions and could be applied to other elements to understand their spatial heterogeneity pattern. It has also been used to characterise the spatial heterogeneity of vegetation cover and land cover (Garrigues et al., 2007).

2.5 Statistical Model: Prediction Model

2.5.1 Geostatistics and classification of remote sensing data

The classification of remote sensing data could be treated as a prediction process since it is essentially a process that could provide the most likely value of a variable at one location (Stein, 1999). Classification of remote sensing data is an important procedure since it deals with the raw remote sensing inputs and produces outputs for further analysis. The method and accuracy of classification directly influence the analysis results. Various algorithms have been developed and applied to classify the image for both pixel-based classification and object-based classification (Atkinson & Lewis, 2000; Stefanov, 2001; Zhang, 2001; Berberoglu et al., 2007). The most widely used classification methods are unsupervised classification methods such as the K-means algorithm and supervised classification methods such as the maximum likelihood algorithm. Both of these methods are pixel-based and generate pixel-level data, while object-

based methods create objects that consist of homogenous pixels.

2.5.2 Regression model

Traditional statistical methods have been used in geography for quite a long time. Among these, urban growth-related topics such as urban growth mechanisms, urban growth patterns, and urban growth impacts have been explored utilizing a variety of geostatistical methods (Cheng & Masser, 2003a; Stoebner & Lant, 2014; Zhao et al., 2017; Wang et al., 2020; Gielen et al., 2021). Various regression models have been applied at the local, regional, or even national level to study urban growth-related topics (Cheng & Masser, 2003a; Yu, 2006; Riitters et al., 2017). For example, the regression model has long been used to study the relationship between urban growth and population growth or between urban growth and economic growth (Hsu, 1996). Logistic regression has also been widely used in studying determinants of urban growth or urban spatial patterns and has proved its effectiveness in addressing this sort of problem (Zhao et al., 2017).

The regression model has been employed in the study of urban patterns. This geostatistical model is effective in describing the spatial characteristics of urban patterns, reflecting the heterogeneity of spatial patterns, and revealing the determinant of variation in such patterns (Aspinall, 2004; Stoebner & Lant, 2014; Liu & Wang, 2016). Since space is not homogenous, global statistical models may have a weakness in characterizing local variations. To address such problems, some localized statistic models have been developed to characterize local variation, such as Local Indicators of Spatial Analysis (LISA) (i.e., the local Moran's I index) (Anselin, 1995) and Geographically Weighted Regression (GWR) (Brunsdon et al., 1996). This type of model has been successfully applied to some regions and proved to be effective in revealing local change and its influencing factors (Wheeler & Tiefelsdorf, 2005; Bitter et al., 2007; Huang et al., 2015).

These regression methods have been combined with other statistical methods to model urban land use from an economic perspective. For example, a regression model was employed with a Granger causality analysis based on economic, demographic, and land use data to analyse the drivers of urban land use change in the Pearl River Delta in China (Seto & Kaufmann, 2003). This research was conducted at a macro-level to reveal macro-level socioeconomic factors that drive urban land change. The results indicated that at a macro level, the urban land conversion was primarily caused by exogenous factors such as Foreign Direct Investment (FDI). The relative ratio of agricultural land, industrial land, and urban land productivity was identified as the main drivers of natural and agricultural land conversion to urban land. This method provided a better understanding of the macroeconomic drivers of urban land change and supported further research on identifying the drivers of urban land change at different levels.

The logistic regression model has been used to detect the influencing factors of urban growth and urban patterns. For instance, the logistic model was used to study and compare the influencing factors of urban patterns between two border cities in the US and Mexico (Zhao et al., 2017). These two adjacent cities provided an excellent case to explore and compare the underlying factors influencing urban patterns such as transportation, population, and economics. This research characterized the historical urban growth in these two cities first. Then a logistic regression model was utilized to evaluate the effects of a variety of factors on the urban pattern and compare the differences in driving mechanisms. The results suggested that different economic and development backgrounds were underlying the different urban growth patterns and that some local factors were the main determinants of this growth. The results indicated that the city in the US exhibited a more dispersed pattern, and population and highway density showed different effects in these two cross-border cities.

A spatial logistic model has been used to explore the determinants of urban growth in Wuhan

(Cheng & Masser, 2003b). Unlike most research-based study areas in coastal or large cities, this research studied the urban growth pattern in Wuhan, a central medium-sized city which provided a unique case to compare with other large coastal cities and western cities. This research first performed an exploratory data analysis to make a hypothesis. Then a logistical regression model was used as a confirmatory analysis. To deal with the spatial dependence, this research designed a spatial sampling scheme to reduce its effect on the analysis. The result suggested that after the land reform and before 2000, major urban infrastructure and newly developed zones played an essential role in promoting urban growth during this period, while the role of local government's role and master planning was weakened. This method has provided a useful approach to studying the influencing factors in urban growth. The results could be further used in the dynamic model of urban growth.

A logistic GWR has been applied in Nanjing city in China (Luo & Wei, 2009). This large city remains compact in form in the rapidly urbanizing context of contemporary China, which makes it a good case to study how the impacts of factors influencing urban patterns vary among different cities. Both the global logistic regression model and GWR were applied to this city. The results indicated that the GWR fitted better than the global regression model and performed better at revealing the determinants of spatial variation. The GWR allows the variation of parameters across space. This approach could provide a better understanding of variations of urban patterns and the different impacts of determinants. GWR has also been applied at a regional scale to identify the spatial non-stationarity characters in regional development mechanisms (Yu, 2006). This model was applied in the Greater Beijing Area which consisted of 13 cities to investigate the spatial variation of mechanisms in regional development. The results indicated that the regional development mechanism produced significantly different local characteristics and that spatial non-stationarity played a crucial role in the regional development. This method provides a useful tool for understanding regional development

mechanisms and their spatial variation. Apart from that, GWR has also been used to study the urban sprawl and landscape fragmentation multi-scale relationships (Torres et al., 2016). Scholars employed both the global regression model and GWR together with landscape metrics to explore the mismatches between urban sprawl and landscape fragmentation across scales. Based on the quantification of the urban sprawl and landscape fragmentation spatially, this research performed the global regression model first, then used GWR to explore the spatial variation of this urban sprawl and landscape fragmentation relationship and its scale-dependent behaviour. The results indicated that the relationship between urban sprawl and landscape fragmentation does not prevail. It is rather non-stationary, and scale-dependent. This research provided support for better land conservation and management.

LISA have been applied to measure inter-building distances when studying local urbanisation patterns in Southern Brussels (Caruso et al., 2017). This method first employed the Minimum Spanning Tree (MST) to build a connected urban and suburban graph and utilized this inter-building distance as a direct measure of built land. LISA were then used to calculate this distance to measure urban patterns at a fine scale. Together with LISA, this method is based on fine-scale inter-building distance and measured local scale spatial pattern which supports better planning and management.

The regression method has also been used to study the urban growth pattern at multiple scales (Cheng & Masser, 2003a). Treating the city as a self-organized hierarchical system, this research constructed a logistical regression model to study the determinants of urban growth at different scales. Since studying microscale determinants requires fine resolution of land cover/use data and more social, economic, and other factors, this research only focused on macro and meso levels (the probability of change and the density of change respectively). The results suggested that the urban growth pattern was scale-dependent. This multiple-scale

analysis helped to provide a deeper understanding of urban growth patterns, as well as a better understanding of the temporal process of urban growth. Given increasing study of urban dynamics from a network perspective, network weight matrices have been incorporated into regression models to study the processes driving urban growth. This approach seems to produce more accurate results, is better at revealing underlying process (He et al., 2023), and suggests that the network perspective should be given more attention in future studies.

Since urban dynamics involves a variety of processes at different temporal and spatial scales, research conducted at one single scale, a pure bottom-up, or top-down method cannot fully capture the drivers of urban land change and reveal its complicated growth mechanisms. For instance, regional scale methods usually reveal that macro-scale urban growth is influencing factors such as population, economy, and land market. While the local-level method usually reveals micro-level driving factors such as infrastructure, biophysical factors, and individual or group behaviours (Cheng & Masser, 2003a; Fragkias & Seto, 2009). To incorporate factors at multiple scales scholars developed a coupled system dynamics spatial logit (CSDSL) model which coupled both a local scale logistic regression model and a regional scale system dynamic model (Güneralp et al., 2012). This model not only incorporates both regional and local level factors but also allows interactions between local and regional scales of land change. This model was utilized to analyse and forecast the amount of urban land change and the urban land pattern change. The results indicated that the integrated model performed better at analysing and forecasting both the change in the amount of urban land and its pattern. This method captures spatial complexity and variation of the urban land better. This research indicated that local urban land change is tightly linked with regional-scale processes. However, this method showed its limitation in forecasting isolated urban land change and had a weakness in capturing development projects.

It is argued that these regression models usually have a low degree of explanation and small sample size (Irwin et al., 2009; Luo & Wei, 2009). Even though statistical methods could not fully capture the dynamics of urban land change and the characteristics of the urban growth process, and have weaknesses in modelling urban growth process and multiple scale relationships and feedback, they have still provided much useful information in identifying the determinants of urban growth at different levels. They have illustrated the complexity of urban dynamics, the multi-scale characteristics of urban land change, as well as the multi-scale relationships among urban land change and its driving process (Yu, 2006; Torres et al., 2016; Zhao et al., 2017). Statistical methods also work as a crucial component of dynamic models to provide useful information such as selecting factors, setting parameters, and helping to determine the transition rule in dynamic models.

2.6 Dynamic Model

2.6.1 Complexity in modelling urban systems

Urban systems are a complex, dynamic and hierarchical. They involve a variety of interactions and feedback among different kinds of individuals, groups, and different levels of government at different levels. Their interaction and feedbacks are also cross-scale (Irwin et al., 2009). Individual and group behaviour shapes the city from the bottom up, for instance, individuals' choices of residence location and transportation have an impact on the urban spatial structure, urban form, and intra-city flow. In contrast, the government usually impose urban dynamics from the top down, for example, the government's policy and planning contribute to shaping the urban form and influence the location choice of individuals and groups.

2.6.2 Cellular Automata models

Cellular Automata (CA) Models have been widely used to model complex systems. CA models

are typically cell-based, with the model simulating the change in state of each cell at each time point following a defined transition rule. In a CA model, all cells are assigned with an initial state (Santé et al., 2010). The state of each cell depends on the state of its neighbourhood cells and the transition rules (Syphard et al., 2005). Time is considered discrete. The model updates each cell's state-based transition rule at each time interval and repeats this calculation process iteratively. At each time interval, the model generates the new state of all cells.

CA were first introduced in the late 1940s and further developed by Wolfram who demonstrated that they could be used to model complex natural phenomena (Wolfram, 1984). CA models were initially used in modelling physical processes and natural processes. In 1979, Tobler introduced the CA model in geography and discussed the neighbourhood and transition rules in the CA model. In the discussion, Tobler introduced the first law of geography: "Everything is related to everything else, only near things are more related than distant things" (Tobler, 1979). Based on this theory, the land use at a location is dependent on the land use of its neighbourhood locations, which laid the foundation of the CA model's application in geography. He stated that in geographical space, the state of a cell, e.g., the representation of land use in the model, is the function of the size, shape, orientation of the cell, and other characters of its neighbourhood and transition rules (Tobler, 1979).

Later, with the development of computers and increasing discussion of CA theory, a variety of CA models have been applied in geographical and ecological research, including research on landscape pattern change, land use and land cover change, forest fire diffusion, urban expansion, rural-urban land transition, risk assessment, agricultural or grassland protection, and ecological security. Research has been conducted at both local and regional scales (Fang et al., 2005; Hagoort et al., 2008; Santé et al., 2010; Liu et al., 2013a).

Among this research, the application of the CA model in urban dynamics is the most

extensively studied. CA models have been applied to simulate urban spatial dynamics, and various CA models were built to simulate urban growth. Built based on self-organization, the CA model views urbanisation to be the product of complex, self-organizing dynamic systems (Wolfram, 1984; Chen et al., 2014; Montero et al., 2021; Guan et al., 2023; Lin et al., 2023; Yao et al., 2024). Application of the CA model in urban dynamics is based on the assumption that the previous state of the urban land pixel has an impact on future urban dynamics through the interaction of the land pixel and its surrounding land pixels (Tobler, 1979; Clarke & Gaydos, 1998; Li et al., 2017). In these examples, the spatial resolution of land cells varied from 30m to 1km. The state of the land cell also varied from urban and non-urban to several types of land use. Regarding neighbourhood, researchers usually select the Moore rule, or a radius or a square of a selected number (usually 2 to 9) of cells (Santé et al., 2010). For transition rules, some models use strict transition rules while others use transition rules based on transition potential (growth potential) or probability (Wu, 1998a; de Almeida et al., 2003). Some researchers even use transition rules based on artificial intelligence or fuzzy logic (Wu, 1998b; Li & Yeh, 2002). For example, researchers have integrated Markov chain analysis with the CA model to simulate urban growth under different scenarios and used landscape metrics to analyse and compare simulation under different scenarios (Dietzel, et al., 2005a; Zhang et al., 2011). The integration approach has been proven to be effective in representing, simulating, and forecasting urban evolution over space and time. Some CA models have been used to analyse the influencing factors of urban land change, while others have been used to forecast urban change in the future which is followed by a model validation and a comparison of simulated urban patterns and real urban patterns (Aguilera-Benavente et al., 2014; Fang et al., 2005; Han et al., 2009; Zhang et al., 2023).

It is recognized that urban growth and its spatial-temporal pattern are the results of multiple factors interacting with each other at multiple scales and across scales. Thus, some researchers

stated that as a bottom-up model, CA models emphasise the interaction and state of individual cells at the local scale, and lack adequate information regarding policy, economic, and other influencing factors at higher levels. For instance, urban growth is not only spatially constrained by topology and related policy (e.g., urban planning, natural resources management practice, and preservation zones) but is also impacted by regional economic development and population flows (He et al., 2008; Chen et al., 2014). To overcome this shortcoming and better incorporate influencing factors at multiple scales, some researchers have integrated the CA model with other exogenous models which usually reflect the population, economic, and other factors at a higher level to simulate urban growth patterns (Santé et al., 2010). For example, some researchers utilized an Urban Expansion Dynamic (UED) model which incorporated a CA model based on urban transition potential to simulate urban growth patterns and forecast future expansion in Beijing city (He et al., 2008). This model integrated the spatial distribution of Gross Domestic Product (GDP) and population at the macro-scale and overall urban spatial pattern to provide transition potential. The results indicated that the simulation without transition potential underestimated the agglomeration effect of the urban core area and sub-central urban areas. To better understand and model urban dynamics, researchers have integrated the CA model with the system dynamics model to incorporate urban growth driving forces at macro scales (Chen et al., 2014). The results showed that the integrated model performed well at both simulating urban growth and future expansion forecasting. Through this integrative method, macro-level urban growth driving forces such as population migration, policy, economic growth influence and their interactions are considered in the simulation. Furthermore, the CA model has also been integrated with Multi-Agent Systems (MAS) to simulate the transition of rural settlements to townlands (Liu et al., 2013). This integration facilitated both the behaviour of agents and their interactions with the environment in the simulation. This method builds transition rules based on both the neighbourhood state and

agents' behaviour. The application of this method in three fast-developing towns in China indicated that this simulation method is effective in analysing micro-interactions between the environment and multi-agents and their influence on land conversion.

In the modelling of urban expansion, most CA models utilize transition rules based on the weighted sum which is calculated from logistic regression or fuzzy approaches which allow uncertainty in the simulation. Both of these approaches are based on adjacent urban transition which assumes that the non-urban pixel adjacent to an urban pixel has more probability to transit to an urban pixel. However, previous research has revealed that urban growth occurs at both non-urban pixels adjacent to urban pixels and non-urban pixels away from urban pixels (Liu, et al., 2010a). The former can be classified into two categories: i.e., infilling and edge growth, which refers to growth at a non-urban pixel surrounded by urban pixels and growth at a non-urban pixel at the edge of urban patches respectively. The latter one is outlying growth which refers to urban growth at non-urban pixels adjacent to non-urban pixels. This type of growth usually occurs at a location away from urban patches. In the disperse-coalescence urban growth theory, this is viewed as the early stage of urban growth. Since most CA models are based on neighbourhood transition rules, they have proven their ability to capture urban growth near urban pixels in a variety of research settings (i.e., the infilling and edge growth). However, these neighbourhood transition rules cannot capture outlying growth (Liu et al., 2014). To incorporate urban growth that occurs away from the urban patch, some researchers have used t the SLEUTH urban growth model which selects new urban cells that deviate from the urban patch randomly (Clarke & Gaydos, 1998); some scholars proposed a LEI-CA model which integrates the CA model with LEI landscape index. In the LEI-CA model, scholars utilize different rules to simulate the adjacent growth and outlying growth (Liu et al., 2014). The model was applied in the Dongguan city in China and has successfully simulated urban expansion patterns. The comparison between the LEI-CA model and the logistic-based model

has proven that the LEI-CA model could better simulate outlying urban growth.

However, some scholars have argued that cell-based methods have limitations in simulating future urban land patterns since they cannot adequately reflect the evolution of urban land patches (in the real world, urban growth usually occurs as land parcels increase in size or amount), and especially in China where most urban growth is spontaneous which is not fully reflected in cell-based models (Chen et al., 2014). Thus, patch-based CA models have been proposed to simulate urban growth using patch-based methods (Chen et al., 2014; Yang et al., 2023; Yao et al., 2024). For example, a Patch-Logistic-CA model and a patch-based CA model using the patch-growing algorithm. A patch-based logistic CA model has been used to simulate the urban growth pattern in Guangzhou city and compared with the results of a cell-based CA model. The results indicated that the patch-based CA model worked better for simulating realistic urban growth, and the cell-based CA model could only simulate new urban cells connected to urban cells initially.

Apart from these efforts to advance the technical aspects of CA models in simulation spatial dynamics, some researchers have focused on the central neighbourhood rules and the model fitness of the real world. For instance, research has been concentrated on explicitly revealing the neighbourhood interactions by incorporating the spatial externality in simulating urban dynamics (Hagoort et al., 2008). More specifically, how the land use change in the neighbourhood influences the land use change at one location and how this impact varies with distance. Furthermore, the single neighbourhood rule ignores the intraregional and interregional differences which may influence the simulation results. Based on this consideration, one researcher incorporated spatial externality in a CA simulation and generated a set of neighbourhood rules (Geertman et al., 2007). The regionalized rules and a general rule were then used to simulate urban dynamics. The comparison and validation of the results

indicated that a better-founded neighbourhood rule and regional-specific rules could support the CA model to produce a better-fitted simulation and better practical use.

2.6.3 Agent-Based model

Another dynamic model that has been widely used in modelling urban dynamics is the Agent-Based Model (ABM). Unlike most CA models that are based on cells, ABM models simulate urban dynamics based on agents which could be land parcels, individuals, or groups (Rounsevell et al., 2012; Filatova et al., 2013). In the CA model, most transition rules are spatial based which reflects the interaction and relationship among cells. In ABM, the transition rule is more varied. It could be spatial, such as distance to the city centre, or reflect an individual's decision-making, or interactions between individuals and space (Matthews et al., 2007; Walsh et al., 2013).

ABM's ability to represent adaptive and interactive agents makes it useful in simulating processes which involve multiple agents interacting with each other. For example, in the simulation of land use change, ABM could capture the behaviour of different agents, e.g., individuals, households, companies, and local governments, and their interaction which is usually nonlinear (Crooks et al., 2008; An et al., 2014). In an ABM, the behaviour of agents could be passive or proactive, and the agents may have different types, e.g., individuals, groups, and some influencing environmental or economic factors. These characteristics make ABM widely applied in environmental and geographical research since they can capture the features and dynamics of a variety of related agents. However, this also increases the complexity and uncertainty in simulation due to the complex behaviour of different agents and the nonlinear relationship among those agents (An et al., 2005; Walsh et al., 2008).

In an urban system, urban dynamics and evolution processes involve various agents' decision-

making. The behaviour of one agent could impact other agents' decision-making directly or indirectly. The choice of these agents plays a crucial role in influencing the urban dynamic, and their spatial preferences have an important impact on the resulting spatial pattern. Therefore, as a dynamic model which could simulate the adaptive behaviour of multiple agents, ABM has been widely used in modelling various geographical processes, such as urban growth, population mobility, land use and land cover change, agricultural dynamics, crime spatial dynamics, land or housing market, and epidemics (Filatova et al., 2013; Magliocca et al., 2015; Fu & Hao, 2018). Unlike static models, ABM can be used to simulate urban systems dynamics at the level where the system's components are interacting with each other. Modelling the process could also help to reveal how the decision-making of different agents influences urban dynamics.

Researchers have built ABM to analyse how the heterogeneity of residential preferences affects urban sprawl in southeastern Michigan (Brown & Robinson, 2006). This research utilized social survey data as source data to simulate the behaviour of agents in the ABM. This model has defined two different types of heterogeneity in terms of agent preferences, i.e., variability and categorization which assume agent characters are independent and correlated respectively. The results of this simulation suggested that the urban sprawl could be viewed as a process driven by various preferences to some extent.

Most ABMs have been applied at a local scale since when applied to a large scale, the complexity and diversity of adaptive systems may increase substantially which increases the difficulty and uncertainty to simulate, and large-scale modelling may require large data which limits the simulation. Efforts are still being made to apply ABM at regional scales. Scholars have proposed a conceptual framework to apply ABM at a regional scale to analyse land use and land cover change and apply this model in the Netherlands (Valbuena et al., 2010). This

research defined the internal and external factors that influence the decision-making of agents and linked the environmental factors with agents' actions. Combining individuals, an agent typology, and a probabilistic decision-making method could simplify the variability of decision making which helps to fulfil this simulation at the regional scale. The results suggested that this integrated approach is flexible and generic and could be applied in different regions to simulate the land use and land cover change process.

ABM has been used to study what factors influence the land use decision-making of landowners. For instance, an ABM model was built to study to what extent land suitability, land use preferences, and spatial externalities influence landowners' decision-making (Kelley & Evans, 2011). This model built a household-based spatially explicitly land portfolio ABM and revealed that land suitability and spatial externality played a more critical role in determining land use change than preferences. These results could contribute to support policy management, especially in forest or agricultural management.

ABM has been integrated with other theories or models to simulate the various spatial processes. Researchers have integrated economic models with ABM to build an economic ABM to study the dispersed urban pattern and its influencing factors in the urban fringe area (Magliocca et al., 2014). This method simulated the behaviour of agents based on basic microeconomic decision making which is agent optimisation and market price and allowed more heterogeneity in agents. This simulation could help to reveal the fundamental economic features of the urban dispersal process and its influencing factors.

2.7 Forecasting

Forecasting urban dynamics is an important topic in urban studies since forecasting could provide essential information for supporting urban planning, assessing urban growth impacts,

policy making, and land and resources management. However, due to the inherent complexity of urban systems, the variety of urban systems components, the complicated interaction and feedback among components, as well as the existence of external shocks, the forecasting of urban growth and urban dynamics remains difficult (Syphard et al., 2005; Seto, Güneralp, et al., 2012). The forecasting results may vary due to factors such as data quality and data quantity, the resolution of spatial or temporal data, a different understanding of urban systems, and model fitness (Pijanowski et al., 2002; Seto, Güneralp, et al., 2012). Various methods have been employed to model urban growth and urban dynamics, such as statistical methods, scenario-based modelling, Markov transition matrix, and dynamic simulation methods (Guan et al., 2011; Wang & Li, 2011; Pijanowski et al., 2014). Forecasting related to urban dynamics has mainly focused on urban land change and urban land growth since urban land change is one of the most fundamental changes and most influencing aspects of urban growth (e.g., the amount, location, and spatial pattern of urban growth), urban population growth which put heavy pressure on both urban and environment, urban economic growth, and urban impacts (Li & Yeh, 2002; Herold et al., 2003). With the advance of technology (both the development of remote sensing to provide higher resolution data to obtain more detailed topological and morphological features of spatial objects and the advance of modelling technique) and more in-depth understanding of urban systems, more sophisticated methods have been developed to simulate and forecast urban dynamics.

For example, the CA model has been recognized as a useful tool in both simulating and forecasting urban growth. Researchers have built an Urban Growth Model based on the CA model to forecast the spatial extent of the urban area in southern California and its impact on habitat patterns based on three scenarios from 2000 to 2050 (Syphard et al., 2005). A statistical method was used to test the model's fitness with the comparison of the forecasting results for past years and data for those years. A comparison was also made between the forecasting results

and the results of a GIS overlay model using landscape metrics. The results suggested that all scenarios produced an increasing cluster of urbanized areas separating the main mountain area, and more significant habitat loss would occur in the scenario in which urban growth is located on steeper slopes. The CA model produced a similar future urban growth patch as the GIS overlay method and forecasted more patches and edges than the GIS overlay model. This method performed well at producing spatially explicit results and capturing local interactions and non-linear behaviour in forecasting urban growth. A similar method has also been applied in the Algarve region in Portugal to forecast urban growth in 2020 (Aguilera-Benavente et al., 2014). This research also built three scenarios based on different socioeconomic pathways representing variations in socioeconomic drivers of urban growth. Other developed CA models such as the SLEUTH model have also been applied to forecast the spatial and temporal form of urban growth to 2030 (Wu et al., 2010). The results indicated that the forecasting of the amount and location of the new urban area still needed to be improved. It is also suggested that landscape metrics might be used as constraints in the simulation of urban growth patterns to improve the forecasting results. Apart from that, the Markov model has also been integrated with the CA model to simulate and forecast urban land change. A Markov-CA model was used to analyse the spatial distribution and temporal change of land use and forecast the land use change from 2015 to 2042 (Guan et al., 2011). This method incorporated both natural and socioeconomic data to conduct the simulation. In this method, the transition probability matrix from the Markov method could help to determine the number of transition cells in the CA forecasting.

A basic urban growth forecast could be conducted using the growth rates of population and GDP with a regression model, especially at a large scale to make a comparison and produce overall urban growth trends. Scenarios have been widely used in forecasting representing different growth paths (Wu et al., 2010).

Some other methods have been applied to forecast land change. For instance, a neural network was used to forecast land use change combined with GIS. A Land Transformation Model was built based on these two techniques at both regional and national scales. Utilizing High-Performance Computing (HPC) and big data, the simulation and forecasting of national urban growth was conducted in the US (Pijanowski et al., 2014). This method has provided a useful tool for a large-scale approach to model and forecast land use change.

2.8 Summary

Urban systems are not only the aggregation of subsystems involving various activities such as individual activities, economic, ecological, and political activities but also the result of interactions and feedback between these activities. These activities also take place at different levels which lead to urban systems exhibiting hierarchical behaviour. The urban system is also a spatial entity that exhibits spatial dynamics and spatial heterogeneity at multiple scales. The spatial patterns and characteristics of the urban system reflect the impacts and interactions of local, regional, national, and even global activities. To understand the dynamics of urban systems, both spatially explicit methods and process-based methods are important in providing information on spatial pattern change and the underlying driving processes. For example, geostatistical methods, landscape metrics, and fractal methods may be used to reflect the physical characteristics and processes of urban systems. They characterize the spatial form, spatial distribution, and spatial pattern of urban systems. In contrast, process-based models can reveal the underlying process such as an individuals' behaviour and socioeconomic processes that drive urban growth and changes in urban pattern. Incorporating processes at multiple levels is also essential in urban modelling. The process at a lower level could influence higher-level spatial patterns and higher-level system dynamics.

A variety of approaches have been adopted to study patterns of urbanisation, urban growth

processes, and their relationships. Studies provide lots of empirical examples of the characteristics of urban growth, urban growth process and their driving forces; have advanced theories on urban growth and urban pattern change; and contributed to developing better methods of urban study. For example, research on the single-city growth patterns has revealed urban growth trajectories and provided empirical examples to advance the development of dispersal-growth-coalescence-growth theories. Similarly, research on both the inter- and intra-city levels of urban growth patterns have contributed to a better understanding of urban evolution and underlying processes. However, few researchers have utilized object-based methods to study urban growth. Urban entities are not just an accumulation of urban pixels, but systems, comprising various activities and both internal and external interactions. Object-based methods could be used to represent urban entities directly, allowing for explicit analysis of urban growth patterns and growth processes at the patch level by studying per-object dynamics and at the city level by accumulating object dynamics.

The dynamics of urban entities are not fully considered in the current urban growth literature. Relationships between urban entities during phases of urban growth can only be inferred through the analysis of raster data. Object-based methods could address this gap by explicitly modelling relationships between objects, providing new perspectives on growth patterns and processes. This research will employ an object-based method to study spatial and temporal patterns of urban growth. It will first characterize urban growth by treating urban land as urban objects and explore its advantages compared to existing methods. It will then explicitly analyse urban growth processes at object and city level by building temporal connections between objects, and reflect on the additional insights this approach offers over previous studies. Finally, by treating urban objects as parts of a system that are spatially and temporally connected, the dynamics of urban objects will be predicted at object level.

3 Revealing the scale and synchronicity of rapid urban growth in China in the 2000s in response to reform and regional policies by treating provincial capital cities as sets of spatial objects

Abstract

While urbanization in China has accelerated since the 'Reform and Opening-up' policy of 1978, little is known about the precise trajectories and patterns of per-city urban growth, and the relation of these patterns of growth to national and regional policies. We used a reliable annual time-series dataset of land cover and a logically consistent object-based approach to reveal the scale and patterns of growth from 1992 to 2014 in 13 provincial capital cities, treated as sets of 100s of spatial objects. The results provide precise quantification of the space-time distribution of per-object urban growth between and, importantly, *within* the 13 provincial capitals of China. The urban area of most core cities doubled, and in some cases tripled, over the 23 years. Most surrounding smaller cities also experienced rapid growth, following expansion of the core city. The growth was surprisingly synchronous across most cities, but asynchronous in a few notable others. We demonstrate how this extraordinary synchronous and asynchronous growth was related to the timeline of key national and regional government policies, respectively. The results provide a new evidence base with which to consider urban growth in China, its impacts on society and environment, and future government policy interventions.

3.1 Introduction

China, as one of the largest developing countries in the world, has experienced rapid urbanization, especially since the 'Reform and Opening-up' policy in 1978 (Schneider & Mertes, 2014). According to the Chinese National Statistical Bureau, the level of urbanization (the percentage of the population classed as urban) was 17.9% in 1978, 36% in 2000 and 59.6% in 2018. Since 1978, the high level of rural-to-urban population migration in China has brought around 640 million people into cities. This represents an extraordinary growth rate when placed in the long-run history of civilization. This rapid urban expansion has had significant impacts on the environment, such as increased air pollution, reduced biodiversity and carbon pools, and climatic change (Kalnay & Cai, 2003; Seto, Guneralp, & Hutyra, 2012; Silva et al., 2013; Zhou et al., 2015). It has also influenced social and political systems, for example, linked to social inequality, social welfare and urban governance (Wu, 2002; Liu & Diamond, 2005; Meng, Gregory, & Wang, 2005; Acuto, Parnell, & Seto, 2018; Weiss et al., 2018; Suel et al., 2019). Here, as a crucial step towards better understanding and mitigation of the impacts of rapid urbanization in China, we analyze the temporal trajectories and spatial patterns of urban growth in China, post-Reform, with a focus on a period of rapid transformation in the mid-2000s.

Since 1978, the Reform has had a profound influence on the Chinese economy and society as a whole, with China shifting gradually from a central planning economy towards a market-oriented economy (Lin, 2002). Accompanied by remarkable

economic growth, cities in China have expanded rapidly, and increased productivity in agriculture after the Reform has allowed surplus labor to be re-employed in industrial and service activities in cities (Lin, 2001). Population migration policy has also loosened gradually, leading to a significant increase in urban population (Lin, 2007). Concurrent with this population increase, urban land cover has expanded, particularly because land and urban housing Reforms introduced value to land and boosted the real estate industry, which has accelerated urban expansion (Ding, 2003; Wei & Zhao, 2009; Chen, Guo, & Wu, 2011). Meanwhile, decentralization of decision-making and fiscal power has stimulated regional governments to lease land use rights to acquire more local revenue (Schneider, Chang, & Paulsen, 2015). Furthermore, several types of special development zone have been established, initially in the coastal regions and then across China more widely, to attract more Foreign Direct Investment and boost economic growth (Schneider, Seto, & Webster, 2005). Usually located in suburban areas, these development zones have had an important impact, not only on economic growth, but also on urban form and urban expansion (Schneider, Chang, & Paulsen, 2015). Understanding the combined impacts of these national and regional policies on the temporal and spatial characteristics of urban growth across China is a pre-requisite to building effective urban development strategies for the future and ensuring sustainability.

In 2019, the population of China reached 1.4 billion, nearly one-fifth of the global population. Thus, ongoing urbanization in China is significantly impacting environmental, economic and ecological dynamics, not only within China, but globally.

Since the Reform and Opening-up in 1978, urbanization in China has accelerated (Fei & Zhao, 2019). However, while urban land and the urban population are known to have increased on a massive scale, this growth, including the rates of growth and the timings of growth, have not been quantified adequately per-city. Moreover, the relationships between the rates and timings of growth in different cities have not been explored. Finally, the relationship between growth in specific cities and related national and regional policies has not been established, not least because of the lack of a consistent method of quantifying per-city urban growth over this period.

To address the above gaps, this research used a consistent dataset to quantify urban growth rates for 13 capital cities and their surrounding urban areas across China over 23 years. In this research, the term “city-object” is used for convenience to represent distinct urban spatial objects that may be found inside cities and their surrounding regions. We focused here on the growth characteristics of the different-sized city-objects that can be found inside cities, rather than the growth of a single city. This allowed the evaluation of differences in growth characteristics with distance from the city centre, and differences between the 13 capital city regions across China. We focused specifically on urban transformation in the 2000s as specific policies were in place to support rapid urban growth during this period. By disentangling the growth characteristics of cities by city-object, it was possible to relate this growth to a series of policies at the national and regional level after the Reform, with synchronicity of growth rate being a strong indicator of national policy.

To achieve the above aims, we first extracted the urban class for selected cities from a well-established and high accuracy annual time-series of land cover data spanning 1992 to 2014. We calculated the magnitude of growth and annual growth rate of each of 1000s of city-objects over this period. We then classified the city-objects according to their total area and compared the growth characteristics of these as constituents of the 13 different capital cities across China. We further characterized the growth trajectories of the 13 sets of 100s of city-objects at the regional level and explored how these relate to key national and regional policies.

3.2 Data and Methods

Most previous research on urban change utilized the raster data model and, thus, raster-based approaches to characterize urban spatial patterns (Liu et al., 2010). Raster-based methods can be used to monitor detailed spatial patterns of change in selected areas. While applied much less commonly, object-based methods provide an alternative that have the capability to capture directly and consistently the time-series dynamics of each urban city-object (i.e., urban city patch), where each city is comprised of the *set* of all such city-objects. Hence, we used an object-based approach to analyze city growth characteristics in China, where each city is considered as a set of spatial objects, based on an annual time-series of land cover data. This object-based approach provides a clear and consistent way to measure the time-series growth of each urban city, considered as a set of objects.

3.2.1 Data

Our study used the global land cover data produced under the Climate Change Initiative Land Cover (CCI-LC) project (ESA, 2017). With an annual temporal resolution, and a spatial resolution of 300 m, data were available for 1992 to 2015. The CCI-LC data were acquired through the processing of several remote sensing data sources which included the full archive of Advanced Very-High-resolution Radiometer (AVHRR) (1992-1999), SPOT-Vegetation (1999-2013), Medium Resolution Imaging Spectrometer (MERIS) (2003-2012) and PROBA-Vegetation (2013-2015). The quality of the land cover product was assessed by external parties using independent reference data. The weighted-area overall accuracy of the 2015 map is 71.7%. The urban class has a larger accuracy (86%) (ESA, 2017). These land cover data consist of 37 land cover classes based on six groups corresponding to the United Nations Land Cover Classification System (Di Gregorio, 2005). Change in the urban class from 2014 to 2015 is not included in the CCI-LC dataset. Hence, we used urban land cover data of mainland China from 1992 to 2014 for this research.

3.2.2 Method

Previous research has been conducted mainly on the characteristics and dynamics of urban growth, its drivers, and its impacts on China (Seto & Fragkias, 2005; Yue, et al., 2013; Tong et al., 2017). Of the research that focused on cities, rather than urban area more generally, most focused on a single or several large cities to explore or compare changing spatial form (Luo & Wei, 2009; Zhang et al., 2011; Chen, Gao, & Yuan, 2016).

Studies that compared the growth characteristics of different-sized cities are still limited. When analyzing urban growth, most studies used administrative boundaries to define the study areas (Luo & Wei, 2009). However, in many cases, urban areas have expanded beyond their administrative boundaries, especially in some metropolitan areas where several urban areas have become spatially connected with each other. Thus, for many large cities, the use of administrative boundaries to define the study area results in an underestimation of growth.

To detect urban growth, we employed an object-based method. Each contiguous urban land parcel was treated as one urban city-object, which in almost all cases will map to a named city or town. Importantly, we used the end year (i.e., 2014) as the baseline to monitor the growth of each urban city-object over the 1992-to-2014 period. Each contiguous urban city-object in 2014 was assigned a unique ID. Then, for each year before 2014, all the urban land within the 2014 boundary was labelled with the same ID. This specific approach was carefully designed to bring the specific benefit of being able to track urban city-objects through time.

Figure 3.1 illustrates the measurement of urban land for three time points. The urban land boundary of an urban land parcel (U1 in Fig. 3.1) at time T3 is used as the boundary to measure the total area of urban land in T1 and T2. The total area of urban land within the dashed line at T1 and T2 is calculated as the area of urban land at times T1 and T2, respectively. This measurement means that in previous years, one ID may represent several urban land parcels. That is, they existed as independent urban land parcels and

became connected before 2014, or in 2014, as one contiguous urban area. All the urban land growth that occurred within this boundary is included in the growth statistic for this urban area and treated as one city-object.

We calculated the total area of urban land and the growth rate for each city-object ID from 1992 to 2014. This approach ensured that per-object urban land growth was measured based on spatial extent rather than an administrative boundary. In some cases, the urban area consisted of several spatially interconnected city areas. In such cases, we treated them as one urban object and assigned them the same ID. Thus, this method provides a simple and logically consistent approach to measure how each urban city-object existing at the end of the study period has developed over time.

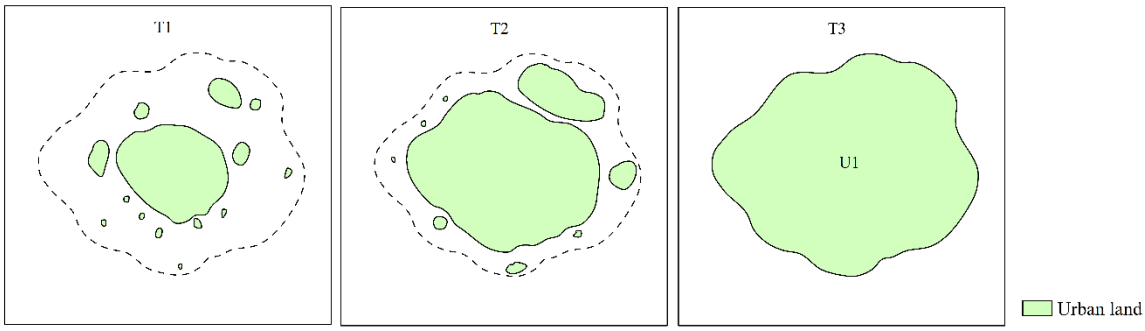

Figure 2.1 Illustration of the method used to measure urban growth over time. From the first time point (T1) to the last (T3).

To examine the variation in urban growth trajectories across China, we sampled 13 cities based on their populations (larger than 1 million in 2014), *per capita* GDP (ranked relatively high in the region), and location (distributed across the country) (Fig. 3.2). They are the national capital city (Beijing) and the provincial capital cities. The capital cities are usually regional centres and, thus, represent regional urban growth. These 13

cities are distributed across the northeastern, eastern, central and western regions of China.

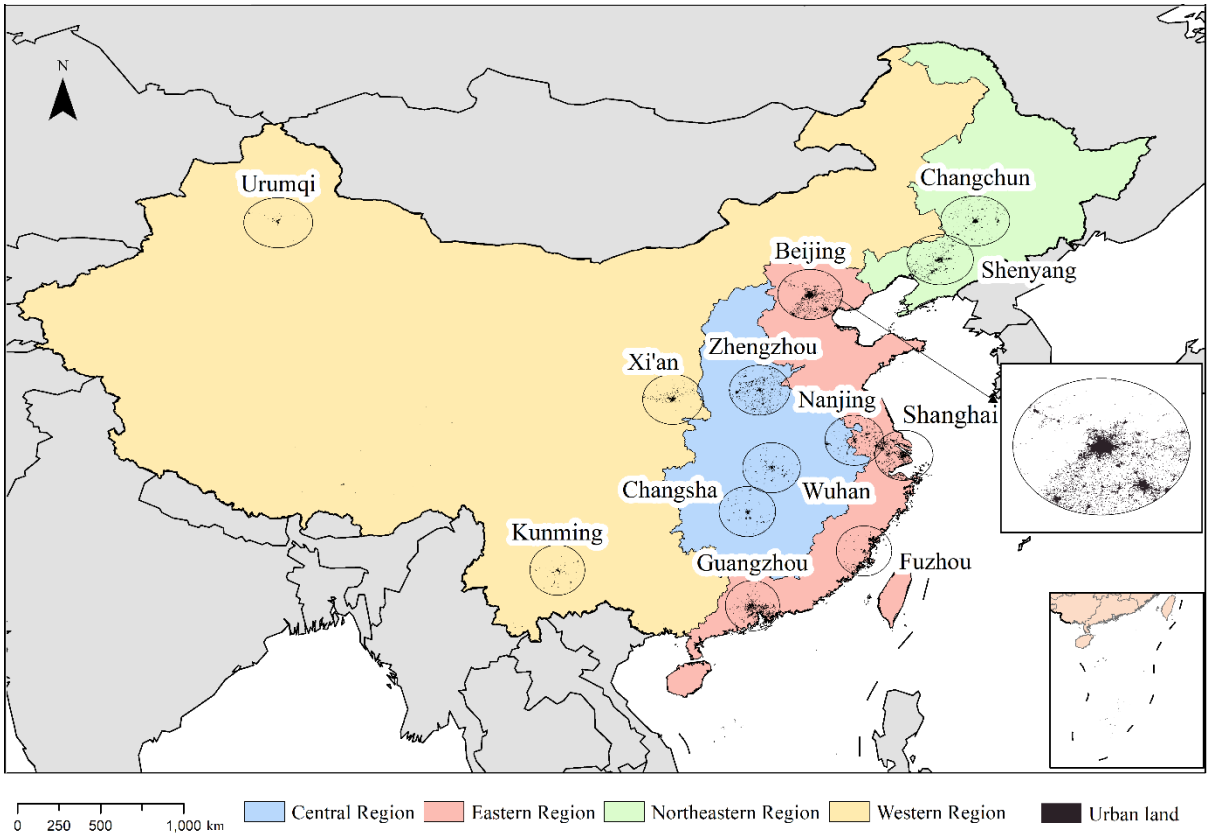

Figure 2.2 The location of the 13 provincial capital cities investigated in this research. The circles reflect each 150 km buffer zone used in the analysis of urban growth.

We used a 150 km buffer zone around each of the 13 provincial capital cities to analyse the growth trajectory of all urban area objects within these buffers. The largest contiguous urban area within each buffer was defined as the core city. An exception occurs when a river runs through the core city and divides it into two parts. We treated these parts as one urban area and used the sum of these two parts as the total urban land of the core city. The core city approach allowed us to link the growth trajectories of major cities with those of surrounding urban area objects and permitted analysis of urban growth characteristics at the regional, rather than the city level.

To characterize the growth trajectories of cities of different sizes, we categorized them according to the total area of urban land cover in 2014. Specifically, we categorized cities into those larger than 100 km^2, and between 50-100 km^2, 20-50 km^2, 10-20 km^2, 5-10 km^2, and 1-5 km^2. Since these categories are based on the area of each city in 2014 only, the same city may previously have belonged to different, smaller categories as its total area is likely to have been smaller in earlier years. For each size category, the average increase in the urban area and the growth rate was calculated for each of the 13 regions from 1992 to 2014.

3.3 Results

3.3.1 Temporal growth trends and regional differences

According to the Ministry of Housing and Urban-rural Development of the People's Republic of China (2016), urban area in China expanded nearly 2.5 times from 40,625 km^2 in 1992 to 139,304 km^2 in 2014. Over the same period the proportion of the population that is urban doubled, from 27% to 54%.

For the 13 regions selected, we found that city-objects in all size groups across China experienced unprecedented growth from 1992 to 2014 (Fig. 3.3). This is most obviously pronounced for the 13 core cities (i.e., core city-objects; black lines in Fig. 3.3). For example, for Guangzhou the core city increased by 2,300 km^2, an increase of almost 1.5 times compared to 1992. For smaller city-objects, the absolute increase in area was smaller. However, considering the initial area of urban land, the growth rate was significant. For example, in the Guangzhou buffer zone, the average area of city-objects

in the 5-10 km^2 category increased from 1.27 km^2 in 1992 to 6.82 km^2 in 2014, which is five times larger than the initial area. Figure 3.3 shows that most city-objects expanded rapidly during the period 2000 to 2005. This phase of intensive urban expansion is seen across all of China, from coastal cities to inland cities of all size categories. From 2005 onwards, most city-objects continued to grow, but at a relatively lower and more stable rate.

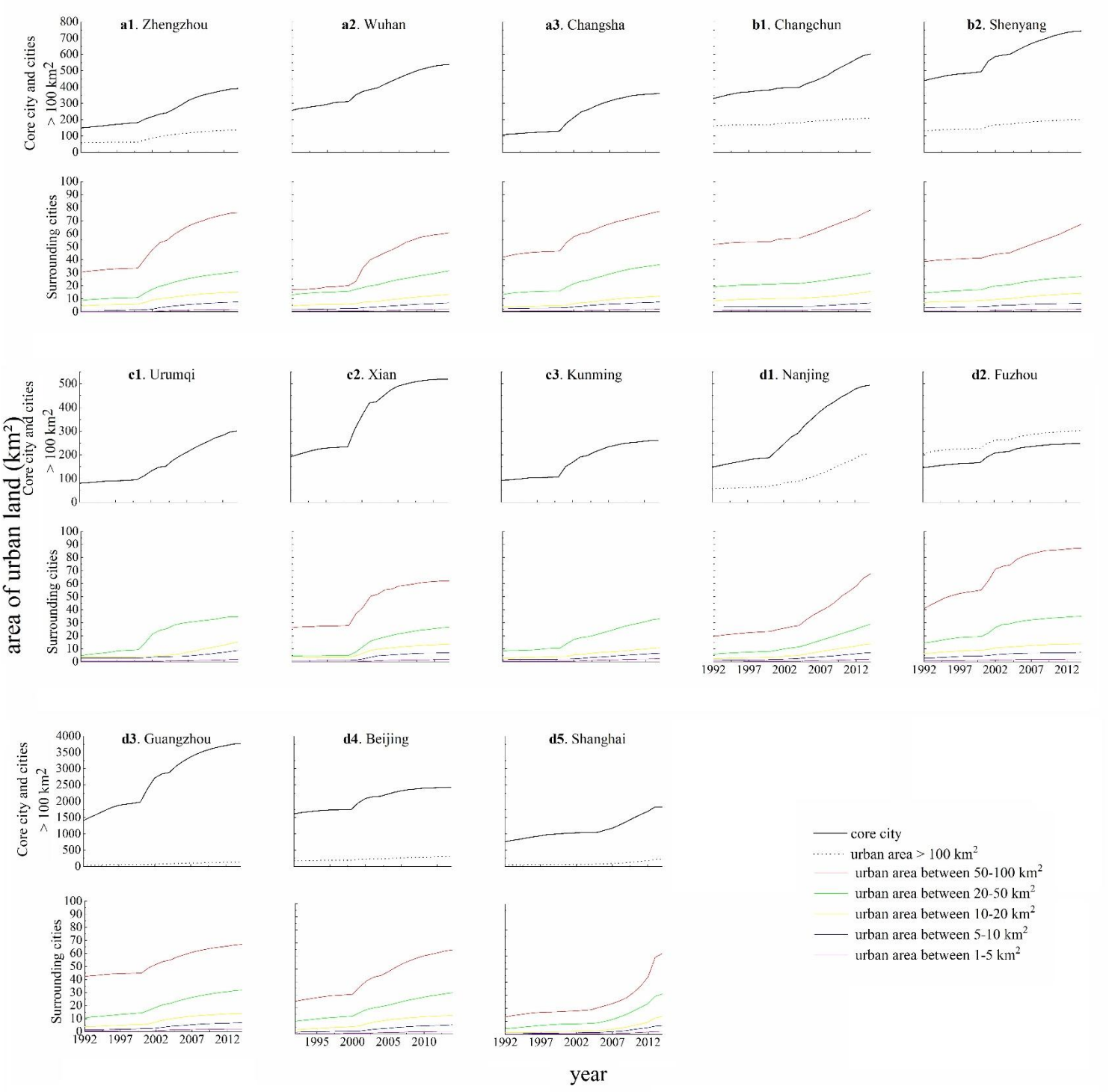

Figure 2.3 Trajectories of the areas of core cities and their surrounding city-objects (based on the average area in each size group).
a1-a3 are cities located in the central region, **b1-b2** are cities located in the northeastern region, **c1-c3** are cities located in the western region, **d1-d5** are cities located in the eastern region.

To explore variation in the growth patterns of cities across China, we first examined the

northeastern region (b1-b2 in Fig. 3.3 and Fig. 3.4; green region in Fig. 3.1). Here, the core city and city-objects with an area of 50-100 km^2 already occupied large areas in the early 1990s. This is likely due to earlier economic development compared to other regions due to abundant natural resources and the role of the northeast as an industrial base in China before the Reform. However, after the Reform, the urban growth rate in the northeastern region fell behind that of other regions. Although the core cities almost doubled in area over this period, in most cases the urban growth rates in the northeastern region were below 10%, even for city-objects of a relatively small area (1-5, 5-10 and 10-20 km^2). This illustrates a major regional difference in the growth trend across China.

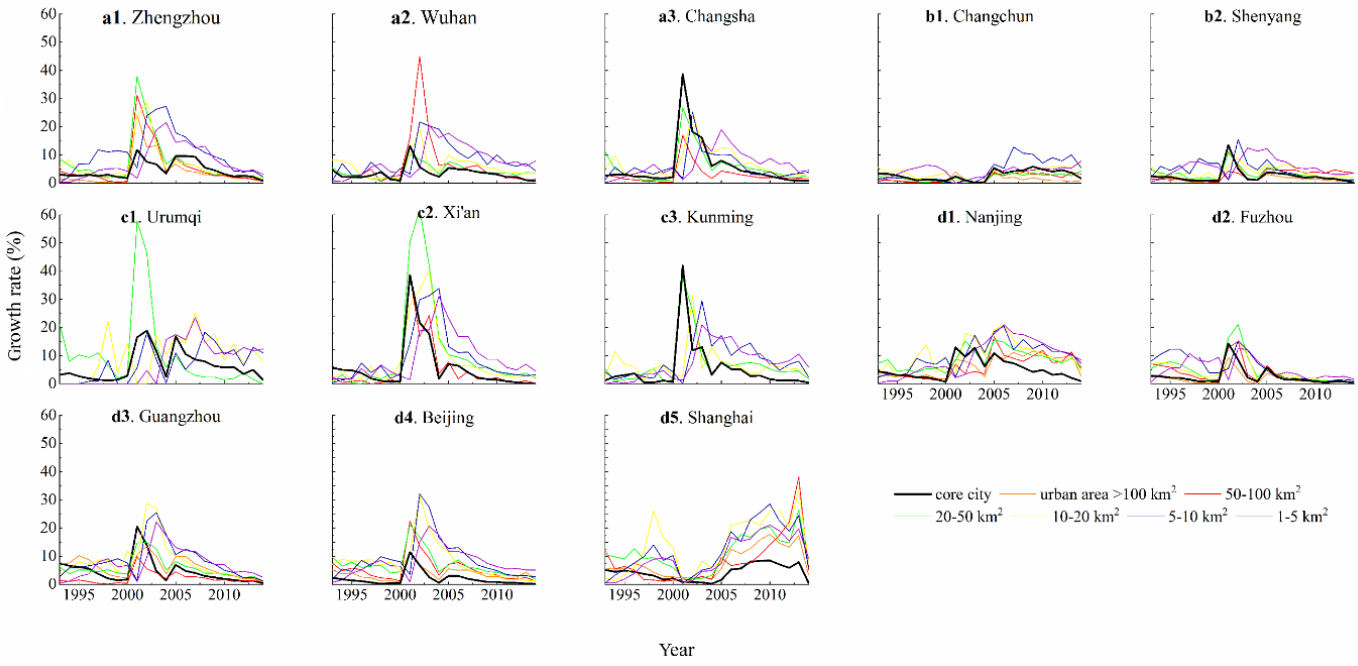

Figure 2.4 Trajectories of the urban growth rates of core cities and their surrounding city-objects (based on the average growth rate in each size group).
a1-a3 are cities located in the central region, **b1-b2** are cities located in the northeastern region, **c1-c3** are cities located in the western region, **d1-d5** are cities located in the eastern region.

Unlike the northeastern region, most city-objects in the western region occupied a

relatively small land area in the early 1990s (c1-c3 in Fig. 3.3; yellow region in Fig. 3.1). The exception is Xi'an, whose core urban area was nearly 200 km^2 in 1992. Urban expansion in this region was not as apparent in the 1990s, but started increasing rapidly after 2000 (c1-c3 in Fig. 3.4). Xi'an and Kunming share a similar growth trend during this period. Their growth rate was greatest in the early 2000s and decreased afterwards. By comparison, Urumqi had two growth peaks around 2001 and 2005 and sustained a higher growth rate compared with Xi'an and Kunming after 2005. Although the western region is considered less developed than other regions of China, this region experienced the highest growth rate after 2000, and this growth was highly synchronized.

In the central region (a1-a3 in Fig. 3.3 and Fig. 3.4; blue region in Fig. 3.1), the core city areas show a similar growth trend to core cities in the western region, with a slight expansion in the 1990s, rapid expansion in the early 2000s, and relatively low and stable growth afterwards. The only exception is Zhengzhou, which grew rapidly around 2006. The core cities of both Wuhan and Zhengzhou had a relatively lower growth rate compared with the western region, but Changsha expanded significantly in the early 2000s, synchronously with growth in the Western region.

Finally, turning to the eastern region (d1-d3 in Fig. 3.3 and Fig. 3.4; red region in Fig. 3.1), we found that urban expansion was unique in the 1990s when most cities grew more rapidly than cities in the other regions of China. For example, the Guangzhou core city area (this core area covers another large city, Shenzhen), increased by 500 km^2 in the 1990s, far beyond the growth of other core cities. In the early 2000s, urban land in

eastern China grew at an unprecedented rate, with the highest level between 2001 to 2005, mirroring the synchronous growth reported above in the western and central regions. The notable exception is Shanghai, which reached its highest growth rate only after 2005 and which maintained a high growth rate afterwards. The core city area of Nanjing maintained rapid growth longer than Fuzhou and Guangzhou whose growth rates decreased to less than 5% per year after 2005. As one of the largest urban agglomerations in China, the Guangzhou core city area increased by nearly 2,500 km^2 over the study period. The national capital Beijing, one of the largest urban agglomerations in China, showed a similar growth trend to that of Guangzhou, but with a lower growth rate for the core city area. Beijing increased by 1000 km^2 over the study period.

Interestingly, most surrounding city-objects followed the growth trend of the core city. A rapid expansion of the core city usually coincided with significant growth of the surrounding city-objects, especially for city-objects of area >100 km^2 and 50-100 km^2. The growth rates of surrounding city-objects in the smaller size categories exhibited similar growth trends to the core city area, but with greater variability. For example, the expansion by 5.31 km^2 (from 9.18 km^2 in 2000 to 14.49 km^2 in 2001) of the urban area surrounding Urumqi represents a growth rate of 57.8%.

A 1-to-2-year time lag in the growth of city-objects in the small-sized category was observed in some cases, which may imply spillover effects from the growth of larger city-objects. Moreover, variation exists in the rate of growth between the core and

surrounding city-objects. Taking the mega-urban agglomeration of Beijing as an example, the growth rate of the surrounding city-objects was greater than the growth rate of the core city. This trend was also observed in the Zhengzhou, Xi'an and Wuhan regions. In contrast, the growth rates of the surrounding city-objects in the Changsha area, for example, were smaller than that of the core city. This difference may imply different regional growth trajectories.

3.3.2 Dynamics of regional urban spatial patterns

Figure 3.5 illustrates the expansion of core cities and the rapid growth of surrounding city-objects in the buffer zone of four selected cities at the regional level across China. All four cities grew rapidly in both the size and number of their constituent city-objects. The expansion of the core city area (black areas in Fig. 3.5) caused some surrounding small urban areas to become part of the core (our method is robust to this occurrence; see Methods). In some cases, as the core city area continued growing some nearby city-objects joined the core creating a mega-agglomeration. For example, in the mega-agglomeration of Guangzhou, the contiguous core city area is composed of Guangzhou and several nearby cities including Foshan, Dongguan and Shenzhen. Physically, these core cities grew into large contiguous urban areas consisting of several different administrative regions extending out towards the 100 km buffer zone.

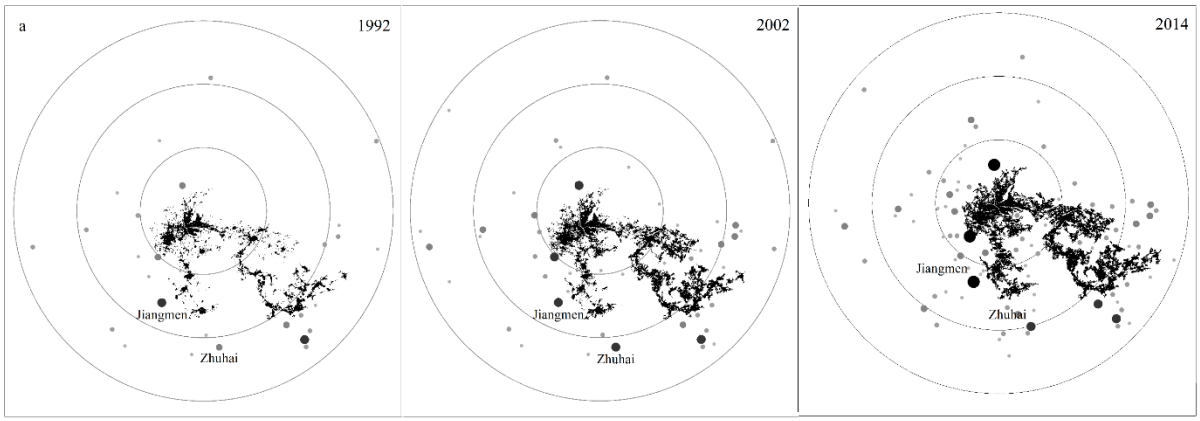
a
1992
2002
2014
Jiangmen
Zhuhai
Jiangmen
Zhuhai
Jiangmen
Zhuhai

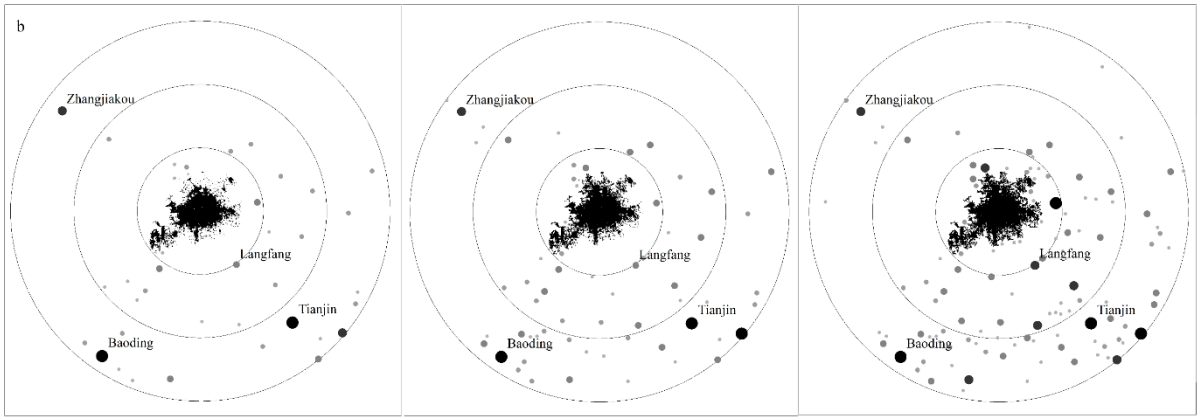
b
Zhangjiakou
Langfang
Tianjin
Baoding
Zhangjiakou
Langfang
Tianjin
Baoding
Zhangjiakou
Langfang
Tianjin
Baoding

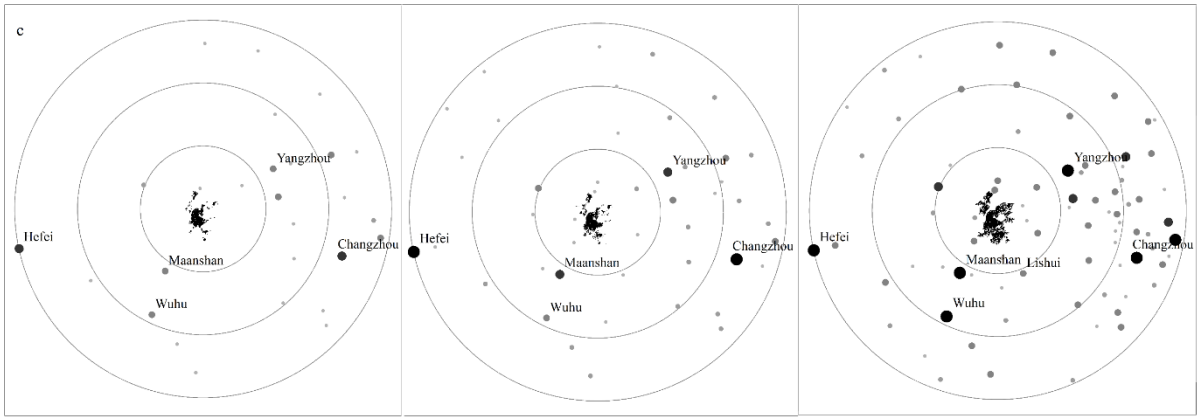
c
Yangzhou
Hefei
Maanshan
Changzhou
Wuhu
Yangzhou
Hefei
Maanshan
Changzhou
Wuhu
Yangzhou
Hefei
Maanshan
Lishui
Changzhou
Wuhu

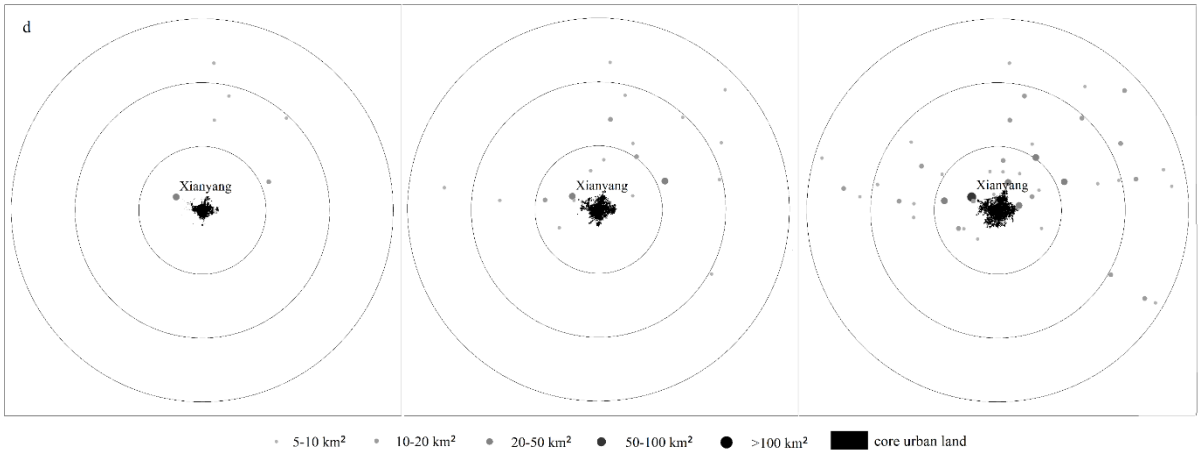

Figure 2.5 Maps of four core cities and the locations of their surrounding city-objects in different area categories in 1992, 2002 and 2014 (from left to right).
The rings are the 50 km, 100 km and 150 km buffers from the urban core. **a**. Guangzhou, **b**. Beijing, **c**. Nanjing, **d**. Xi'an. The black areas represent urban land within the 2014 core city boundary for each year. Urban areas smaller than 5 km^2 are not shown.

Figure 3.5 illustrates that the number of medium and large-sized (>20 km^2) cities increased significantly in the four cases. The maps show how many city-objects grew into the large-sized category (>100 km^2) between 1992 and 2012. For example, in the buffer zone around the Nanjing core area, several city-objects in the large category distributed in the 50-150 km buffer area such as Maanshan, Wuhu and Yangzhou, grew from a medium size (20-50 and 50-100 km^2) (map a in Fig. 3.3). This trend suggests that, at the regional level, the urban spatial pattern transformed from a monocentric to a polycentric form allowing the surrounding cities to serve as subcenters.

3.4 Discussion

This research quantified the unprecedented urban growth that occurred across China between 1992 and 2014. Over the study period, the growth of cities (i.e., city-objects) of all sizes across China was extraordinary. Across the 13 provincial capital city buffer

zones analysed, Guangzhou, Nanjing and Beijing experienced the most extensive urban expansion, increasing by 4,540 km^2, 3,953 km^2 and 2,074 km^2, respectively. Most core city areas doubled or even tripled in size. For Beijing and Guangzhou, the core city area experienced the most extensive growth with more than half of the new urban land occupied by the core area. Cities in western China also witnessed rapid urban growth. Even Urumqi, whose buffer zone experienced the smallest increase in urban land, increased by 490 km^2 in urban area. This extraordinary transformation has potential influence on the environment, food security and eco-systems, especially in the western region, which contains particularly vulnerable ecological systems and environments (Zhou et al., 2015; Xing et al., 2021).

3.4.1 Analysis of the results in a policy context

In urban growth studies different theories have been applied to explore why cities grow over time. It has been suggested that urban growth could be attributed to numerous endogenous and exogenous factors such as economic growth, population growth and proximity to transportation hubs (Eaton & Eckstein, 1997; González-Val, 2023). Additionally, some researchers have modelled urban growth as a function of its inherent attributes such as its initial size (Fragkias & Seto, 2009; Batty, 2023). When considering these two theories together, urban growth should be stable if all other affecting factors are stable. For example, if the endogenous and exogenous factors are consistent, the urban growth trend, which is modelled as a function of them, should also be stable. Therefore, any changes in growth trends could reveal changes in potential influencing

factors. In the present research, the influencing factors are themselves potentially dependent on a background of a series of reform policies. Thus, changes in growth rate might suggest changes in policy since these policies can lead to changes in related influencing factors. For example, the household registration reform allowed large population migration from rural to urban areas which increased the urban population. A series of reforms aiming to boost economic growth increased income in cities which contributed to attracting more people to cities which further led to urban growth. Meanwhile, economic growth itself is also a key factor influencing urban growth. Therefore, identifying the changes in the trends and characteristics of urban growth could help to infer the underlying effects of reform policies.

We observed a remarkably synchronous growth pattern (increase and subsequent decrease in growth rate) in several cities, which suggests a strong link between national policies and urban growth since it implies synchronous changes in the underlying influencing factors. Such national-level synchronous changes are likely to be linked with national-level policy changes given their ability to strongly influence the overall dynamics of the underlying factors. For example, from 2000 to 2004, Zhengzhou, Wuhan, Changsha, Shenyang, Urumqi, Xi'an, Kunming, Nanjing, Fuzhou, Guangzhou and Beijing all witnessed significant urban growth. This synchronous behaviour suggests that national policy is likely to have influenced all these provincial capital cities to respond simultaneously. It provides strong evidence for the efficacy of changes in national policies in driving significant urban growth. In contrast, some provincial capital cities grew asynchronously to this main response, for example, the

asynchronous rapid urban growth from 1992 to 1995 in Guangzhou and the delayed urban growth in Shanghai after 2005. From the perspective of modelling, which treats urban growth as a function of various influencing factors, urban growth can be regarded as the result of decision-making *at different levels* which can affect the dynamics of the underlying factors both nationally and regionally. Specifically, urban growth dynamics may be affected by both top-down behaviours such as national-level reforms and bottom-up behaviours such as regional policies and the decision of local governments and local land use entities (Li & Wu, 2018). At the micro level, individual decision-making may also contribute to the dynamics of growth trends although its magnitude is likely to be marginal compared to national and regional policies. From this perspective, national policies can be regarded as a global effect that influences the underlying factors everywhere in the same way and leads to a spatially consistent changes in the growth trend. At the regional and city levels, local factors could cause deviations spatially from the overall growth trend. Therefore, comparing changes in the growth trends between regions can help to understand the potential effects of regional policies and how they have shaped urban growth in different regions. In our results, the observed asynchronous urban growth patterns, relative to an overall synchronous pattern, suggest a deviation from the overall trend which is likely to reflect the influence of local factors, such as regional-level policies and local conditions.

We further take Guangzhou and Xi'an (Fig. 3.6) as examples to illustrate how national and regional policies affect the growth trends of cities since they are located in different regions in China and have experienced different regional policies. The marketization

and opening in the early stages of Reform (in the 1980s and 1990s), which targeted coastal areas, stimulated growth in the Guangzhou buffer zone in the early 1990s, especially for the core city area including Shenzhen which reached a very high annual growth rate of around 8%. The ensuing reforms in the 1990s, such as the housing reform, tax reform and relaxation of population migration, contributed to maintaining a high growth rate above 5% in the 1990s, especially for cities in the medium and small-sized groups. By contrast, even though development zones were established in the 1990s to attract foreign investment into some inland provincial capital cities such as Xi'an, the urban growth rate remained lower (mostly below 5%) over this period compared to Guangzhou. This is because many small- and medium-sized cities in the coastal provinces benefited from Reform especially in the early stages, while in the west, opening policies and investment were focused on provincial capital cities.

After 2000, the city-objects in both Guangzhou and Xi'an experienced significant growth. City-objects in the small-sized category also witnessed this trend, but reached their largest growth rates one-to-three years later than the core cities. Considering this time lag, the combination of the marketization of the economy including land, housing and tax reforms, increasing openness, and population migration in the 1990s may help to explain the significant urban expansion in the early 2000s. The growth rates of cities in the Xi'an buffer zone are greater than those of cities in the Guangzhou buffer zone, especially those in the large and medium-sized categories. This significant growth may have been accelerated by the West Development Drive, which aimed at boosting development in the western region and narrowing the gap between west and east.

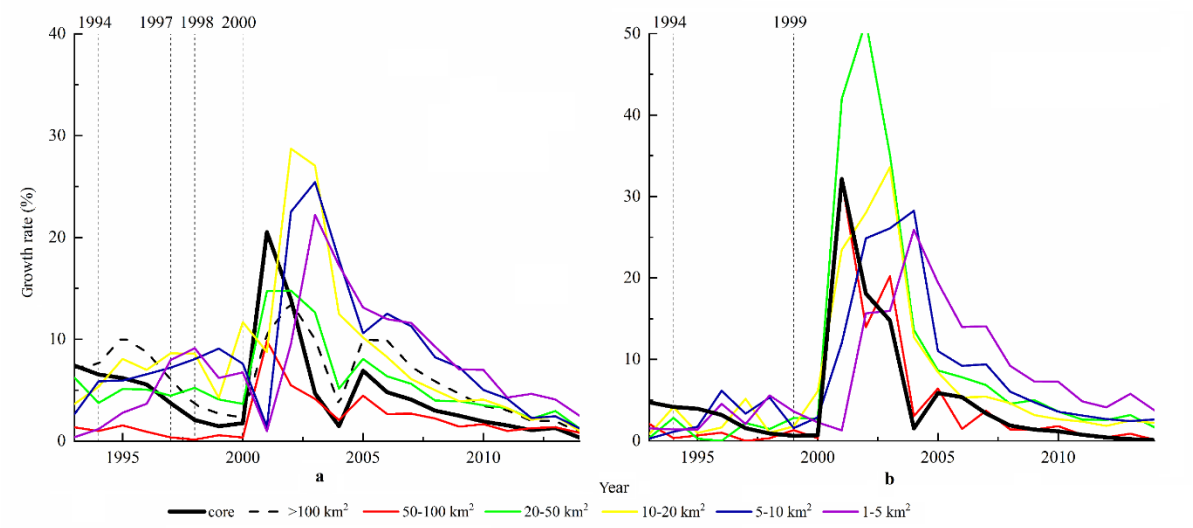

Figure 2.6 Urban growth rates for cities of different sizes in the a. Guangzhou and b. Xi'an regions.

The dashed lines indicate the timing of the relevant reform policies (see Table 3.1).

3.4.2 Analysis of differences by size and across regions

Our results demonstrate how urban form has transformed at the regional level (i.e., within the 150 km buffer zones) as well as at the city level (i.e., each city-object) over the period 1992-to-2014 (Fig. 3.5). This allows us to consider the relationships between core city areas and their surrounding city-objects, and the regional differences in these relationships. First, at the 50 km scale (i.e., within a 50 km buffer), the number of city-objects in the small-sized group increased significantly. City-objects in the small-sized category appeared clustered around the core city. Some city-objects in the small-sized category transitioned into the larger-sized category. This trend was observed in both coastal cities and inland cities. These small city-objects in the 50 km buffer zone were close to the fringe area of the core city. Their growth may be due to spillover effects

from the core city area. The expansion of the core city area is likely to have promoted urbanization in the periphery, for example, through the “diffusion” and “coalescence” processes of urban growth (Dietzel, et al., 2005a). Our approach also contributes to greater understanding of urban growth theory, especially at the regional level. The emerging small-sized city-objects around the core city-object, as seen in figure 3.5, can be regarded as the result of the diffusion of urban growth from the core city-object. Meanwhile, with the expansion of core city-objects, several urban objects finally connected with each other and coalesced to become one large object. This is especially obvious as shown for Guangzhou which gradually became a continuous metropolitan area.

Within the 50-150 km buffers in the eastern region, the growth of city-objects in both the small-sized and large-sized categories was observed. For large city-objects, one should note not only their expansion, but also the increasing number of these city-objects over the period. The city-level polycentric or multi-nucleated spatial pattern has been studied for some large cities in China (Liu & Wang, 2016). Our results identified a transformation towards a morphological polycentric or multi-nucleated pattern at the regional level. However, the degree of polycentricity differs across China. Most eastern regions exhibit a greater degree of polycentricism compared to western regions. For example, in the Nanjing area, even in the 100 km buffer zone, four large cities (Yangzhou, Zhenjiang, Wuhu and Maanshan; represented as city-objects) had a population larger than 1 million in 2014. In Guangzhou, this mega-urban core area consists of several large urban agglomerations, including Guangzhou and Shenzhen,

each with a population of more than 10 million. Nanjing and Guangzhou exhibit different regional spatial patterns. Nanjing is a core city area surrounded by several rapidly growing large city-objects, and Guangzhou is one continuous core city-object consisting of several cities, respectively.

In contrast to the above, the provincial capital cities in western China exhibited a dominant centric pattern at the regional level. For example, in the Xi'an area, the core city is surrounded by only one large city-object (Xianyang) and several small or medium city-objects. Even though the growth of small and medium city-objects in this region is significant, the number of large city-objects in the region is limited. The core city, Xi'an, continues to play a dominant role in the region. The relatively lower levels of integration to global trade, combined with natural and social conditions such as lower population density, population migration to the east, challenging terrain, arid climate and lack of water in some western provinces may constrain the development of small- and medium-sized city-objects. The "Belt and Road" initiative may provide opportunities for the western region to become increasingly integrated into international trade, which could boost its economic growth since the Silk Road Economic Belt in China covers most western provinces. With further development, whether cities in the west will follow the regional urban pattern in the east remains unknown.

3.4.3 Rethinking the object-based method from the results

We proposed an object-based method and the city-object concept to characterise the urban growth trends in China and further explore how the growth relates to reform

policies. Most urban growth studies either focus on overall growth at the single-city level or utilize a raster-based method to study the changing urban growth pattern over time. Some research further developed growth metrics such as urban growth modes (Shi et al., 2012; Li et al., 2013) which classify urban growth into different types based on the spatial relationship between new urban land and existing urban land; and urban sprawl metrics (Sahana et al., 2018) which delineate the spatial pattern of urban expansion. However, these methods lack consistency in measurement. They can characterise the overall growth and map the spatial pattern of urban growth, but changes to urban objects cannot be represented in a consistent manner by these raster-based methods. Urban objects represent directly urban entities allowing consistent measurement and characterization of their dynamics, which is key to studying urban growth. Our object-based method consistently measures the growth trends of city-objects and the results are comparable between different regions and different-sized objects. The similarities and differences in the growth characteristics of city-objects across different regions and for different object sizes suggest how underlying policy changes shaped them and, thus, reveal the underlying effects of reform policies. The approach could be further applied in other regions or countries to explore their urban growth trends.

3.4.4 Future urban development

After the unprecedented urban expansion in the early 2000s, urban growth rates in China remained relatively stable and positive, albeit at lower levels than before. Growth

is likely to continue in the future, since the National Population Development Plan (2016-2030) issued by the State Council, projects that urbanization will reach 70% by 2030, which means that nearly 140 million people will migrate to cities in the next decade. Together with this projected rapid urban growth, China will aim to achieve the United Nations Development Programme Sustainable Development Goals (UNDP SDGs) by 2030. This commitment presents an opportunity to achieve social, economic and environment sustainable development, but also a huge challenge. Significant urban growth places great pressure on environmental, ecological and social systems through increased demand for a variety of natural resources and social welfare provision (Kalnay & Cai, 2003; Alberti, 2005). The supply of more public services such as education, medical services and sports and leisure activities require effective urban planning and governance. Moreover, our defined buffer is essentially at the city-region scale and the results indicate that some synchronous behaviour was observed within the buffer. The given observed and continuing growth in both the core and surrounding cities implies that cooperation amongst cities in planning, economic activities, mitigating pollution, infrastructure construction and social welfare provision is becoming increasingly important. For example, recently, Beijing transferred some of its industry to nearby cities, especially those in Hebei province (Wang et al., 2016), to both mitigate congestion in Beijing and promote development in surrounding areas. At the national level, an initiative in underway that aims to transfer industrial activities, especially labour-intensive industries, to the central and western regions further contributing to achieving sustainable development and reducing the gap between

different regions (Liu & Zhang, 2022). These initiatives require cooperation between local governments.

3.5 Conclusion

We quantified the temporal and spatial patterns of urban growth across China in 13 provincial capital city regions between 1992 and 2014, a period of rapid urban transformation with only a few parallels in human history. To do this we developed a reliable and consistent object-based GIS analysis method that treated each provincial capital city region as a *set* of spatial urban objects including the large core area and 100s of surrounding city-objects. This conceptualization of provincial capital cities as sets of objects allowed, for the first time, a comprehensive analysis of the growth of both the 13 core city areas and their surrounding city-objects. The urban growth rate was found to be exceptionally large for core cities and city-objects of all sizes for all regions across China throughout period from 1992 to 2014, especially from 2000 to 2005. For most core cities, urban land area doubled or even tripled.

A major finding is that the majority of cities and their associated city-objects experienced rapid, *synchronized* growth in the early 2000s, implying the influence of a series of changes to national-level policy. However, some city regions such as Guangzhou and Shanghai developed asynchronously, which implies the additional influence of regional policy or local conditions. A further regional difference was observed in that the western region experienced growth of the dominant core cities with fast-growing small- or medium-sized surrounding city-objects, while cities in the

eastern region transformed into large, polycentric patterns.

The rapid growth trends and morphological changes revealed here pose significant challenges for both coordinated regional urban planning and urban governance. Moreover, attention needs to be given to how to address the environmental and social issues caused by the scale of this growth. These insights may be useful in developing future national and regional level strategies for further urbanization of the major Chinese cities.

4 The Geographical Analysis of Megacities Through Changes in Their Individual Urban Objects

Abstract

This research utilized global coverage, annual, high-quality land cover time-series data to explore the urban growth process in the core area, and in several buffer zones, of Beijing, Guangzhou, Shanghai, and Tokyo. We developed a conceptual model in which growth is characterized at the per-object level by four active growth events: introduction, establishment, dispersal, and coalescence, with a fifth inactivity event, stability. We developed a rule-base which allowed the direct measurement of establishment, dispersal and coalescence from observed inter-annual changes in the urban objects over time. By aggregating the object-level events to the landscape level we showed that these three events generally followed a synchronous temporal trend in terms of magnitude within the core area and within each buffer zone. There was no evidence for a logical sequence of events through time. The identified events dominated alternately over time, although synchronicity in magnitude far outweighed any differences in proportion between them. This points to a single underlying urbanization process: urban growth with a specific dynamic rate. Interestingly, synchronicity was not generally observed between the core and buffer zones. This proposed object-based method provides insights into the underlying urban growth process and could be used to build new urban growth models.

4.1 Introduction

The world has witnessed extraordinary and continuing urban growth since the

beginning of the 20th century, with urbanized areas expanding rapidly and the population increasing at an astonishing rate (Schneider & Woodcock, 2008; Jenerette & Potere, 2010). The acceleration of population has been accompanied by rapid urbanization. Moreover, there were 548 cities with a population of more than 1 million in 2018, and this is projected to rise to 706 cities by 2030 (UNDESA, 2014). Cities provide pivotal habitats for human populations since they promote economic growth and technological innovation (Bettencourt et al., 2007). Moreover, they support the interaction of population, information and capital flow (Krings et al., 2009; Matsumoto et al., 2016).

Rapid urban growth has had a profound influence on the world's ecological and socioeconomic processes from local to global scales (Wilson et al., 2003; Grimm et al., 2008; Zhou et al., 2015; Li et al., 2017; Suel et al., 2019). Urban expansion is linked closely with carbon emissions (Seto, Güneralp, et al., 2012), natural resource consumption (Wu et al., 2010), biochemical cycles, air pollution (Alberti, 2005; Riitters et al., 2016), social injustice and spatial inequality (Lin, 2001; Robinson et al., 2012). Thus, in an era of rapid urbanization it is essential to mitigate the negative impacts of urban growth to achieve sustainable development. Crucial steps to achieving this goal are to: (i) quantify urban growth trajectories and evolving urban spatial patterns and (ii) use this information to infer the urban growth processes that underlie these trends.

There exists a long tradition of geographers characterizing and modelling the dynamics of urban growth. Early theories characterizing urban spatial form such as bid-rent

theory (von Thünen, 1826), central place theory (ChristallerW, 1933) and the sector model laid the foundation for subsequent research. More recently, efforts were made to analyze changing urban forms (Fleischmann et al., 2022) and the relations between the observed dynamics of urban patterns and the underlying processes (Lin, 2001; Kontgis et al., 2014; Li et al., 2017). In the urban form studies, some research focused on defining the urban shape and developing urban shape index (Medda et al., 1998; Wentz, 2000).

To study urban dynamics, some research explored the urban evolution from the city systems perspective, such as analysing the dynamics of metropolitan regions using a set of variables (Salvati & Serra, 2016) and studying change of city size and growth rate distribution incorporating spatial interaction and innovation cycles (Favaro & Pumain, 2011). These studies explored urban growth in the context of urban systems other than focusing on a single city. In order to express the dynamics of urban objects in the urban systems in a spatially explicit way, the concept of urban growth phases was also developed to characterize and model urban growth processes. In particular, the 'early wave' analogue, subsequent 'urban expansion' phases and 'urban cycles' were introduced (Clark, 1951; Blumenfeld, 1954). It was later suggested that the growth of cities could be described as diffusion-limited aggregation and fractal growth processes (Batty, 1986; Makse, Andrade Jr., et al., 1998; Benguigui & Czamanski, 2004). More recently, the process phases of diffusion and coalescence of urban systems were developed and examined based on empirical observations (Dietzel, et al., 2005a). In the context of urban systems, diffusion refers to the spread of an urban area from an origin

or an urban seed area (usually the core urban area) into its surrounding area. In this phase, through the expansion of the urban seed area, the city spreads to new land. With continued diffusion of an urban area, some urban areas become connected (i.e., the coalescence phase).

A major branch of the quantitative study of urban spatial dynamics in the last two decades has been the application of landscape metrics to characterize urban dynamic patterns and, thus, infer urban growth processes (Luck & Wu, 2002; Angel et al., 2012; Jiao et al., 2015). For example, a series of landscape metrics were used to explore and project the urban growth dynamics in California's central valley (Dietzel, et al., 2005a). The analysis confirmed the diffusion and coalescence phases and reported cycles of these two phases with changing spatial extents. Similar wave-like diffusion and coalescence phases were demonstrated in the Houston metropolitan area and Dubai with the application of a series of landscape metrics (Nassar et al., 2014). The results suggested that oscillation between the diffusion and coalescence phases could occur over a short period. In contrast, when applied in Phoenix and Las Vegas, only one landscape metric exhibited a wave-like pattern; others metrics revealed a monotonic behaviour (Wu et al., 2011). A diffusion-coalescence phase was also observed around Guangzhou using metrics calculated within buffer zones (Liu et al., 2012). Jenerette analysed 120 cities around the world and argued that diffusion and coalescence were not two alternative processes of urban growth, but that cities were on a continuum of diffusion and coalescence (Jenerette & Potere, 2010). These processes were also observed in cities in the Yangtze river delta region in China (Li et al., 2013). These

empirical observations provide valuable information and evidence which can be compared against hypothesized processes and theories to improve the modelling, and increase our understanding, of the dynamics of urban systems.

In this research, we replace the above concept of growth phases with four definite, measurable growth *events*: introduction, establishment, dispersal and coalescence, borrowing from ecological theory (Turner and Gardner, 2001). Importantly, these events are attributable at the individual object level and, thus, are measurable directly once each individual city is represented appropriately as a geospatial object.

We define *introduction* as occurring when an urban object is first introduced into the landscape. From a geographical analysis point of view this equates to a nonurban pixel (or contiguous pixels) changing into an urban pixel (or contiguous pixels) that is identifiable as a separate urban object (i.e., it is bounded spatially by non-urban pixels). After the introduction of an urban seed into the landscape, the urban area expands causing an *establishment* event. From a spatial analysis point of view establishment equates to an urban object in the present year being larger in spatial area than itself in the previous year. With continued growth of the urban area, a *dispersal* event may eventually occur introducing a new, separate urban seed as a function of the nearby established or establishing city or cities. This is equivalent to introduction, but through proximity to neighbouring urban objects, dispersal can be inferred. Such inference is not undertaken here. Rather, due to the proximity of the core mega-city area in each region, all cases of introduction and dispersal are classed together as dispersal. With

continued urban growth, some urban areas may become connected and merge to form one contiguous urban object in a *coalescence* event. From a geographical analysis point of view this event is identified by the appearance of more objects with the same ID in the previous year than the single object in the present year. This identification is only possible by allocating the object ID in the final year and working backwards. Viewed from a graph perspective, the final year single urban object has historical roots that bifurcate going backwards through time. Note that since introduction represents the initiation of the core city and most existing cities will currently be experiencing the establishment, dispersal or coalescence events, we focus mainly on analysing urban growth based on these three measurable "ecological" events. The null event is stability (i.e., unchanged). These four events and the null event cover the full space of possibility, and no other events are possible at the per-object level. From a formal perspective this means that measurement of these events characterizes the system fully in the two dimensions of existence (introduction and dispersal, with coalescence as loss; null = stability) and growth (introduction, dispersal, establishment, coalescence; null = stability).

Direct analysis of urban growth process phases at the object-level is limited. Most studies were conducted at the landscape level using landscape metrics. The landscape metrics approach measures urban pattern change through time and, thus, attempts to infer the underlying urban growth events and processes indirectly. However, since the relations of processes and patterns is complicated, different growth events could lead to similar urban patterns. Thus, a direct measure of dynamics of urban growth events

as proposed here is advantageous for studying urban growth process.

Empirical observations of megacities could potentially increase our understanding of urban growth processes and contribute to advancing urban growth theories. However, previous research has focused mainly on a single metropolitan area (Xu et al., 2007; Yu & Ng, 2007; Li et al., 2013) and only a few studies have analysed the urban growth dynamics of megacities. Megacities not only cover a larger land surface area, but also consume more energy and materials and have a greater influence on surrounding urban and rural areas (Gurjar et al., 2008, Baklanov et al., 2016). In the context of the hypothesis of urban growth phases, the character of megacities and the regional behaviour of urban growth processes remain to be studied. Furthermore, inter-city comparisons, and especially cross-country comparisons, of urban growth processes in megacities, are rare. Thus, in this research, we selected and studied four megacities in East and Southeast Asia: Beijing, Shanghai, Guangzhou and Tokyo, using a carefully designed, object-based methodology applied to a high quality, coarse spatial resolution, standardized remotely sensed urban land cover dataset from 1992 to 2018.

A key issue quantitative geography, and particularly when studying the evolution of urban systems is scale. This is especially relevant where the dynamics of urban patterns are analysed to explore the potential urban growth process. First, urban patterns are scale-dependent (Li et al., 2013; Wu et al., 2014). Urban patterns exhibit different characteristics at different spatial scales. Second, processes influence the dynamics of urban patterns at varying degrees at different spatial scales (Sexton et al., 2013). For

example, a process that influences street-level patterns significantly may play only a small role in influencing regional urban patterns. Thus, characterizing urban growth patterns at different levels is essential for understanding urban growth processes. At the per-urban object level, urban growth will manifest as one type of growth event at a time and follow a *sequence* of such events. However, when analysing at the population level, based on the set of growth events of all urban objects at a given time, the whole region may experience several events simultaneously, with one dominant event type. Therefore, we analysed urban growth patterns at both the per-object and population levels to provide a deeper understanding of the evolution of urban systems.

In urban growth theory, it is also suggested that growth phases are scale-dependent (Dietzel, et al., 2005a). It is hypothesized that when urban areas join together (i.e., the coalescence phase), the new urban form becomes a new urban seed area at larger scales (Dietzel, et al., 2005b). In the next phase, the new urban seed area expands (i.e., establishment) and the dispersal of urban land occurs at a coarser scale because the new urban growth process operates at the coarser scale. This suggests that the urban seed area and its surrounding areas may exhibit different growth characteristics. Thus, to increase understanding of the growth characteristics of megacity *regions*, we analysed the development of urban patterns across large regions around four core cities, specifically the core area and three buffer rings (zones), and linked the evolving patterns of objects and events to the underlying urban growth process, as introduced above.

The main contributions of this research were, thus:

1. A rigorous object-based GIS methodology was introduced for defining and analysing individual urban objects through time.
2. Borrowing from ecology, a new paradigm was suggested for analysing urban growth via the time-series of change events occurring per-object (the change events are: introduction, establishment, dispersal, coalescence, stability).
3. Based on this methodology a very large time-series database of urban objects and their events was created for each of four mega-city regions (Beijing, Pearl River Delta, Shanghai and Tokyo).
4. From this database, for the first time, it was possible to analyse the time-series of individual urban object events at the population level for each mega-city region and (a) compare between each mega-city region and analyse their differences and (b) compare between each mega-city core area and three buffer zones.
5. The time-series analysis included for each mega-city and buffer zone: (a) a count of each object-level change event type, (b) a count, at the population-level, of dispersal, loss and net change, and (c) the relative proportion of each event type.
6. We used the evidence from our proposed per-object methodology and the results to suggest a re-evaluation of the key geographical theories of urban growth.

4.2 Study area, data, and method

4.2.1 Study area

We selected four megacities in east Asia selected for this research (Beijing, Guangzhou, Shanghai and Tokyo) (Fig. 4.1). They are all identified as megacities by the United Nations. This selection covers megacities in both developed and developing countries and, thus, potentially provides suitable examples with which to examine urban growth in cities at different stages of development. In Guangzhou and Tokyo, the core urban area is connected to several surrounding cities. In this case, we treated the continuous urban core area as the core urban patch. Thus, in Guangzhou, the core area is the urban agglomeration in the Pearl River Delta region, and we use the term Pearl River Delta to refer to this study area in the following analysis.

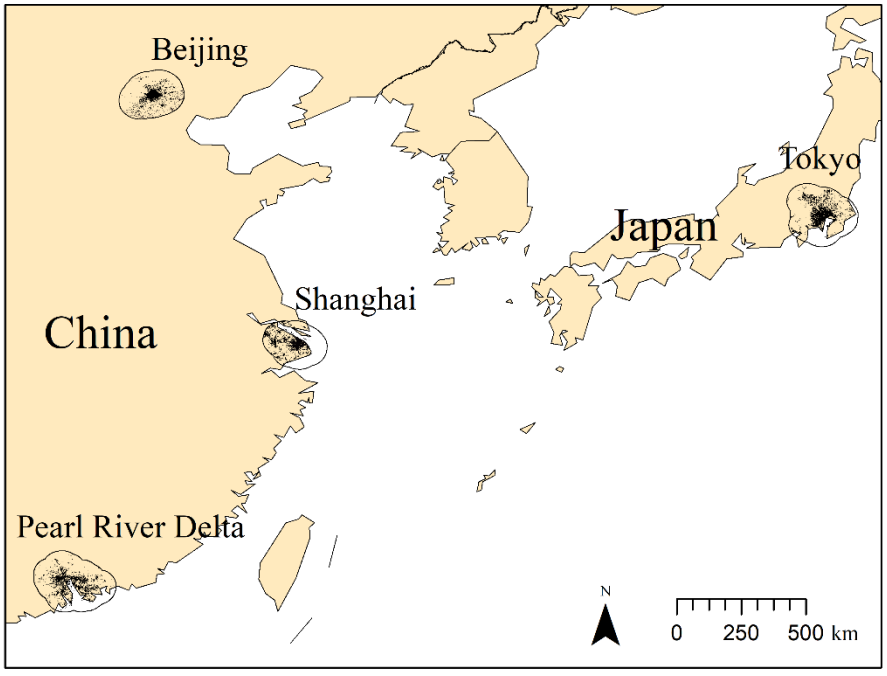

Figure 4.1 Location of the four megacities investigated in this research.
The 60 km buffer zone around each core urban area was used to define the surrounding region within which to analyse urban growth characteristics. Urban land in 2018 is shown in black in the four study areas.

4.2.2 Data

We used global land cover data produced by the European Space Agency (ESA) Climate Change Initiative Land Cover (CCI-LC) project, available at http://maps.elie.ucl.ac.be/CCI/viewer/index.php. With an annual temporal resolution and spatial resolution of 300 m, data are available from 1992 to 2018. The CCI-LC dataset was then obtained through back- and up-dated change detection using a combination of several remote sensing data sources including the full archive of Advanced Very-High-resolution Radiometer (AVHRR) (1992-1999), SPOT-Vegetation (1998-2012), Medium Resolution Imaging Spectrometer (MERIS) (2003-2012), PROBA-Vegetation and Sentinel-3 OLCI time-series (2013-2018). These land cover data consist of 37 land cover classes based on six groups corresponding to the United Nations Land Cover Classification System (Di Gregorio, 2005). The quality of the land cover product was assessed by external parties using independent reference data. The weighted-area overall accuracy of the urban class in the 2015 map was reported as 86%, which is very high for a global product.

4.2.3 Methods

We first extracted the urban land in the raster data model from the ESA dataset for 1992 to 2018. All contiguous urban pixels were combined into urban 'objects', thus, invoking the object-based model. The contiguous urban land areas in the core centre of Beijing, Pearl River Delta, Shanghai and Tokyo in 2018 were defined as the core extents for each city. Since each city itself may extend beyond its administrative boundary and

become physically contiguous with its surrounding urban areas, our approach treated these connected parts as one urban object and, in this case, as the core urban area. A series of 20, 40 and 60 km buffer rings around the core extent was generated for each city to facilitate analysis of the surrounding cities in addition to the core city. The core extent and each buffer ring were then intersected with the urban land objects from 1992 to 2018.

Per-object level analysis

In contrast to quantitative approaches based on landscape metrics, which are generally spatially aggregate representations at the population level, we propose a methodology to infer directly the urban growth event occurring for each urban object and for each annual time increment. Using the GIS, we assigned each urban object a unique ID annually from 1993 to 2018. A key modeling decision from a geographical analysis perspective is that given an urban patch $P_{i,j}$ in year i, all the urban patches $P_{i\text{-}1,k}$ within patch $P_{i,j}$'s boundary in year $i-1$ were labelled with the same ID of $P_{i,j}$. This process was repeated for all urban objects going backwards annually in time from 2017 to 1992. Given this coding scheme, when comparing the IDs of urban patches in year $i-1$ and year i and their corresponding area, the following logic holds true. First, for Coalescence; all IDs that exist repeatedly in year $i-1$, identify separate urban objects that coalesce from year $i-1$ to year i, becoming one urban object. Second, for Establishment; all IDs appearing uniquely at time $i-1$ and with a larger urban land area in year i than in year $i-1$ are urban objects that are subject to an establishment event

as their area grows. Third, for Introduction (and Dispersal); all IDs that appear for the first time in year *i*, and which did not exist previously, represent either the introduction or dispersal events since they are new urban objects in the landscape. Dispersal implies that the introduction is related to a seeding object and, thus, dispersal is used here where the core city object dominates the landscape.

Fig. 4.2 illustrates the above system of coding and its importance for characterising urban growth dynamics. The following processes are illustrated. First, Urban object labelled with ID 1, in year 0 (i.e., $P_{0,1}$), appeared only once in year 0 and its area grew from year 0 (i.e., $i = 0$) to year 1 (i.e., $i = 1$), representing the process of *establishment*. Second, urban objects labelled with ID 2 (i.e., $P_{0,2}$) appeared twice in year 0 indicating that these two urban objects eventually *coalesced* to one urban object ($P_{1,2}$) in year 1. Third, urban objects labelled with ID 3 ($P_{1,3}$) and 4 ($P_{1,4}$) appeared only in year 1, indicating that they were *introduced* (or *dispersed*) into the landscape and did not exist in the previous year. Finally, urban object labeled with ID 5 (i.e., $P_{0,5}$) appeared only once in year 0 and its area remained the same in year 1 ($\text{Area}(P_{0,5}) = \text{Area}(P_{1,5})$), indicating that this urban object was *stable* (i.e., dormant or established).

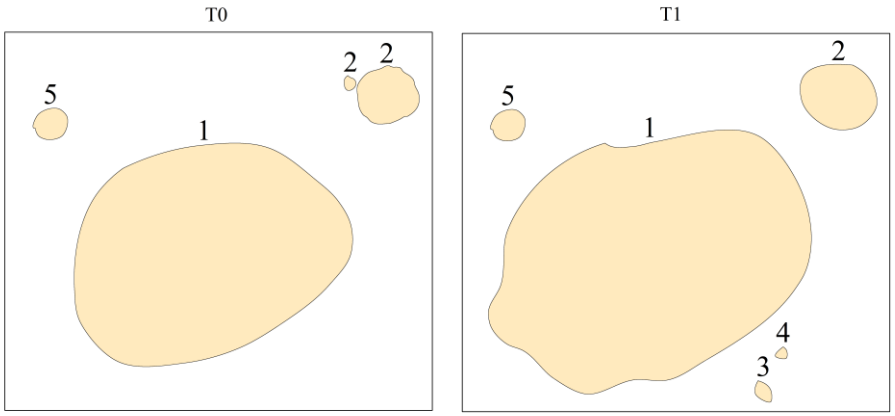

Figure 4.2 Illustration of measurement of urban growth events from time 0 (T0) to time 1 (T1).
1=establishment; 2=coalescence; 3 and 4= introduction; 5=stable. Linked IDs are necessary to support measurement of these events.

It should be noted that in some cases, when the newly introduced urban object is close to another large urban object, it could be labelled as coalescence (not establishment) in the next year. This is because under rapid urban growth, first, the one-year time period may be too long for the establishment event to be observed and, second, our object data are generated from raster data and in some cases, the pixel size may be too coarse to detect the establishment event.

The above coding system applied within a GIS allowed the inference and attribution of growth events to the inter-annual changes observed, per-object, from 1992 to 2018. This process is fulfilled using ArcGIS. It is important to understand that once the time-series graph of objects is established within the GIS, the above coding system is automatic and comprehensive. It is automatic because each event type is identified directly by comparing the present state of an object to its previous state, such that per-object events arise with zero ambiguity in the differences between years. No thresholds are needed; the events either happen or they do not. It is comprehensive because the set of all four

events (and the null-event) cover the space of possibility completely. No other alternatives are possible. These are key advantages of the approach.

After acquiring the growth event of each urban object annually over the study period, we further calculated the total number of objects that experienced the establishment, coalescence and dispersal events, as well as the total number of stable objects, inter-annually from 1992 to 2018, in the core area and buffer zones of the four megacities. Through this per-object calculation, it was possible to analyse inter-annual urban growth events at the population level. At the population level, the spatial and temporal dynamics of the dominant growth event(s) were analysed, thus, allowing inferences on the underlying urban growth process. Fig. 4.3 illustrates the differences between measuring urban growth events at the per object level (in which case a finite set of possible events exists) and at the population level (where distributions are produced across all events).

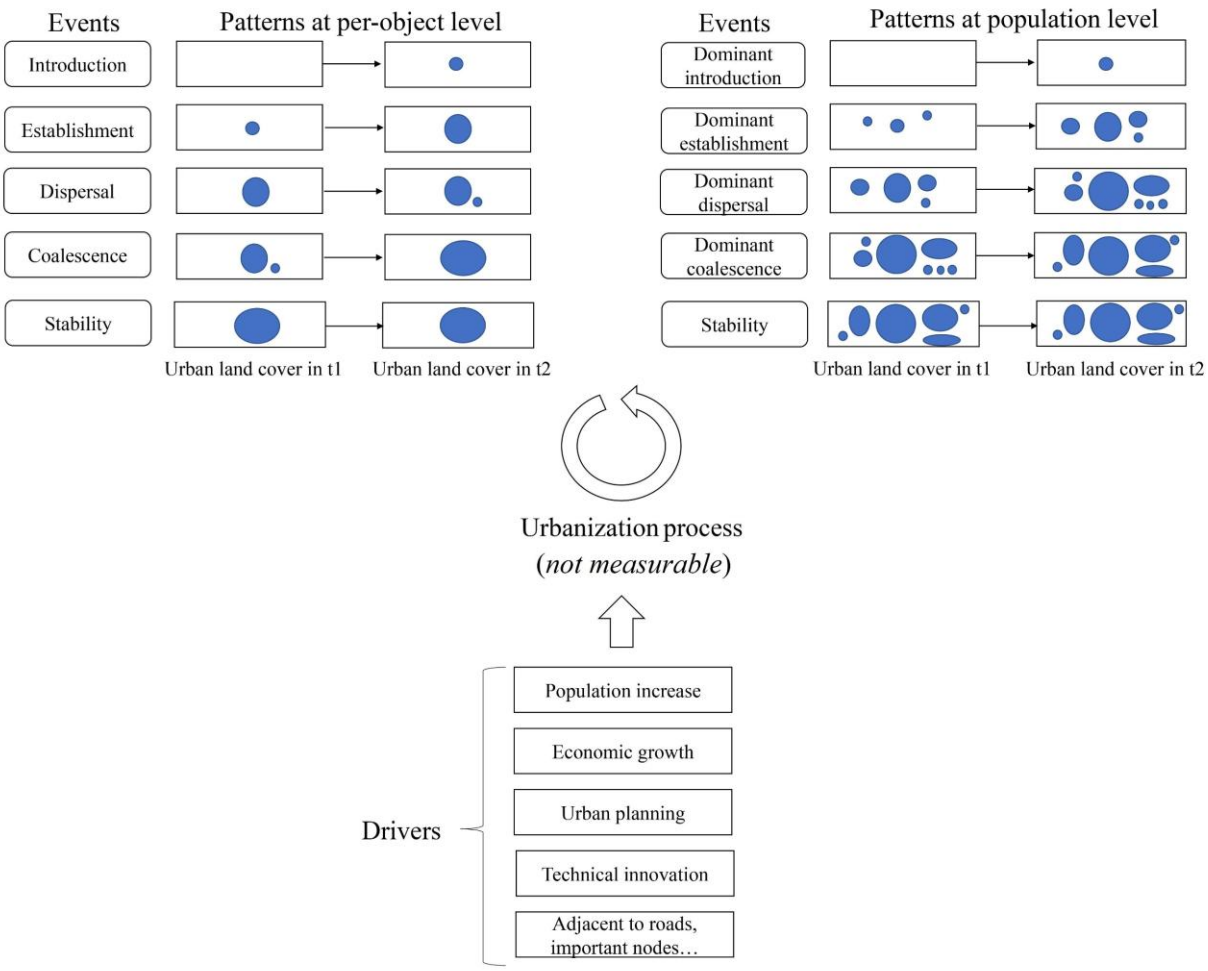

Figure 4.3 Illustration of (left) urban growth events at the per-object level and (right) dominant events at the population level during the urbanization process.
The blue ovals represent urban objects.

4.3 Results

4.3.1 General urban growth trends

We examined the overall urban growth for each megacity over the 26-year period. All four megacity regions experienced rapid urban growth (Fig. 4.4). Fig. 4.4 shows the extent of growth by mapping urban extent in 1992 and 2018. The core area is shown in black, while other urban objects are shown in grey. The three buffer rings are

superimposed over each area. It is surprising to see the enormous urban growth in Tokyo over this period since the urban population in Japan has maintained a relatively constant level since the 1970s. Tokyo's core urban land area increased by around 1000 km^2 over this period.

The three megacities in China all witnessed tremendous urban growth in both the core area and buffer areas. Their core areas almost doubled in size. In terms of urban growth in the buffer rings, the 20 km buffer ring included a larger area of urban land over time, except for Shanghai where the 60 km buffer covered the largest urban land area. The core city in the Pearl River Delta region maintained rapid urban growth over time, while the core area in Beijing experienced its most rapid urban growth from 1997 to 2008 and the core area in Shanghai grew most rapidly from 2007 to 2018.

Urban growth in the buffer rings for Shanghai and Tokyo followed the growth trends of their core areas. In Beijing, the urban land in the buffer rings witnessed rapid growth since 2002. In the Pearl River Delta, urban growth in the 40 and 60 km buffer rings showed a slower growth trend compared to the same buffer rings around Beijing and Shanghai.

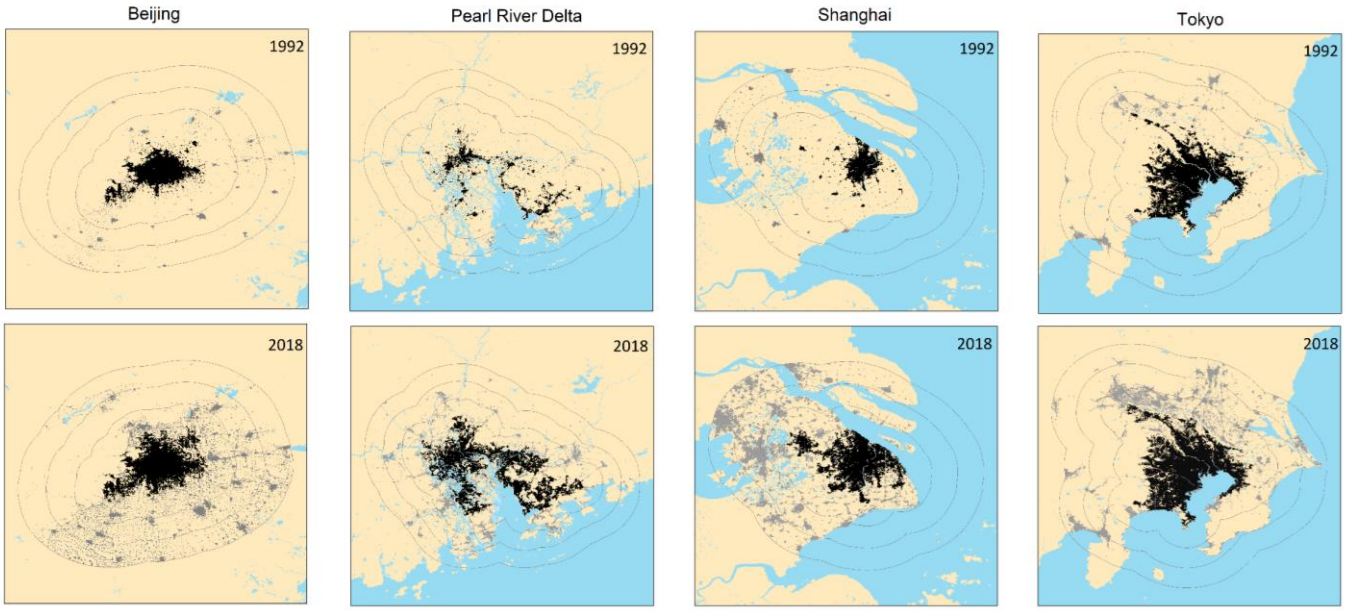

Figure 4.4 Maps of urban extent for the four megacity regions in 1992 and 2018. The core urban area is shown in black and peripheral urban areas in the buffer rings are shown in grey.

4.3.2 Urban events and inference on the growth process

Using the rule-set established above, and specifically because we adopted an object-based methodology, we were able to measure *directly* the prevalence of the three growth events in each of the core and buffer zones through time. This was achieved by applying the rule-set to each urban object annually, such as to infer growth events through time at the per-object level. Fig. 4.5 shows the number of objects allocated to each event over the 26-year period.

The results show that all core and buffer zones for the four megacities experienced all three events almost consistently over time. Fig. 4.5 captures the detail of the dynamics of the urban growth events over time. The magnitude (i.e., total number) of these urban growth events fluctuated over time. However, in Shanghai and Tokyo, general

synchrony is observed among the three growth events. In Shanghai, the total number of urban objects experiencing the growth events grew significantly from 2004 and 2005, reaching a peak around 2010, and then decreased afterwards and increased again in 2017. This trend is observed in the core urban area and buffer zones, suggesting a synchronous urban growth process in the region over time. It should also be noticed that the peak level of coalescence was reached roughly two or three years later than the peak level of dispersal and establishment. This implies that, at the landscape level, a mass coalescence of urban objects occurred after the intensive introduction and expansion of urban objects. In Tokyo, the overall trend in growth events is similar in three buffer zones, with a high prevalence of the three events around the late 2000s and early 2010s. This trend is not observed in the core urban area where the magnitude of dispersal and establishment in the late 2000s and early 2010s was similar to the early 1990s.

In Beijing, the total number of urban objects involved in these events was smaller compared to the other three core urban areas, with a peak level around 2003. In the buffer zones, the total number of dispersal and establishment events showed a general increasing trend before 2016 and a high level in the 2010s. Unlike Shanghai and Tokyo, the total number of coalescence events was smaller compared to the other two events. This suggests that introduction and establishment are the main urban growth events, outstripping coalescence.

In the Pearl River Delta region, the core urban area showed a relatively greater number

of urban objects experiencing dispersal and establishment in the 1990s compared to the other three megacities. The three events exhibited a peak around 2003 and decreased afterwards. This trend is also observed in the 20 and 40 km buffer zones, while in the 60 km buffer zones, there is greater fluctuation. This suggests that the urban growth process is complex and dynamic here. Local drivers could influence the growth process and lead to differences in the growth events.

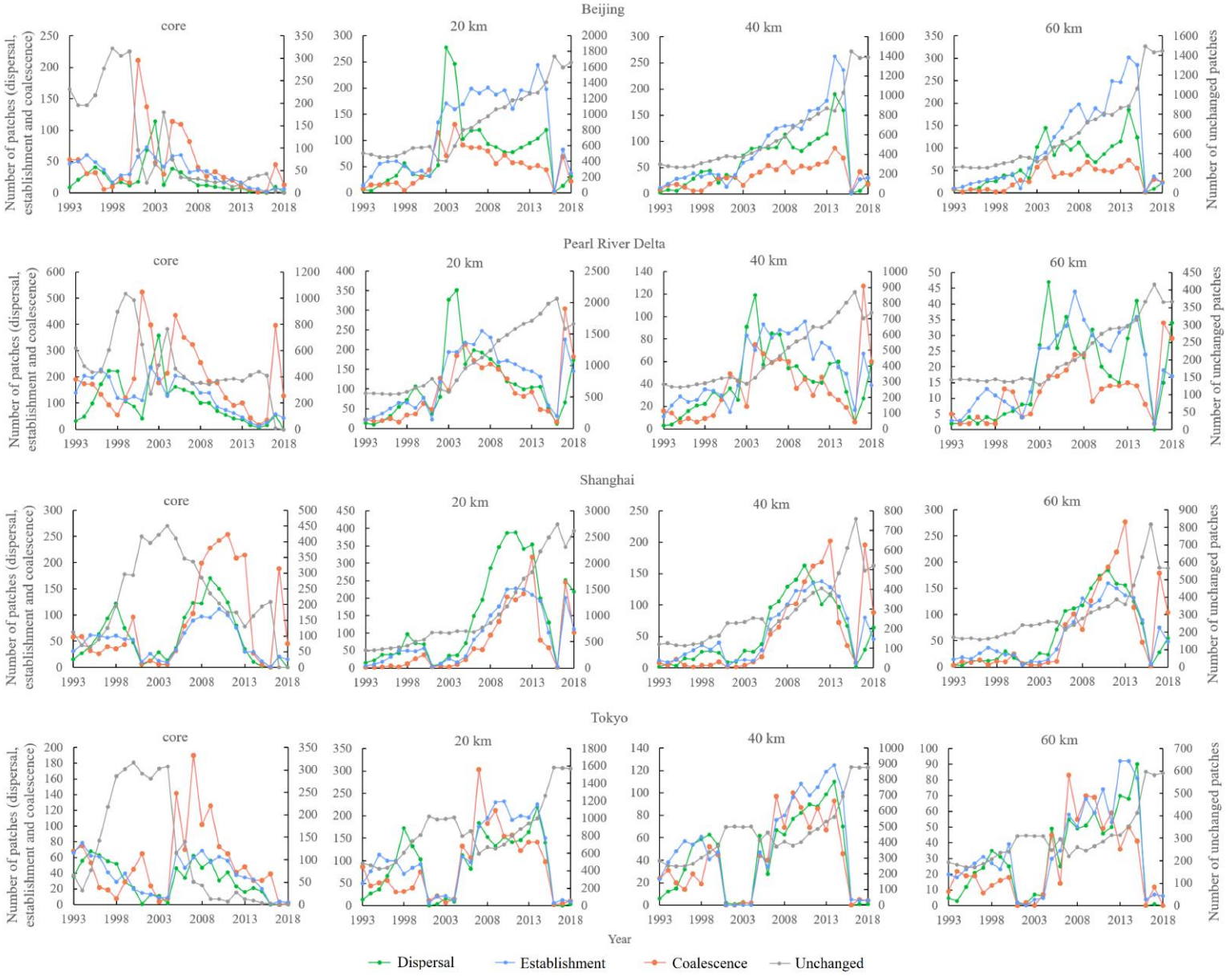

Figure 4.5 The number (i.e., count) of urban patches experiencing the coalescence,

dispersal and establishment events and stable patches in (top to bottom) the four megacity regions for each year from 1992 to 2018.
The data of 1993 suggests the changes from 1992 to 1993 and so on). Time-series plots are shown for (left to right) the core area and buffer zones.

We plotted the number of new urban patches (i.e., dispersal events), the loss of urban patches (the total number of coalescing urban patches minus the number of urban patches that they coalesced into in the subsequent year), and the net change in urban patches (the total number of new patches minus the lost patches) against time (Fig. 4.6). This shows the overall urban dynamics and details the gains and losses of urban patches in the landscape over time.

For the core urban area, Beijing, Pearl River Delta and Tokyo gained urban objects in the 1990s and early 2000s. Shanghai continued gaining urban objects in the 2000s until 2007. The net flux was negative in the four megacities in the 2010s, indicating continuous merging of urban objects. In the buffer areas, Beijing and Tokyo gained urban objects for most of the period. In Beijing, the increase in the net flux was much greater than in the other megacities, suggesting intensive and increasing urban complexity in the landscape related to a more fragmented landscape pattern.

In the Pearl River Delta, the 20 and 40 km buffer zones gained urban objects until 2016 and experienced a loss in urban objects in more recent years suggesting the dominance of coalescence. In Shanghai, the only net loss in urban objects is observed in more recent years in the 40 and 60 km buffer zones. The 20 km buffer zone gained a large number of urban objects in recent years, indicating the intensive introduction of urban objects around its core urban area.

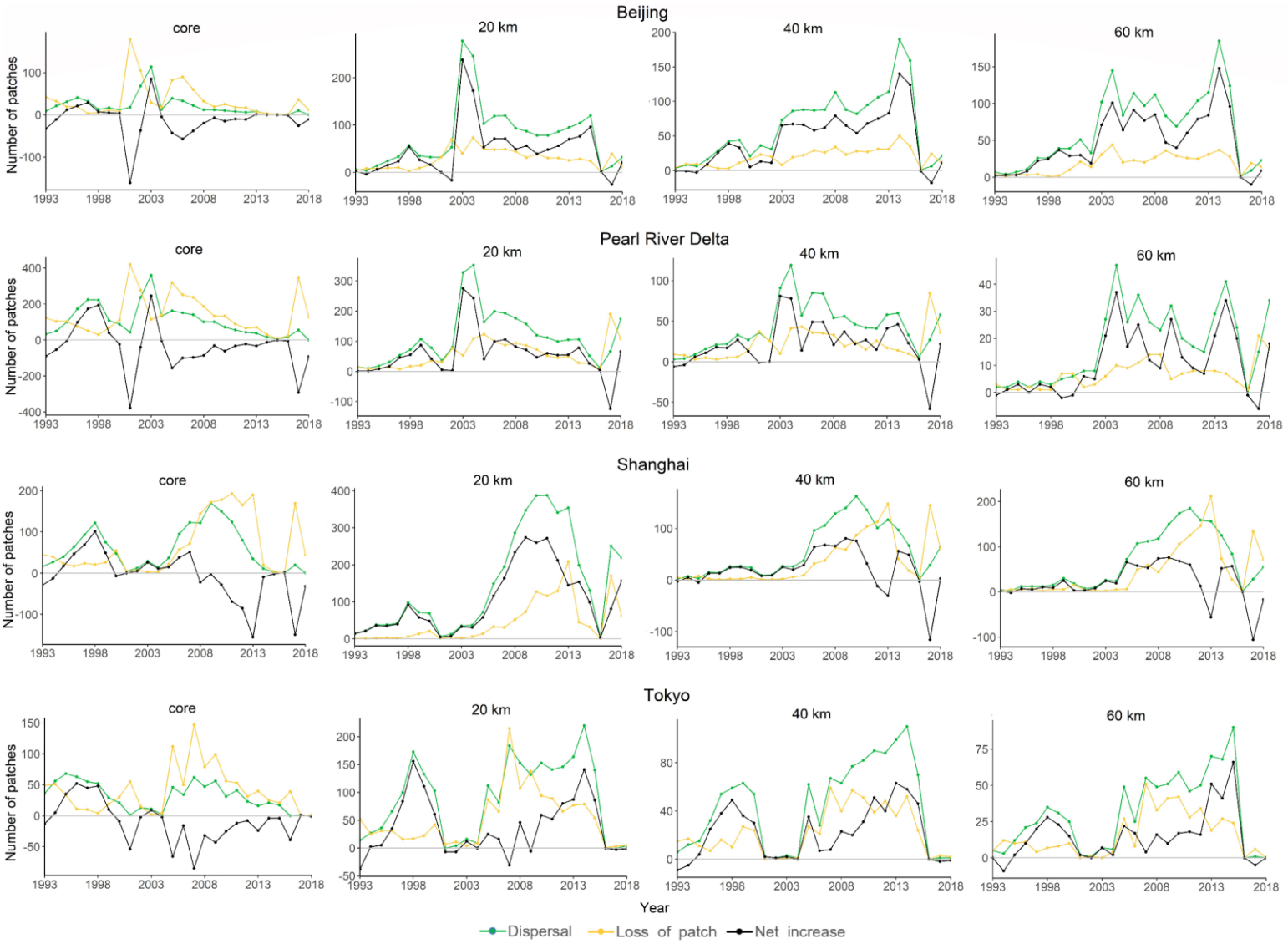

Figure 4.6 The dispersal, loss and net change in the number of urban patches in the core area and buffer zones in the four megacities.

To better capture the relative dynamics of the urban growth events, we normalised the number of objects falling into each growth event by dividing each by the total number of objects and then plotted the relative proportions through time (Fig. 4.7). In the core urban area, the coalescence event is dominant for most of the period. In Beijing and Tokyo, the establishment event accounted for a large number of changed urban objects in the late 2000s and early 2010s. In the Pearl River Delta, dispersal and establishment accounted for a similar proportion for most of the period. In Shanghai, dispersal

increased notably and occupied a relatively large proportion in the 1990s and late 2000s. In Shanghai, Tokyo and Pearl River Delta, the overall dynamics and proportion of unchanged objects was similar in the three buffer zones, suggesting that the urban patterns changed synchronously in the periphery. In Beijing, the 20 km buffer zone showed a different overall trend. In all three buffer zones of Beijing and Pearl River Delta, dispersal and establishment occupied a larger proportion than coalescence, indicating that coalescence is still limited in the periphery compared to other events. In contrast, in the buffer zones of Shanghai, the proportion of dispersal events was larger than for the other megacities, especially in the 2000s. In the 40 and 60 km buffer zones, the proportion of coalescence events is greater than for the other megacities, probably due to the relatively larger size of the satellite cities located in this area and the merger of urban objects clustering around these satellite cites. Lastly, in the buffer zones of Tokyo, the proportions of each event are similar in the late 2000s.

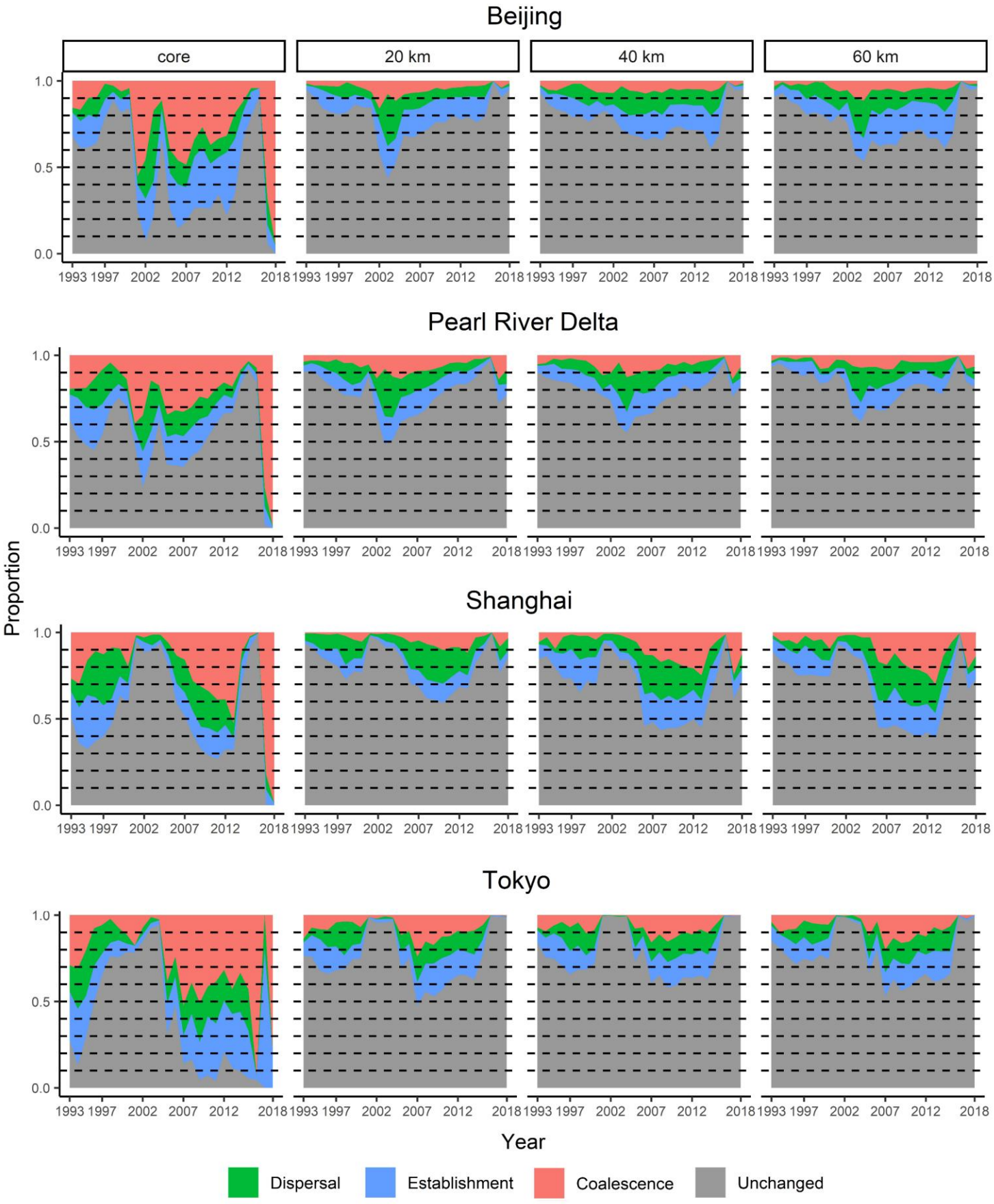

Figure 4.7 The proportion of urban objects experiencing the three urban growth events

(and no change) in these four megacities in the core area and buffer zones over time.

4.4 Discussion

This research explored the urban growth process over a 26-year period in four megacity regions in South-East Asia (Beijing, Pearl River Delta, Shanghai and Tokyo). For these four megacities, a rule base was established from which to measure directly the occurrence of growth events on an inter-annual basis at the per-object level over time.

4.4.1 Inference on underlying growth processes and phases

Urban growth is the result of multiple factors interacting at different scales, such as population increase, economic growth, planning strategy, and development policies. Changes in the level of each event type through time could potentially be used to inversely infer changes in the underlying growth process because these events necessarily occur due to growth drivers, and collectively they *define* the overall areal growth rate. Therefore, changes in the counts of the change events through time can potentially be interpreted as implying a physical amplification, constraint or "disturbance" in the underlying urban growth process. For, example, if growth increases as a function of a change in policy, then this should be observed in increases in the numbers of all types of change events per object.

However, some caution should be exercised over the above interpretation because changes in the level of each event are also a function of the availability of space. Given a fixed space, one might expect the number of events observed to be eventually

conditioned by the space left available to fill, in addition to the policy. Thus, while changes in the counts of change event types necessarily reflect changes in the overall areal growth rate, and that growth rate may be due to policy and other drivers, the ability to infer changes in the underlying growth process is conditional upon the relation between the urban pattern and the proportion of the space that it fills. Related to this, it should also be noted that our analysis of urban growth focused on spatial expansion and we did not measure the intensification of urban land use, and vertical expansion in particular. The dynamics of these other dimensions of urban growth, especially during decreasing trends in the growth rate, should be considered in future research.

Of course, the space available need not be regarded as fixed, and as a mega-city grows so too can the definition of its spatial extent. Such an interpretation invokes the geographical concepts of fractality and scale-invariance and, consequently, in this interpretation *overall* differences in the count of each event may not be observed as the city grows to occupy new space.

For a fixed space, the dominance of the different object-level change events may be expected to vary through time as the space is increasingly filled. Indeed, this thinking underlies much of the earlier work on urban growth phases: introduction events dominate in the early phases, establishment/dispersal dominates in the middle phase and coalescence dominates in the final phase as the space is increasingly filled. In this paper, we defined *fixed* buffer zones around each mega-city core area and tested the hypothesis that as a city expands within a fixed space, the predominance of each event

type should change depending on proximity to the core area. The assumption underlying this experimental approach is that space (distance from core) can be exchanged for time (phase of growth). Through the object-based approach, we were also able to explore whether there exists any geographical variation across regions in the event types and whether the event types change synchronously with each other through time. In this paper, we explored these questions through a geographical analysis of the pattern of changes in the event types within, and between, regions, and through time.

4.4.2 Temporal changes in the number of growth events per mega-city and policy interpretation

In Tokyo, growth events occurred at a relatively lower level in the early 2000s, suggesting urban growth slowed or entered a stable state: after years of rapid urbanization, a relatively high level of urban development was reached and the possibility space for urban transition was limited. The growth that was observed subsequently, especially in the buffer zones, may have arisen because in 1999 planning promoted the development of nearby cities in the periphery.

In Shanghai, the core area witnessed a decrease in the magnitude of growth events around 2000, probably because in the 1990s, with a series of opening policies and the construction of the Pudong district, the urban areas experienced a relatively rapid increase and remained relatively stable in the late 1990s. The area experienced significant growth around 2003 and afterwards, probably due to the enforcement of the

Shanghai Master Plan (1999-2020) and further opening, which promoted further rapid urban growth.

In the buffer zones of Beijing, especially the 40 and 60 km buffers, the magnitude of growth events increased steadily, indicating a stable urban growth process. In the Pearl River Delta, the growth trend in the number of objects experiencing growth events slowed around 2005 and decreased thereafter, suggesting that after the rapid development of the 1990s, such as within the special economic zone in Shenzhen, the opening policies and foreign direct investment in the region, urban growth entered a new state, with a general decreasing trend in the magnitude of growth events. This was also observed in the early 2010s in Shanghai as mentioned above. After years of intensive urban growth (i.e., an increasing trend in the magnitude of growth events), the rate of urban growth slowed.

4.4.3 Geographical analysis of event sequencing and synchronicity across the core-buffer, across buffers and across mega-cities

A general synchronous trend in the three growth events is observed among the various buffer zones, which suggests that urban growth drivers have similar effects on the dynamics of the different events and leads to similar behaviour of these events at the population level. It implies a general similar urban growth process for the core urban area and its hinterland. For example, in all three buffer zones of Shanghai, the magnitude of all events experienced rapid growth in the 2000s and decreased thereafter, suggesting factors that influence all the buffer areas.

However, the observed growth events and patterns differ in some cases between the core urban area and buffer zones. For example, the buffer zones of Beijing exhibited a different pattern of growth events from the core area. This suggests that the factors influencing urban growth in these regions affect the core urban area and buffer zones differently. This may be because Beijing is the capital city of China: the core urban area experienced rapid urban growth and economic development with a weaker connection to its hinterland compared to the other megacities, revealed as different growth trends. The number of coalescence events was also smaller than for other megacities in the buffer zones, suggesting a more dispersed pattern.

The hypothesized sequence of the three urban growth events was not observed at the landscape level. Unlike the suggested cycles of diffusion and coalescence or the oscillation behaviour of urban growth reported in previous studies (Dietzel, et al., 2005b; Martellozzo & Clarke, 2011) our results indicate that, in reality, the establishment, dispersal and coalescence events are realised concurrently as a result of a single growth process of given intensity occurring in the urban landscape, and they dominate alternately.

In contrast, at the patch (object) level, the hypothesised dispersal, establishment and coalescence events were observed to follow a sequence as expected. This is axiomatic: first, a new urban object is introduced (or dispersed) into the landscape. Then, it may remain stable or grow in area (i.e., establishment). When it is close enough to another urban object, as it continues growing, it merges to form a new urban object (i.e., coalescence). This new urban object may experience the same establishment-

coalescence phase sequence or another coalescence event.

When accumulating the object-level events at the landscape or population level, the hypothesized sequence is not generally observable. In real urban systems, the factors influencing urban growth are dynamic and complex. When a set of factors promotes rapid urban growth, as urban land expands the number and size of urban objects are *both* likely to increase, shown as an increase in both introduction/dispersal and establishment events, and with this urban expansion coalescence may also increase. This leads to a synchronous behaviour of the events and hides the sequence occurring at the per-object level, as observed in this research. This is a key contribution from this study—that from a geographical analysis perspective it is more precise to identify and analyse change events at the object level first and *then* aggregate them to represent more comprehensively the urban system at the population level.

In future research, the sequence analysis of growth events at the per-object level could help to provide valuable information for understanding the evolution of urban systems and, thus, building urban growth models. The object-based method provides a way to trace the growth process at the per-object level. Fig. 4.8 represents succinctly the urban object-level growth process and demonstrates the effectiveness of our method in capturing the spatial–temporal links between urban patches. It shows how urban object 8911 grew from several small urban objects into one larger urban object from 2005 to 2011. According to our method, all the objects from 2005 to 2010 are located within the boundary of object 8911. From 2005 to 2008, the objects are quite small and most of them remain unchanged.

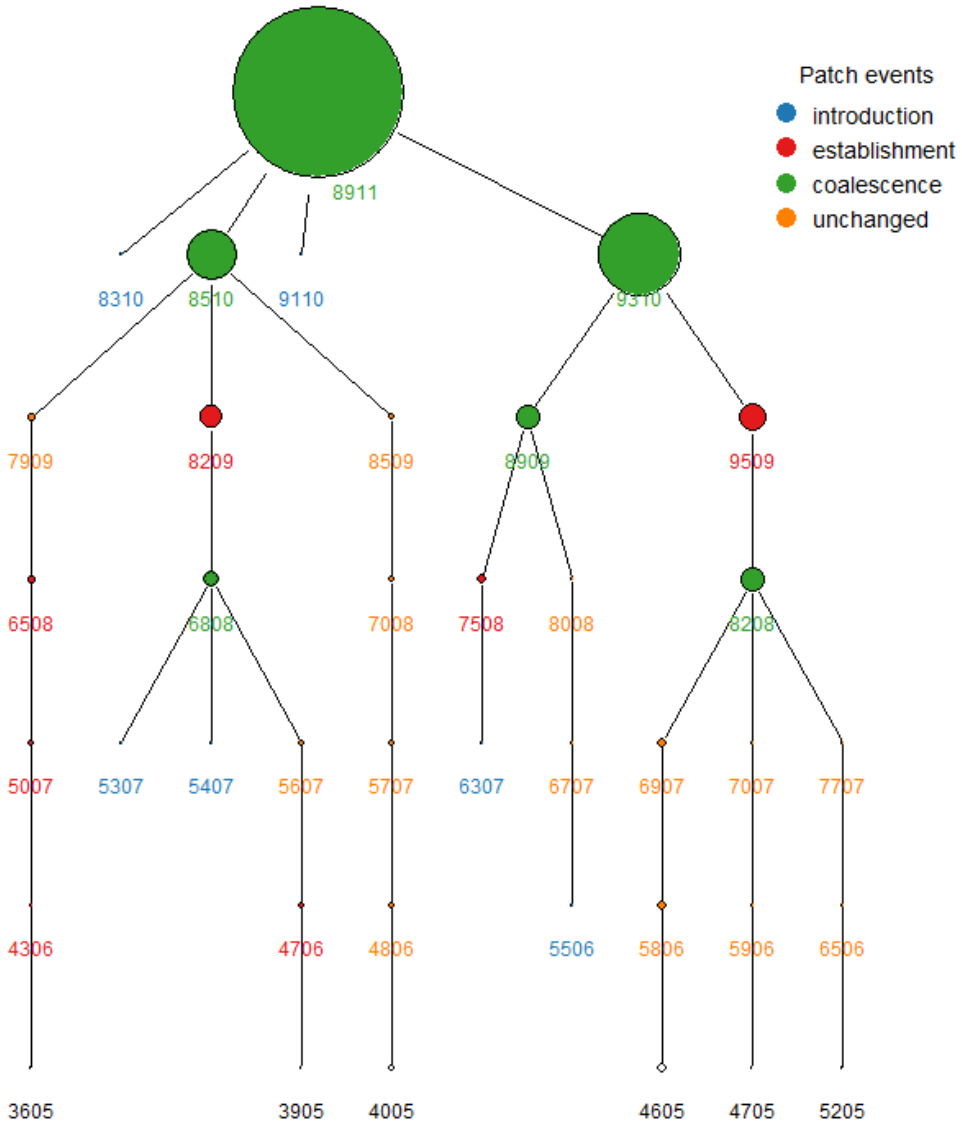

Figure 4.8 An illustration of the urban object growth process from 2005 to 2011. Object 8911 is an urban patch in Shanghai. Each circle in the figure represents an urban object, with its colour referring to different events and its size proportional to its area. To avoid confusion, it should be noted that the labelled IDs do not correspond to the IDs used in the calculation of events. Each circle has one unique ID, with the last two digits in the labelled ID referring to the respective year. All the objects in 2005 are coloured black since in this example they are treated as initial patches which do not inherit any of the four events.

From 2008 to 2011, the patches grew rapidly and coalescence became the dominant process. By identifying the events associated to each urban object, it was then possible to build the spatial–temporal links between them. For example, objects 8909 and 9509

are two isolated urban objects in 2009, but they merged into one urban object (9310) in 2010, thus, defining the underlying link between them. In future research, the well-defined temporal links among urban patches could be further expanded into a spatial–temporal graph structure of urban patches by adding specific spatial links between the urban patches. Such a graph could help to further study inter-urban interactions and the evolution of urban systems. Moreover, most urban growth models are based on raster data which are commonly spatial scale-dependent. The object-based method can be used to overcome this dependency to some extent.

4.4.4 Policy interpretation

Research on the dynamic spatial patterns arising from urban growth processes not only benefits our understanding of the evolution of urban systems and their interactions but also provides supporting information for policy-makers and decision-makers planning growth and managing the effects caused by urban growth. Urban growth influences profoundly the environment and ecological processes from local to global scales. Mitigating the negative effects of urban growth is crucial to achieving sustainable development. At the regional level, we observed a large number of dispersal and establishment events for most of the time in the buffer areas in the four megacities. This suggests that in the periphery, there exist strong drivers, and a consequent high rate, of urban growth. An increasing number of urban objects is usually associated with increasing fragmentation which will further influence ecological processes and social processes. For example, these new urban land areas are usually gained from agricultural

land, forest or grassland. The loss of these areas may lead to habitat fragmentation (Riitters et al., 2016), local climate change (Zhou et al., 2015) and the loss of benefits for local stakeholders (Robinson et al., 2012). With a compact core urban area, the buffer areas usually have a dispersed pattern, which influences different ecological processes. Thus, in these megacities, effective regional planning and environmental management are essential to mitigate the negative ecological and social impacts of urban growth, both in the core and the periphery areas.

4.5 Conclusion

We analysed the spatiotemporal urban growth patterns in the urban core and buffer zones of four megacity regions in South-East Asia. An object-based analysis was undertaken at the per-object level and four change events were defined, borrowed from ecology, at the per-object level. We analysed the object-based time-series data to analyse changes in urban growth events at the per-object level and, by aggregation, at the whole region level. By specifying a logical rule base for application at the per-object level we were able to measure the establishment, dispersal and coalescence growth events. This approach was effective in providing the per-object level data necessary to analyse and quantify changes in the *composition* of these events (i.e., growth phases) at the regional level through time. Subsequently, the time-series of these compositional changes at the regional level was used to make reasonable inferences about the underlying growth process. As such, the insights provided here, cut through existing theory and approaches to characterizing changes in urban patterns.

At the population level, the establishment, dispersal and coalescence events were found to be generally present and concurrent over time, albeit dominating at different times. The growth events exhibited a general synchronous trend in each buffer zone over time rather than following a specific logical sequence (as must occur at the object level). In the buffer zones of Shanghai and Tokyo, the magnitudes of the different growth events were generally similar especially after 2000, whereas in Beijing and the Pearl River Delta, the magnitude of the dispersal and establishment events was much greater than for coalescence. The same was not always observed between the buffer zones and the core area. A general synchronous trend was observed only in the core and buffer zones of Shanghai. Our results also suggested that in the buffer zones, dispersal and establishment were dominant most of the time, indicating a highly active growth process that leads to a more fragmented spatial pattern of urban objects, which is indeed realized in reality.

The object-level rule-based approach developed here for the first time revealed new insights into the dynamics of urban growth events, thus, providing potentially increased understanding of the underlying urban growth process and the urban systems themselves. This new approach and information should be developed further so that it can support effective regional urban planning and environmental management which are both essential to achieve environmentally sustainable levels of urban development and landscape patterns.

5 Modelling urban objects through Bayesian linear mixed-effects models

Abstract

At the macro-level, urban systems consist of urban entities interacting with each other. Exploring the dynamics of such urban systems requires the definition of urban spatial objects, a comprehensive definition of the possible change states that such objects can take, and the systematic linking of these objects through time with unique identifiers. Here, such a data model is extended, for the first time, via a spatial-temporal graph-based structure to facilitate model-based exploration of how the relationships between neighbouring urban objects affect the dynamics of urban entities, leading to better understanding of urban system dynamics. A linear mixed-effects model, fitted through an approximate Bayesian inference framework in Integrated Nested Laplace Approximation (INLA), was applied to the created graph-based dataset to model the coalescence, growth and unchanged states of urban spatial objects based on the previous states of the objects themselves and of their neighbouring objects. The findings reveal that the coalescence state of urban objects in the present year is influenced by their state, *proximity* to neighbours and the states of neighbouring objects in a defined buffer in the previous year. The growth state of urban objects in the present year is associated with their previous state, the *state* of the largest neighbouring object and the states of objects within a close buffer in the previous year. Additionally, the area of objects that grew

was investigated and found to be related to the largest interaction with neighbouring objects, with varying effects for different-sized objects. This research contributes to studies of urban growth by modelling explicitly the relationships between the states of urban spatial objects in the present year and their states, and those of neighbouring objects, in the previous year. The results offer new insights into the evolution of urban systems.

5.1 Introduction

As the most dynamic and rapidly evolving system on Earth, the urban system has attracted the interest of scientists and researchers across various disciplines (DeFries et al., 2010; Derudder et al., 2010; Arribas-Bel et al., 2011; D. Li et al., 2022; Lengyel et al., 2023). Within urban studies, urban growth is a central topic as it relates to a variety of issues such as global environmental change, social equity, public health and food security (Galea and Vlahov, 2005; Grimm et al., 2008; Hatab et al., 2019; Meerow et al., 2019). Understanding how urban systems have changed, why they have changed and the consequences of the changes could help to increase understanding of interconnections with related processes, and ultimately contribute to sustainable development (Derudder et al., 2010; Lengyel et al., 2023). In this context, modelling urban growth is a critical issue and it has been studied intensively.

Urban growth studies generally use one of two main approaches. The first measures

how much cities have grown over time. This could be at the individual city level or sometimes across broader scales ranging from regional to global levels. Urban growth is modelled over time with parametric or nonparametric models, or a combination of both (Hoffhine Wilson et al., 2003; Li and Gong, 2016; Angel et al., 2021; González-Val, 2023). These models represent urban growth by the magnitude of some property such as land area or population, and are mainly based on two underlying theories. The first is that urban growth is a function of various endogenous or exogenous drivers, such as economic growth, population growth, policy effects and accessibility to hubs or resources (Fujita, 1976; Eaton and Eckstein, 1997; Feng et al., 2002; Ding, 2004; González-Val, 2023). Researchers have explored the relationship of urban growth with these drivers through a variety of statistical models (Yue et al., 2013). The other theory treats cities as systems and argues that city growth is random and is a function of its initial size (González-Val, 2023). This approach generally explores urban growth through scaling laws or fractal dimensions within a defined region over a long period (Benguigui and Czamanski, 2004; Arcaute et al., 2015; Lagarias and Prastacos, 2020; Molinero and Thurner, 2021).

The second approach studies how urban growth changes both spatially and temporally. Such studies focus typically on changes in spatial pattern over time, representing cities using raster (i.e., image) data. A classic approach is to utilize landscape metrics to explore the dynamics of urban spatial patterns. Within this framework, some growth types such as dispersal-coalescence, infill, edge-expansion and leapfrog, and indices such as the Landscape Expansion Index (LEI), have been developed to characterize

urban growth from a process-based perspective (Liu, et al., 2010; Aguilera et al., 2011; Li et al., 2013; Jiao et al., 2015). Another widely studied approach adopted cellular automata (CA). CA is a dynamic method that simulates urban growth from a micro level (i.e., pixel-level) based on location, geographical and socioeconomic conditions, and interaction with surrounding neighbours through a defined transition rule. It includes different growth drivers and spatial effects to study urban growth from a self-organization view. The CA approach has been developed into a variety of different branches such as object-based CA, ABM-CA and AI-CA (Liu et al., 2008; Liu, et al., 2010; Liu et al., 2013a, 2013b; Abolhasani et al., 2016). Another interesting approach represents cities using raster data, but studies urban growth from a percolation perspective. It treats urban growth as a process where the city diffuses from the seed or the core to the surrounding space over time. Usually combined with fractal dimension, some researchers have utilized this approach to study the dynamics and evolution of urban systems from city level to regional level (Makse, et al., 1998; Arcaute et al., 2016; Sarkar et al., 2020).

Among the above studies, a significant common element is the representation of cities from the perspective of the growth process by incorporating relationships between urban lands. This is because during the urban growth processes, urban lands interact with each other and are affected by each other, suggesting that interactions are crucial in understanding urban land dynamics. For example, dispersal-coalescence, infilling and leapfrog essentially represent cities through different relations between new and existing urban lands (Dietzel et al., 2005a; Li et al., 2013; Dahal et al., 2017).

Percolation theory is also based on an assumption about the growth process.

While the above approaches study urban growth processes by incorporating the relationships between urban lands, urban systems comprise urban entities which include a variety of activities interacting with each other located on urban land. This suggests that the raster representation of urban land (i.e., based on pixels) could not explicitly and adequately capture the relationship between urban entities (e.g., cities, towns, villages). While studies have incorporated spatial or temporal relationships, or both, most are based on the relationships between raster pixels, while studies with an explicit spatial-temporal link between urban entities and their relationships are still limited. Therefore, to fill this gap, this research represents urban entities as spatial objects and explores the relationship between these objects.

Some research on land cover change and landscape ecology has developed network or graph-based methods by representing land cover or habitat as objects to study their spatial-temporal evolution (Cantwell and Forman, 1993; Urban et al., 2009; De Cola, 2010; Cheung et al., 2015; Wu et al., 2021). For example, studies have built spatial graphs based on landscape habitat objects to study connectivity and its implication for conservation (Fall et al., 2007; Urban et al., 2009). This general approach has been further developed into a spatial-temporal graph, incorporating temporal transitions between objects, to study the land cover evolution over time (Wu et al., 2021; Zou et al., 2023). Such methods provide detailed insights into the spatial-temporal relations of land objects tracing their transitions over time. In urban studies, the object-based

method has been applied rarely.

In previous research, we represented cities as objects and characterized them by four states based on the urban growth process, including introduction (commonly through dispersal), establishment (or growth), coalescence and 'unchanged', which essentially necessitates a temporal link among objects (Fan et al., 2024). However, urban objects exhibit not only temporal links, but also spatial links through interactions with each other across space. Their direct spatial-temporal relationships have yet to be studied explicitly. Therefore, based on the aforementioned states of urban objects, we here introduce spatial links to allow exploration of the spatial-temporal relationships between objects and how these affect likely future state transitions. Specifically, we build graph networks among urban objects and integrate them with the states of objects to establish spatial-temporal links and, thereby, study the states of objects and their relationships with other objects, especially their surrounding neighbours. For the four states (introduction/dispersal, establishment, coalescence and 'unchanged'), we concentrate on creating an integrated model for the establishment, coalescence and unchanged states while excluding introduction (and dispersal). Introduction is a separate process which relates to whether an object exists, whereas the establishment, coalescence and unchanged states relate to the fate of an object once it exists. To achieve this, taking Shanghai as an example, we fit models for these different states to explore how its future state is related to the dynamics of itself and other objects.

For the coalescence state which refers to urban objects merging with other objects, we

introduce a set of variables characterizing the dynamics of objects that help to model the state of coalescence (i.e., the likelihood of coalescing) and its relationship with the dynamics of surrounding objects. For the establishment and unchanged states, we treat them collectively within a single growth model since they represent whether an object grows or not. Similarly, a set of variables characterizing the dynamics of objects is also introduced to model the growth state of objects (i.e., the likelihood of growth) and their relationship with surrounding objects.

Finally, we predict the coalescence, growth and unchanged future states of urban objects through the relationships among objects obtained by our model. For objects in the growth state, we further explore how their area is related to surrounding objects. This research, thus, models explicitly the well-defined state transitions of urban spatial objects through extensive characterization of the spatial-temporal relationships among neighbouring urban spatial objects.

5.2 Data and method

5.2.1 Data

The land cover data were acquired from the European Space Agency (ESA) Climate Change Initiative (CCI) Land Cover time-series Product (Defourny et al., 2023). The CCI is a global, annually consistent land cover dataset with a spatial resolution of 300 m. It covers the period since 1992 and is still updated with the latest plan being to release the 2021 land cover data. The data are derived from a combination of multiple

satellite sensor datasets including Advanced Very-High-resolution Radiometer (AVHRR), SPOT-Vegetation, Medium Resolution Imaging Spectrometer (MERIS), PROBA-Vegetation and Sentinel-3 OLCI time-series data. The CCI classification system used is the Land Cover Classification System (LCCS) developed by the United Nations (UN) Food and Agriculture Organization (FAO). In addition to this system, the identification of urban areas also relies on the Global Human Settlement Layer in the Global Urban Footprint dataset. The overall accuracy of urban areas reaches 86% to 88%. We extracted urban areas for Shanghai from 1992 to 2018 with a 60 km buffer from the boundary of its centre object defined in 2018 using the CCI dataset. This original raster-based urban dataset was then transformed into an object-based dataset for the present analysis.

5.2.2 Labelling ID for objects

To model and explore the relationship between the state of urban objects and the dynamics of their surrounding neighbours, it is necessary to identify whether an urban object has coalesced or grown. The coalescence state occurs when an object merges with another object. The growth state arises when an object increases in area.

When modelling changes in the area of objects, a pre-requisite is to identify the continuous object that is changing, but if one object coalesces with others, it will cause a change in object identity and a sudden and, in some cases, great change in area. Coalescence can, thus, cause confusion and difficulty in identifying a continuous urban object and modelling changes in its area. For example, if several objects merge into one

object, the increase in area is clear, but to which object the increase should be attributed is not. Thus, we introduce "birth" and "death" processes for urban objects to deal with the identification of the individual objects before considering changes in their areas.

At the initial time point, there are a variety of different-sized urban objects in the space of interest. Influenced by a variety of urban growth drivers, an urban object will tend to expand outwards. Through its expansion, an object could be connected with other objects and merged into one object. At this time point, we treat the several connected objects as "*dead*", and the new coalescence object as "*born*". Based on this concept, if an urban object exists from time *i* to *i*+*n* and coalesces or is "dead" at time *i*+*n*+1, we will treat it as a continuous object from time *i* to *i*+*n,* and if its area at *i*+1 is larger than that at time *i*, it will be labelled "growth".

To label the coalescence and growth state for each object, we assign each urban object with a unique ID. First, to detect the "*death*" and "*birth*" processes, we utilize a backward method by labelling urban objects starting from the last year. We first intersect layer *i*+*n* with layer *i*+*n*-1. For all the objects in year *i*+*n*-1, when conducting $object_{i+n-1}^{j} \cap object_{i+n}^{k}$, $object_{i+n-1}^{j}$ acquires the ID of $object_{i+n}^{k}$, which is ID_{i+n}^{k}. We then check the appearance frequency of ID_{i+n}^{k} in year *i*+*n*-1. If the frequency equals 1, suggesting that it is a continuous object, the object will retain this ID; if the frequency is larger than 1, then new IDs are assigned to all the objects that have ID_{i+n}^{k}.

The details of this process are illustrated in Figure 5.1. In the example, at time *i*+3, the

object is labelled as *a.* Then at time *i*+2, all the objects within the boundary of object *a* are first labelled as *a* (shown in the bracket). We then check the frequency of this labelled ID, that is, *a.* If its frequency equals 1, this suggests that within this boundary there is only one object and it is a continuous object. If its frequency is larger than 1, this suggests that a coalescing process exists from time *i*+2 to *i*+3. In this case, new IDs are then assigned to these objects. At time *i*+2, there are two objects within the boundary of object *a.* So new IDs, *b* and *c* respectively, are given to them. Because of the coalescence of objects *b* and *c*, we treat them as coalesced or "*dead*" at time *i*+3 and a new object, *a* is "*born*" at time *i*+3. This process is repeated every year. In the given example, at time *i*+1, within objects *b* and *c,* there is only one object labelled as *b* and *c*, respectively. So, they are still labelled as *b* and *c,* indicating that they are continuous objects from time *i*+1 to time *i*+2. At the time *i*, the frequency of *b* equals 1 suggesting that it is a continuous object, but within object *c*, there are several isolated objects. In this case, object *d*, *e*, *f*, *g* is "*dead*" at time *i*+1 and object *c* is "*born*" at time *i*+1.

From the above unique labelling process, we acquire IDs that can help to trace the state of urban objects through time. For example, from time *i* to time *i*+3, object *b* is a continuous object from time *i* to time *i*+2 and object *c* is a continuous object from time *i*+1 and time *i*+2. According to the frequency of IDs, we can obtain coalesced objects and continuous objects (i.e., non-coalesced objects). Then for a continuous object, if the area at one time point is larger than that at the previous time point, it will be labelled as growth, otherwise, it will be labelled as unchanged. We, therefore, acquire all the coalescence, growth and unchanged states of *all* objects.

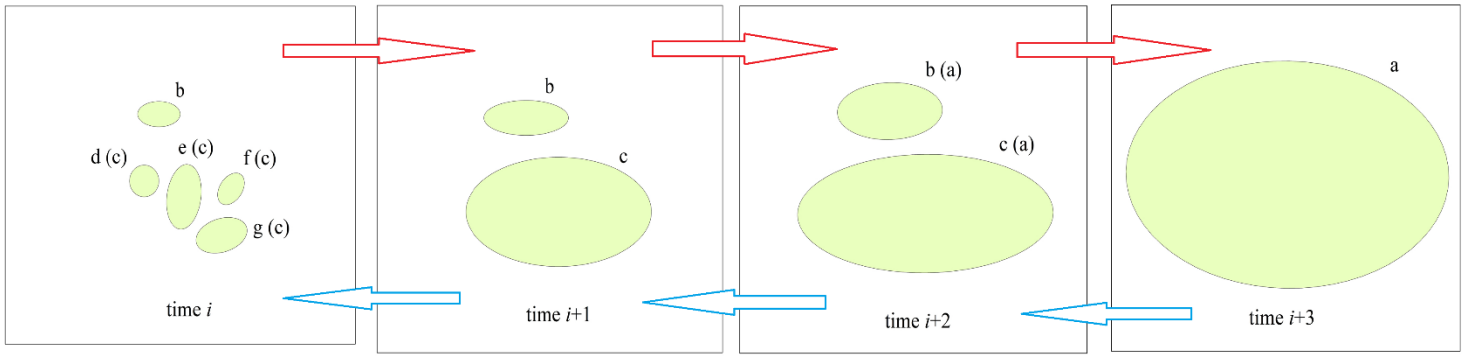

Figure 5.1 An illustration of the ID labelling process for objects.
The red arrow represents the temporal sequence of urban growth while the blue arrow represents the sequence of the labelling process.

5.2.3 Neighbouring objects

The second step is to calculate the influence of other objects on the state of the core object (i.e., the object of interest). In this research, we concentrate on urban objects that are defined as neighbouring objects by building a graph or network structure. To acquire the neighbouring objects around one core object, we first transform all objects into points using the centroid point, and then a *triangulated irregular network* (TIN) is generated from these points for every year. The *Delaunay triangulation* is used to create the TIN. The Delaunay triangulation is associated with Voronoi polygons. In the Delaunay triangulation, points are linked by an edge of the Delaunay triangulation. A triangle is then formed by connecting three points whose corresponding circumscribing circle contains no other points within it. This process results in all points being connected through a set of triangles. Due to the nature of Delaunay triangulation, for one point, all the points directly connected to it through the edges of the Delaunay triangulation are regarded as its neighbours. Consequently, a set of neighbouring points

is established for each point in the dataset. An example is given in Figure 5.2. It is part of the Delaunay triangulation we generated for the year 2010 showing the link among objects. The size of each point is shown as proportional to the area of its corresponding object. The red arrow labels the core object and there are 5 neighbouring objects from A to E around it. It is important to note that since urban objects are essentially polygons other than points which we used to generate the network, there could be some cases in which neighbouring objects are not included in the resultant set of neighbouring objects. However, considering the irregular shape of urban objects and the complexity involved in generating a set of close neighbouring objects among polygons, our method can generally assist in identifying neighbouring objects, thereby fulfilling the requirements for the present analysis.

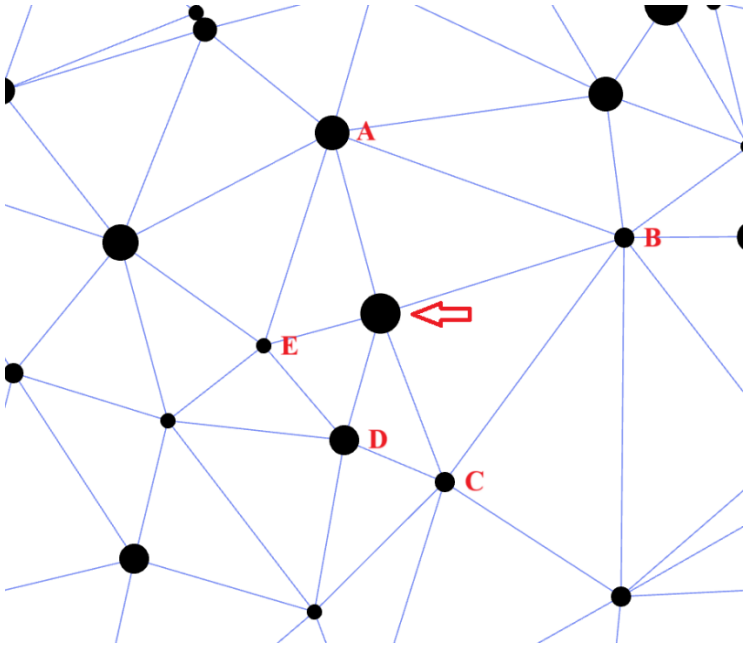

Figure 5.2 Illustration of a set of neighbouring objects for a core object.
The red arrow refers to the core object. A to E represent its neighbouring objects.

5.2.4 Covariates

Based on the generated network, we identify a series of influencing factors or covariates that represent the dynamics of neighbouring objects which could potentially influence the states of the core objects and, thus, could be further used in our model. We assume that each year's state is dependent on its previous year's state and influenced by its neighbours' dynamics in previous years. Consequently, all the covariates used are based on data from the previous year. When we treat urban objects as nodes and establish links among them, factors such as the distance between nodes, and the weight and dynamics of other nodes, play a crucial role in influencing the dynamics of the core node. Therefore, when we study the dynamic of urban objects from this node-link perspective, the question is how the distance, area and interaction of neighbouring objects influence the state of the core objects. To further explore this, a variety of covariates related to distance, area and interactions were explored in the models.

Table 5.1 The list of covariates for the coalescence and growth model

Covariates	**The coalescence model**	**The growth model**	**The area model**
core_changed_preyear	√	√	
nearest_changed_preyear	√	√	
nearest_500_changed_preyear	√		
nearest_500_1000_changed_preyear	√		
percentage_changed_preyear	√	√	
largest_change_preyear	√	√	
nearest_distance_preyear	√		
percentage_nearest_500_changed_preyear		√	
percentage_nearest_500_1000_changed_preyear		√	
time			√
largest_interaction_preyear			√
second_largest_interaction_preyear			√
third_largest_interaction_preyear			√

largest_area_preyear	√
second_largest_area_preyear	√
third_largest_area_preyear	√
nearest_area_preyear	√
nearest_interaction_preyear	√
largest_object_interaction_preyear	√
second_largest_object_interaction_preyear	√
third_largest_object_interaction_preyear	√

A list of all the covariates for the three models is shown in Table 5.1. First, in the coalescence model, for coalescence to occur, objects should expand and be close enough to be connected. This growth could be either of the core object itself or of the surrounding objects. Thus, distance and growth are two crucial factors. We first include a distance factor (i.e., the nearest distance) in the model. Then, the state of the core object is also included in the model since we assume that if the object changed in the previous year, it is more likely to change this year and increase the possibility of coalescence. Last, the set of states of neighbouring objects is also included. If the neighbouring objects changed in the previous year, they are more likely to change this year with a greater chance to coalesce. We plotted a sample core object and its neighbours in Figure 5.3 to help to explain these covariates. A detailed definition of each factor in the coalescence model is as follows:

1. core_changed_preyear: whether the core object changed in the previous year. 1 for changed and 0 for unchanged.
2. nearest_changed_preyear: whether the nearest object changed in the previous year. 1 for changed and 0 for unchanged. This is included because we assume that

coalescence is likely to occur with the nearest object. In Figure 5.3, the nearest object is D.

3. nearest_500_changed_preyear: whether there is an object that has changed within a buffer of 'nearest distance plus 500 m' in the previous year. 1 for changed and 0 for unchanged. In Figure 5.3, the buffer is depicted in green. We first calculated the nearest distance between the boundary of two objects. Any distance exceeding the nearest distance and less than the nearest distance plus 500 m will be classified in this category. This buffer-based approach helps to avoid duplication of the covariate information from the nearest object. Therefore, only objects C and E are considered. We chose this buffer since 500 m ensures coverage of two pixels outwards in all directions, considering that the original raster has a size of 300 m. This factor recognizes that coalescence must occur close to the core object, but not necessarily with the nearest neighbour.
4. nearest_500_1000_changed_preyear: whether there is an object that has changed within a buffer of 'nearest distance plus 500 m to 1000 m' in the previous year. 1 for changed and 0 for unchanged. A similar calculation of the nearest distance between objects is conducted to avoid duplication. In Figure 5.3, the buffer is shown in purple and the objects considered are A and B. This buffer ensures coverage of four pixels outwards in all directions.
5. percentage_changed_preyear: the percentage of changed objects of all neighbouring objects in the previous year. The unit is %. In Figure 5.3, this covariate represents the percentage of changed objects among objects A to E. This factor

provides information on the amount of change amongst neighbours and represents local dynamics. The larger the value, the more dynamic this local area is, and this could influence the dynamics of the core object.

6. largest_change_preyear: whether the largest object changed in the previous year. 1 for changed and 0 for unchanged. In Figure 5.3, this object is A. This factor is included due to the assumption that large objects may grow more and then are more likely to coalesce.
7. nearest_distance_preyear: the nearest distance between two objects. The unit is km. This distance is calculated as the smallest between object boundaries, shown as a blue double-sided arrow in Figure 5.3.

For the growth model, we assume that it is impacted by the state of the core object itself and the dynamics of its neighbours in the previous year. Thus, covariates 1, 2, 5 and 6 in the coalescence model are also included in the growth model. Factor 1 is the growth state of the core object itself in the previous year. Factor 2 represents that the present growth state is likely to be affected by the nearest object's previous growth state. Factor 3 represents a local dynamic suggesting that the growth of local objects is linked to the growth of the core. Factor 6 implies that the growth state is likely to be affected by the state of the largest object. We further include two more factors that represent the local dynamic as follows:

8. percentage_nearest_500_changed_preyear: the percentage of changed objects within the buffer of 'nearest distance plus 500 m' in the previous year. The unit is %.

9. percentage_nearest_500_1000_changed_preyear: the percentage of changed objects within the buffer of 'nearest distance plus 500 m to 1000 m' in the previous year. The unit is %.

These two factors have similar meanings to factors 3 and 4. The difference is that they represent the percentage of changed objects rather than whether they changed. They, thus, provide more detailed information on local dynamics. It is also important to note that when we refer to 'changed in the previous year' in the above covariates, we not only refer to objects that increased in area. Any objects that are newly introduced into the space or experienced coalescence in the previous year are also classified in this category, as they all represent change.

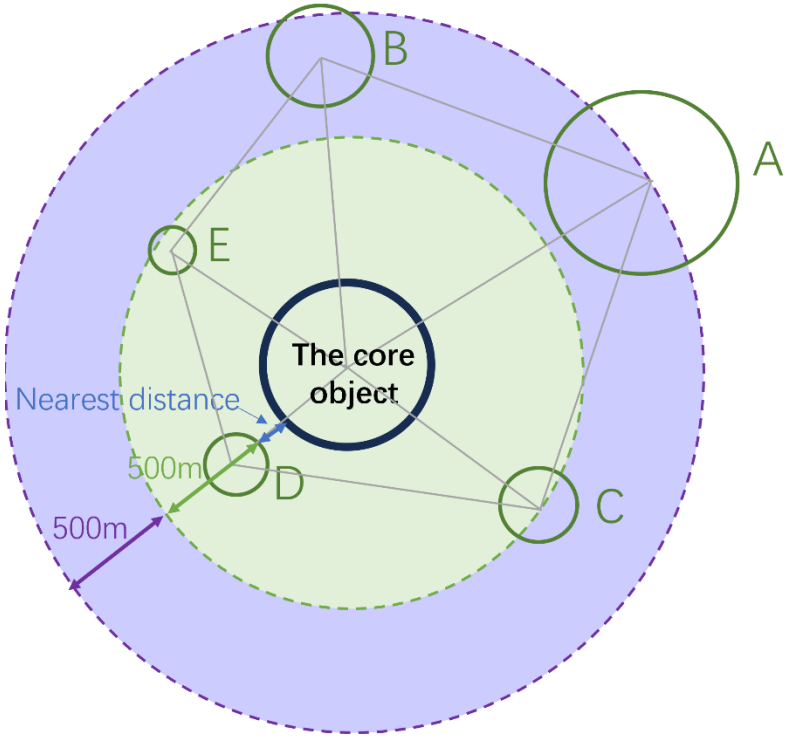

Figure 5.3 Definition of covariates in a set of neighbouring objects.
The green objects are neighbouring objects. The grey lines connecting objects represent the TIN.

For the area model, we assume first that it is influenced by time as area will increase over time. Then we introduce an interaction term which borrows from the well-known gravity model calculated as $\frac{a_0 \times a_i}{d_{0i}^2}$, where a_0 is the area of the core object, a_i is the area of the *i*th neighbouring object and d_{0i}^2 is the square of the distance between the core object and the *i*th neighbouring object. The distance is calculated using the nearest distance between boundaries. The interaction term suggests that area is influenced by the interaction between itself and the neighbouring object represented by their areas and a decay with distance. In this context, the interaction is larger when two objects are larger and closer. We use this interaction to represent the link between the core and the neighbour. It is not merely the neighbour's effect on the core, but a two-way effect, which mirrors the connections between urban objects in reality. As two urban objects are larger, the interactions such as population or information exchange between them is also more intensive which will further affect their respective states. We, therefore, select several different interaction terms for the model. Ultimately, we will check whether the area of the core object is related directly to the area of its neighbours, leading to several area factors also being included in the model.

The detailed definition of covariates for the area model is as follows:

1. Time: represents the temporal effect. We assume that time has a linear effect on the area of the object.
2. largest_interaction_preyear: the largest interaction of all interactions in the previous year.

3. second_largest_interaction_preyear: the second-largest interaction of all interactions in the previous year.

4. third_largest_interaction_preyear: the third largest interaction of all interactions in the previous year. Factors 2 to 4 represent area being likely to be affected by larger interactions.

5. largest_area_preyear: the area of the largest object in the previous year.

6. second_largest_area_preyear: the area of the second-largest object in the previous year.

7. third_largest_area_preyear: the area of the third largest object in the previous year. Factors 5 to 7 represent area being likely to be influenced by the area of larger objects.

8. nearest_area_preyear: the area of the nearest object in the previous year. This represents the assumption that area is likely to be affected by the area of the nearest object.

9. nearest_interaction_preyear: the interaction between the core and the nearest object in the previous year. This represents the assumption that the area is likely to be affected by the interaction between the core and the nearest object.

10. largest_object_interaction_preyear: the interaction between the core and the largest object in the previous year.

11. second_largest_object_interaction_preyear: the interaction between the core and the second-largest object in the previous year.

12. third_largest_object_interaction_preyear: the interaction between the core and the third largest object in the previous year. Factors 10 to 12 represent the area being likely to be affected by the interaction of larger objects.

Considering a same interaction could have a different effect on different-sized objects. For example, if the interaction is between a large and a small object, the same interaction could have different effects on the small object (such as 2 km^2) and the large object (such as 20 km^2). Thus, we classified the core objects into different groups based on their areas in the final year of their continuous period of existence, which could ensure that the object is classified in the same group over time. Also since there is a very limited number of large continuous objects, which increases the uncertainty in estimation, we run the area model only for objects smaller than 9 km^2. Therefore, the group is as follows: A: area < 1 km^2, represents very small objects; B: area between 1 km^2 and 3 km^2; C: area between 3 km^2 and 5 km^2; D: area between 5 km^2 and 7 km^2; E: area between 7 km^2 and 9 km^2 with a 2 km^2 interval for further modelling. We will explore how the interaction term affects different-size core objects differently.

All these covariates are calculated for all objects over time. So, each core object has its own covariates over time. All aspects of the ID labelling process and the calculation of covariates were conducted using R 4.3.0.

5.2.5 Models

Since we model the coalescence, growth and area of objects over time, the state of a

continuous object could be inherently related over time. Thus, a linear mixed model was conducted with a within-group structure, termed the random effects component. This allows for correlation within groups and variability between groups. In our model, each continuous object is treated as a group. Its state at different time points is treated as a different observation within this group. Considering that for the coalescence and growth model, we have a binary response variable (whether the state of an object is changed or not), a generalized linear mixed model (GLMM) was selected to fit to the data. A GLMM with binary response uses a default logit link to transform probability to the linear predictor and also includes a random structure. In this model, Y_{ij} follows a Bernoulli distribution $Y_{ij} \sim B(1, P_{ij})$ with probability $P_{ij}(Y_{ij} = 1)$ for success, and the model is written as

$$\text{logit}\,(P_{ij}) = \alpha + \mathbf{\beta X}_{ij} + \mu_i,$$

where $i = 1, 2, 3 \ldots, n$ represents the nth group, $j = 1, 2, 3 \ldots, m$ represents mth observation in a group, P_{ij} is the probability of success for observation ij, α is the fixed intercept, $\mathbf{\beta X}_{ij}$ is a set of fixed effects and μ_i is the random effects for group i accounting for variability between groups. Let η_{ij} to be the log odds. Then $P_{ij}(Y_{ij} = 1)$ is acquired by $\frac{e^{\eta_{ij}}}{1+e^{\eta_{ij}}}$.

For the coalescence model, the function is further written as

$$logit(P_{it}) = \alpha + \beta_1\text{core\_changed\_preyear} + \beta_2\text{nearest\_changed\_preyear} + \beta_3\text{nearest\_500\_changed\_preyear} + \beta_4\text{nearest\_500\_1000\_changed\_preyear} +$$

$\beta_5$percentage_changed_preyear + $\beta_6$largest_change_preyear + $\beta_7$nearest_distance_preyear + μ_i.

P_{it} is the probability of coalescence of an object in group *i* at time *t*. When P_{it} is 1, it indicates that the object will coalesce with others. α is the fixed intercept, β_1-β_7 are the coefficients for the corresponding covariates and μ_i is the random effect for group *i*.

For the growth model, the function is written as:

$logit(P_{it}) = \alpha + \beta_1$core_changed_preyear + $\beta_2$nearest_changed_preyear + $\beta_3$percentage_changed_preyear + $\beta_4$largest_change_preyear + $\beta_5$percentage_nearest_500_changed_preyear + $\beta_6$percentage__500_1000_changed_preyear + μ_i.

This model is similar to the coalescence model albeit that P_{it} represents the probability of growth of object *i* at time *t*. The differences are that nearest_distance_preyear is removed and two percentage factors are included, as described above.

In terms of the area model, since there are more small-sized objects in our dataset (i.e., the object sizes have a skewed distribution), a Gamma distribution GLMM is employed. The model using a default log-link including a random structure is written as:

$$\log\left[E\left(Y_{ij}\right)\right] = \alpha + \mathbf{\beta X}_{ij} + \mu_i + \varepsilon_{ij},$$

where the expected value of observation is linked with the linear function through a log-link. Y_{ij} is the value of observation *j* in group *i*, α is the fixed intercept, $\mathbf{\beta X}_{ij}$ is

a set of fixed effects, μ_i is the random effect for group *i* that follows a Gaussian distribution $\mu_i \sim N(0, \sigma_\mu^2)$ and ε_{ij} is the error term for each observation *j* in group *i* that follows a Gaussian distribution $\varepsilon_{ij} \sim N(0, \sigma_\varepsilon^2)$.

The model can be further written as:

$$\log[E(core\_area_{it})] = \alpha + \beta_0 \text{time} + \beta_1 \text{largest\_interaction\_preyear} + \beta_2 \text{second\_largest\_interaction\_preyear} + \beta_3 \text{third\_largest\_interaction\_preyear} + \beta_4 \text{largest\_area\_preyear} + \beta_5 \text{second\_largest\_area\_preyear} + \beta_6 \text{third\_largest\_area\_preyear} + \beta_7 \text{nearest\_area\_preyear} + \beta_8 \text{nearest\_interaction\_preyear} + \beta_9 \text{largest\_object\_interaction\_preyear} + \beta_{10} \text{second\_largest\_object\_interaction\_preyear} + \beta_{11} \text{third\_largest\_object\_interaction\_preyear} + \mu_i + \varepsilon_{it}$$

Time is treated as a fixed linear effect and α is the fixed intercept. β_0-β_{11} is the coefficient for each covariate, $core\_area_{it}$ is the area of the core object in group *i* at time *t* and μ_i is the random effect. In the model, we include a random intercept which means each group has an independent baseline level. ε_{it} is the error term for each observation *i* at time *t* that follows a Gaussian distribution $\varepsilon_{it} \sim N(0, \sigma_\varepsilon^2)$, representing any remaining unexplained part after fitting.

Due to the complexity of our models, we undertake inference using an approximate Bayesian framework through the Integrated Nested Laplace Approximation (INLA) package. Unlike traditional Bayesian inference methods such as Markov Chain Monte

Carlo (MCMC), INLA is less computationally expensive and more flexible. A Bayesian framework specifies a prior distribution of model parameters and estimates the posterior distribution of each parameter. The precision for σ_μ and σ_ε is τ_μ and τ_ε are assigned default vague prior distributions, which follows a log Gamma distribution, log (τ) ~ logGamma ($1,10^{-5}$). For each fixed effect parameter β, a default prior is also assigned with $\beta \sim N(0,10^6)$.

We first applied the coalescence, growth and area models separately. For the coalescence and growth models, the number of coalescence and non-coalescence objects are unbalanced, and this is true also of the number of growth and unchanged objects. Specifically, the number of non-coalescence and unchanged objects far exceeds those of coalescence and growth objects. To mitigate bias and uncertainty in predicting the minority group, we implemented a combination of oversampling and undersampling techniques to create a balanced dataset, ensuring similar numbers of coalescence and non-coalescence objects, as well as growth and unchanged objects. The oversampling method randomly replicates the data in the minority group to increase their number and the undersampling method randomly excludes the data in the majority group. The process stops when the two groups are balanced. We conducted this sampling process to acquire a balanced coalescence and non-coalescence dataset. Then for the non-coalescence dataset, which is the continuous dataset, the sampling process was also conducted to obtain a balanced set of growth and unchanged objects. After the sampling process, the coalescence and growth objects can be represented more evenly in the modelling. The coalescence and growth models were applied to the

balanced datasets separately.

The Deviance Information Criterion (DIC) was employed to select the best-fit model. It is a measure of the goodness-of-fit allowing fair comparison between models. DIC is analogous to the Akaike Information Criterion (AIC) but is especially suitable for the Bayesian context. As for the AIC, a smaller DIC suggests a better model fit. We first include all the covariates in the model and then remove insignificant covariates to obtain a model with only significant covariates. Then the DIC is used to select from the remaining covariates. Since the coalescence and growth models have binary dependent variables, The AUC (Area Under the Receiver Operating Characteristic (ROC) Curve) was used to evaluate how well the model distinguishes between 0 and 1. The AUC value is obtained by sweeping the threshold between 0 and 1 and displaying the specificity and sensitivity. The closer the AUC to 1, the better the model performs at classifying between groups. A *k*-fold cross-validation was also conducted to evaluate the performance of the models. This splits the dataset into *k* equal-sized subsets, with *k*-1 folds as a training dataset and 1-fold as a validation dataset. The model was first applied to the training dataset and then fitted to the validation dataset. This process was repeated *k* times so each fold is treated as a validation dataset once. After iteration, the average value of the evaluation metrics is calculated. In our case, the average accuracy was calculated which evaluates the percentage of correctly predicted state events of the total events.

The area model was applied exclusively to grown objects to focus on how the change

of interaction terms influences the area of the core. It is worth mentioning that the coalescence of objects can sometimes lead to a sudden and significant change in the interaction. We, therefore, examined the increase in interaction terms between two-time points. The distribution of the increase of interaction term was checked and any increase larger than 10 was removed as an outlier. These outliers accounted for less than 0.3% of the total observations and do not affect the performance of the area model.

Finally, we integrated the coalescence and growth models together to evaluate their combined effectiveness in predicting the state of objects. Since essentially these three states are mutually exclusive, an object could only have one state at one-time point. The state of an object can be assessed through the process illustrated in Figure 5.4. First, if an object is coalesced with others, it is classified as a coalescence object; otherwise, it is considered as a continuous object. Second, if the object's area increases, it is identified as a grown object; if there is no change, it is considered an unchanged object. Through this process, it is possible to predict the states of all objects in space. Therefore, first, the coalescence model was applied to the entire dataset, through which it was possible to label coalescence and non-coalescence objects. Subsequently, all the non-coalescence objects were extracted, upon which the growth model was applied to distinguish between grown and unchanged objects.

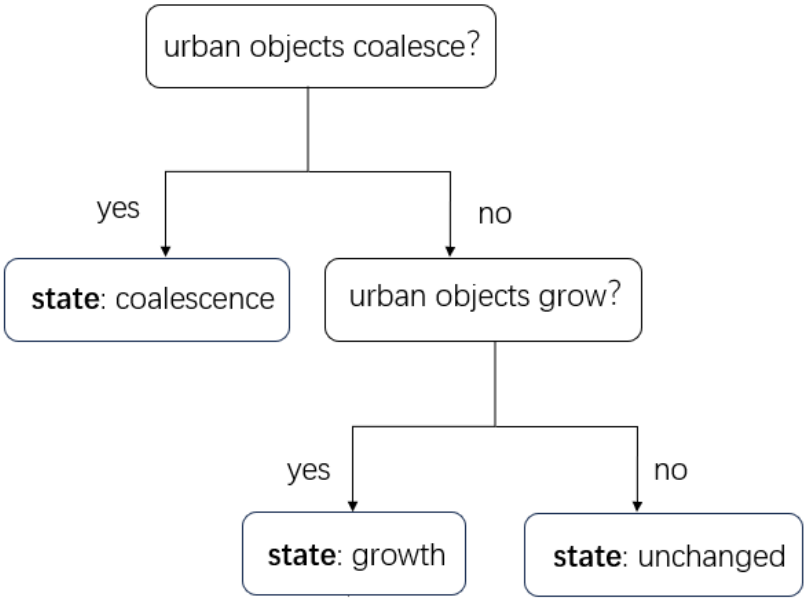

Figure 5.4 The integrated process for predicting the coalescence, growth and unchanged states of objects.

5.3 Results

5.3.1 Coalescence model

5.3.1.1 Model selection and validation

To acquire the best-fit model, we first applied our model with all covariates plus the random structure and checked the posterior distribution of each coefficient. The posterior distribution intervals for nearest_change_preyear, nearest_500_1000_change_preyear and largest _change were not all positive or negative, so they were removed from the model. We then ran the model with the remaining four covariates plus the random structure and checked the posterior distribution again, with all four covariates remaining significant. To further obtain the best-fit model, we used a backward stepwise elimination method to select from these four covariates. We first removed the percentage_changed_preyear which has the least

effect. When comparing the DIC of the model with four covariates and the model excluding the percentage_changed_preyear, the DIC of the latter one decreased slightly from 25647.86 to 25615.29, suggesting that excluding percentage_changed_preyear could increase the goodness-of-fit of the model. Thus, it was removed from the model. We then removed core_change_preyear since it had the least effect. The DIC of the model without core_change_preyear dramatically increased to 44339.17, suggesting that it should be kept in the model. We also excluded the random structure and compared the DIC with the model including the random structure. The DIC without the random structure dramatically increased to 56817.21. Therefore, finally, the best-fit model containing three covariates was identified: core_changed_preyear, nearest_500_changed_preyear and nearest_distance, plus the random structure.

Since we extracted a balanced sub-data-set to fit this model, to further validate how well the model predicts the coalescence of objects, we first fitted the model to all objects in the original dataset and then cross-validation was applied. A 50% probability was used as the threshold to determine whether the objects coalesce or not. If the probability is larger than 50%, object states are classified as coalescence and if smaller than 50% as non-coalescence. By using this 50% threshold, we transformed the mean posterior probability from the model to binary data indicating coalescence or non-coalescence for each object. Then by comparing the predicted value and original value in the dataset, the accuracy of the model was calculated. For the original unsampled dataset, the accuracy reached 91%, indicating an excellent performance. The AUC value was 0.92 which also suggests excellent model performance in terms of distinguishing between 0

and 1. We also checked the integer thresholds between 45% and 55% and compared the AUC and accuracy, but both were outperformed by the 50% threshold. Therefore, a 50% threshold for coalescence was finally selected.

Cross-validation was conducted to further validate the performance of the model. We randomly grouped the original unbalanced dataset into five folds for training (80%) and validation (20%). The model was fitted to the training data and then predicted the validation data. This process was repeated five times. The accuracy was calculated with an average of 86% for the validation data, and the AUC value was 0.84 demonstrating very good performance of the model.

5.3.1.2 Parameter interpretation

The final best-fit model includes an unstructured independent and identical random structure that accounts for variabilities between groups. The precision of this random effect has a mean value of 0.187 with a narrow interval from 0.17 to 0.205, which corresponds to a variance of 5.35 and low uncertainty in estimation. This relatively high variance suggests that between-group variation is relatively high and plays an important role in predicting coalescence. A summary of the fixed intercept and the other three fixed covariates is given in Table 5.2. Since we used a binomial model and a logit link to estimate the probabilities of the observed binary response through a linear combination, the intercept represents the baseline of the log odds when other variables are zero. In the logit model, a positive intercept indicates the baseline probability of the occurrence of predicted events is larger than 50%. In our case, the posterior mean of

the intercept is 1.340, suggesting that the baseline probability of the coalescence of an object is greater than 50%. When converting this log odds into probability, it equals 79.2% ($\frac{e^{1.340}}{1+e^{1.340}}$), implying that the default state of an object is that it is likely to coalesce.

Table 5.2 Summary of the fixed effects of the best-fit coalescence model

parameter	Mean	sd	0.025quant	0.5quant	0.975quant
α	1.340	0.067	1.210	1.340	1.472
β1	0.367	0.048	0.273	0.367	0.461
β3	0.738	0.046	0.648	0.738	0.829
β7	-6.808	0.156	-7.118	-6.807	-6.506

The posterior mean of β_1 and β_3, the coefficients of core_changed_preyear and nearest_500_changed_preyear are positive, suggesting that if the core object changed in the previous year and if there are changed neighbouring objects within the surrounding 'nearest distance plus 500 m' zone, the probability of coalescence of the core object will also increase. Nearest_500_changed_preyear has greater influence with a posterior mean of 0.738, which means that if there are changed neighbouring objects within the buffer, the log odds increase by 0.738, holding other variables unchanged. The log ratio for nearest_500_changed_preyear is $e^{0.738}$= 2.09, indicating that when holding other covariates fixed, the odds increase by 109%. If we use the baseline probability, when nearest_500_changed_preyear equals 1, the probability of coalescence increases to 88.9%. For core_changed_preyear, the posterior mean is 0.367, indicating a log ratio of $e^{0.367}$=1.443, suggesting that when holding other variables fixed, if the core object changed the previous year, the odds will increase by 44.4%.

Similarly, using the baseline probability and converting it into a probability, the probability of coalescence increases by around 5.4%.

The posterior mean of β_7, the coefficient of nearest_distance, is negative but the most significant, indicating that if the nearest distance between the core object and the neighbouring objects increases the probability of coalescence will decrease, and the coalescence of objects is strongly affected by nearest_distance. The negative value is not surprising since if the distance increases, the objects need to grow more to be close enough to another object to coalesce within one time period. It should be noted that the credible interval for β_6 is wider compared to others, indicating greater uncertainty in estimating the effect of the nearest distance.

5.3.2 Growth model

5.3.2.1 Model selection and validation

Similar to the coalescence model, we first applied our model with all six covariates to extract balanced non-coalescence objects. The posterior distribution intervals of percentage__500_1000_changed_preyear and nearest_changed_preyear were not all positive or negative. So, they were excluded from the model. We then ran the model with the remaining four covariates plus the random structure and checked the posterior distribution again, and all these four covariates were significant. Then a backward stepwise method was used to select from these four covariates. Percentage_nearest_500_changed_preyear was excluded first since it was the least significant. The DIC slightly increased to 28305.13 from 28296.47. Therefore, all four

covariates including core_changed_preyear, percentage_changed_preyear, largest_change_preyear and percentage_nearest_500_changed_preyear were kept for the final best-fit model. We also removed the random structure, but the DIC dramatically increased to 35695.88. Therefore, the random structure was kept in the model. A 50% threshold was also used to determine whether an object had grown or not. If the probability is larger than 50%, the object is treated as grown, otherwise, it is labelled as unchanged.

We fitted the final model to all non-coalescence objects in the whole dataset. The AUC value was 0.897 suggesting a good discrimination between grown and unchanged objects. The accuracy was also calculated at 88.8%, slightly smaller than that of the coalescence model, but still indicating an excellent performance overall. 40% and 60% thresholds were also used to compare with the 50% threshold, but the accuracies were slightly lower than for the 50% threshold. Therefore, the 50% threshold was finally used to determine whether an object had grown or not. Cross-validation was also conducted in a similar way as for the coalescence model. The average accuracy was 86.9%, which shows that the growth model accurately predicts the object states of grown and unchanged.

5.3.2.2 Parameter interpretation

Table 5.3 Summary of the fixed effects of the best-fit growth model

parameter	Mean	sd	0.025quant	0.5quant	0.975quant
α	-1.484	0.058	-1.598	-1.484	-1.371

β1	0.316	0.042	0.233	0.316	0.398
β3	0.014	0.001	0.012	0.014	0.016
β4	0.295	0.048	0.200	0.295	0.389
β5	0.006	0.002	0.002	0.006	0.009

The random effects account for heterogeneity within groups, with a mean precision of 0.137 and an interval from 0.124 to 0.150. Compared to the coalescence model, this indicates a larger variance among groups. Unlike the coalescence model, the posterior mean of the intercept is negative, suggesting that for the growth model, the base state is unchanged with a baseline probability of 18.4%. This low probability implies that objects are unlikely to change by default and other covariates must contribute significantly to increase the probability to achieve a growth state.

All other fixed effects are shown in Table 5.3 which are all positive, indicating that all these covariates play a positive role in the probability of growth. Core_changed_preyear (β_1) has the largest log odds of 0.316, suggesting that if the core object changed in the previous year, the probability increases to 23.8% from the baseline probability. Percentage_changed_preyear (β_3) and percentage_nearest_500_changed_preyear (β_5) have a small effect on the log odds, contributing marginal increases. These increases are small, but it should be noted that one unit is only 1% suggesting that the accumulated increase should not be neglected. For example, a 50% percentage_changed_preyear will increase the probability to 31.3% from the baseline. Lastly, Largest_change_preyear (β_4) has a slightly smaller effect than

core_changed_preyear, with a 4.9% increase in the probability.

5.3.3 Area model

5.3.3.1 Model selection and validation

Before running the model with all covariates for the grown objects, we first checked the correlation between the largest interaction and the interaction between the core and the largest object, the second-largest interaction and interaction with the second-largest object, the third-largest interaction and interaction with the third-largest object. The results show that these three pairs have large correlations of 88.6%, 76.1% and 71.5%, respectively. Therefore, we included only the largest interaction, the second largest interaction and the third largest interaction, and removed β_9 to β_{11} in the model. We then applied the model including β_0 to β_8 first. The third_largest_interaction_preyear, largest_area_preyear, second_largest_area_preyear, third_largest_area_preyear and nearest_area_preyear, had intervals crossing zero. Thus, they were excluded from the model. Then a model including β_0, β_1, β_2 and β_8 was applied. They were all significant and so a backward stepwise selection process was conducted. Second_largest_interaction_preyear was removed first since it was the least significant variable. The DIC slightly decreased from -2730.76 to -2743.60, suggesting that the model without second_largest_interaction_preyear is better fitting. We then removed the nearest_interaction_preyear and the DIC decreased to -2756.81. We further removed year and the DIC significantly increased to -1229.96. Therefore, the final model included only year and largest_interaction_preyear. We then added the sized-

group factor for largest_interaction_preyear, and the DIC decreased to -2769.35. Thus, the final model includes year as a linear temporal effect and the size-class varying largest_interaction_preyear.

5.3.3.2 Parameter interpretation

The posterior fixed effect is shown in Table 5.5. The area model has a fixed intercept that has a posterior mean of -1.823 with a standard deviation of 0.040. Since we used a Gamma distribution, the value of the intercept needs to be log-transformed to represent the area of core objects. Thus, the overall mean baseline of the core area is $e^{-1.823} =$ 0.161 km^2. For the fixed temporal effects, one unit (i.e., a one-year increase) corresponds to a 5.2% increase. Time also has an extremely small standard deviation, implying a low uncertainty relating to the effect of time.

For the interaction effects, as shown in Table 5.4, the parameters are positive for all five groups, suggesting that if the interaction increases, the area of core objects also increases. Among the five groups, group E has the least effect with a mean posterior probability of 0.052 and group D has the largest effect with a mean posterior of 0.186. Converting these to the original scale suggests that if the interaction increases by 1 unit, and holding other parts fixed, the area of the core object increases by 5.3% ($e^{0.052} = 1.053$) and 20.4% ($e^{0.186} = 1.204$), respectively. The credible interval for group D is very wide, as shown in Figure 5.4, indicating that the interaction effect for this group has a larger estimation uncertainty compared to other groups. This is probably due to the limited number of objects in this group. In contrast, groups A, B, C and E have much

narrower intervals, suggesting low uncertainty of estimation. Apart from group D, the effect of interaction decreases as the area increases. With a one unit increase in interaction, the area increases by 9.5%, 8.4%, 6.4% and 5.3% for groups A, B, C and E, respectively.

Table 5.4 Summary of fixed effects of the best-fit area model

parameter	Mean	sd	0.025quant	0.5quant	0.975quant
α	-1.823	0.040	-1.901	-1.823	-1.745
β0	0.051	0.002	0.048	0.051	0.055
β1A	0.091	0.008	0.076	0.091	0.106
β1B	0.081	0.009	0.063	0.081	0.098
β1C	0.062	0.011	0.041	0.062	0.084
β1D	0.186	0.063	0.063	0.186	0.310
β1E	0.052	0.013	0.026	0.052	0.078

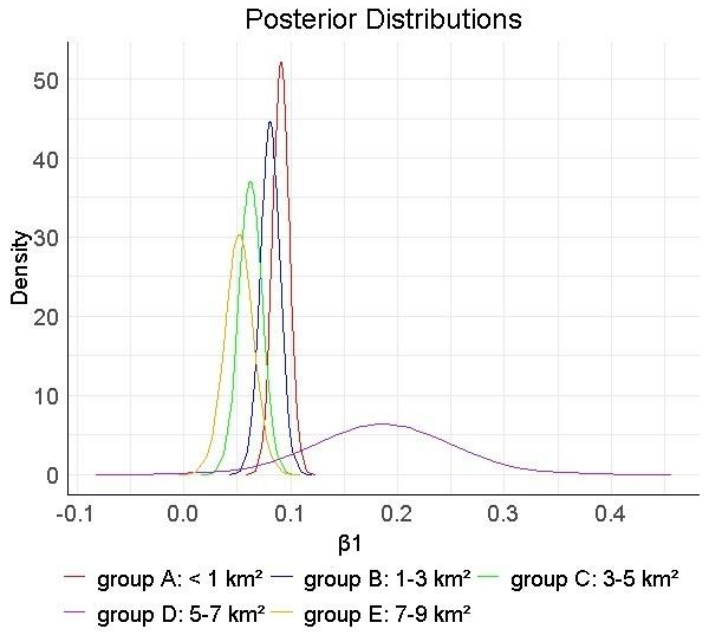

Figure 5.5 The posterior distribution of fixed interaction effect for each sized group.

5.3.3.3 Model hyperparameters

The model includes an unstructured identical and independent random effect to account for between-group variation. Its precision σ_{μ}^{2} has a posterior mean value of 1.42 and a relatively narrow interval, indicating a variance of 0.704 for between-group variation, implying that there is moderate heterogeneity between groups. Finally, the precision for the Gamma observation σ_{ε}^{2} has a high posterior mean value of 19.46 and a narrow interval, representing a low variance of 0.05 implying a narrow interval for each object.

Table 5.5 Summary of the hyper-parameters in the best-fit growth model

parameter	Mean	sd	0.025quant	0.5quant	0.975quant
$\boldsymbol{\tau_{\mu}}$	1.42	0.067	1.29	1.42	1.56
$\boldsymbol{\tau_{\varepsilon}}$	19.46	0.759	18.00	19.44	20.99

5.3.4 Combination of coalescence and growth models

We combined the coalescence and growth models together to predict comprehensively the state of all objects, following the process illustrated in Figure 5.3. First, the coalescence model was fitted to the entire dataset. Then the 50% threshold was used to distinguish between coalescence and non-coalescence objects. Second, the growth model was fitted to all the non-coalescence objects. Similarly, the 50% threshold was used to distinguish between grown and unchanged objects. We then acquired the predicted state of coalescence, growth and unchanged for all objects. The accuracy for the coalescence and growth models was also calculated for each year. Overall, both models demonstrated high accuracies, mostly larger than 80%. The only exceptions were 2017 for coalescence and 1993 for the growth model which both have accuracy over 75%.

We also used 2010 as an example to illustrate the model's prediction of the state of objects. The observed state of each object and the predicted state are mapped in Figure 5.6. The spatial distribution of covariates in 2010 is shown in Figure A1. The mean, lower and upper bound of posterior probabilities for the coalescence and growth models are also mapped (Figures 5.7 and 5.8). The colour scheme is the same in figure 5.7 and 5.8 respectively for lower, mean, and upper maps and it can be seen in the figures that the lower and upper limits generally reflect lower and higher probabilities. It should be noted that the accuracy is calculated based on the number of objects not considering their area. The large coalescence objects in the map are notable, but they account for

only a small number of the whole set of objects. It could be seen from the map that most large objects experienced coalescence this year. This trend is also shown in the probability map where large objects have a larger mean probability. Some variability is shown in the small objects, while growth exhibits more variability.

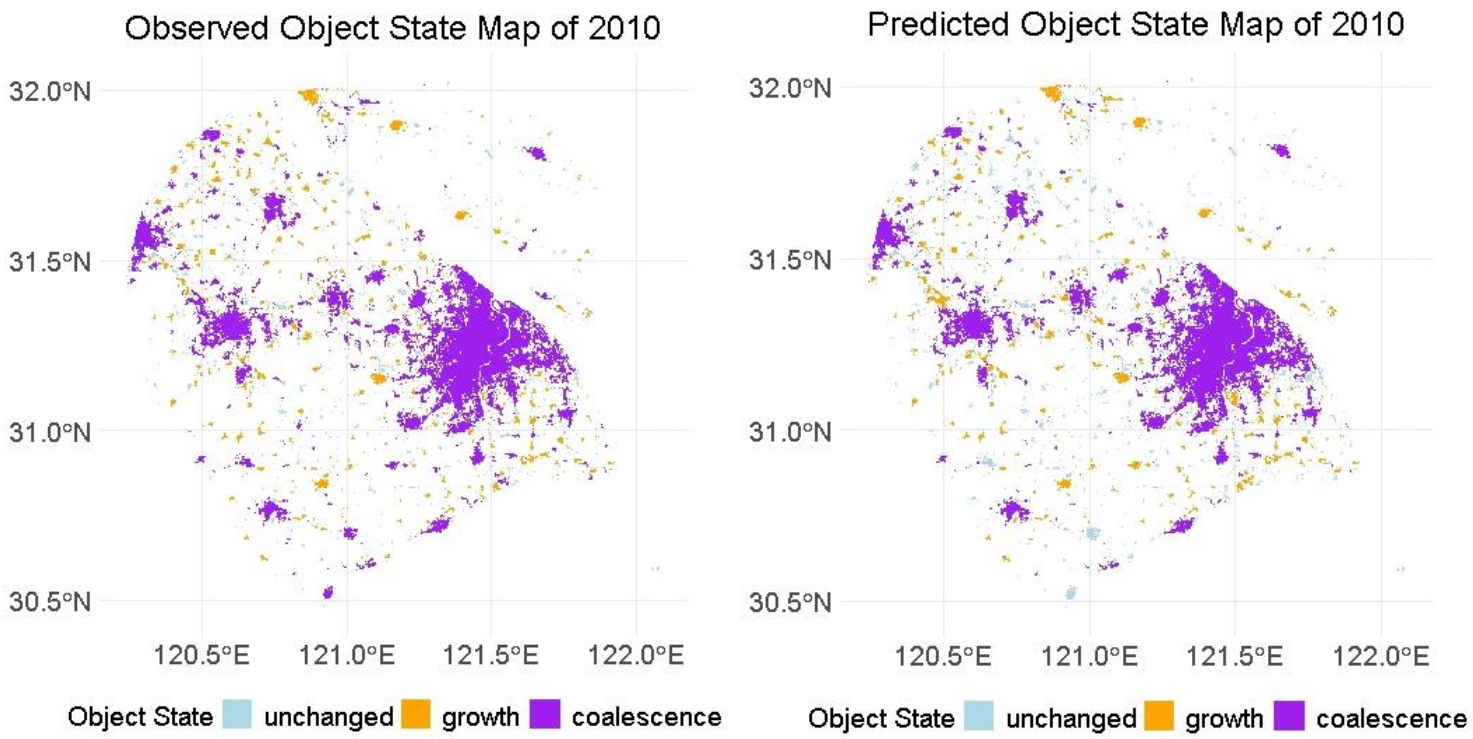

Figure 5.6 Observed and predicted objects in 2010.

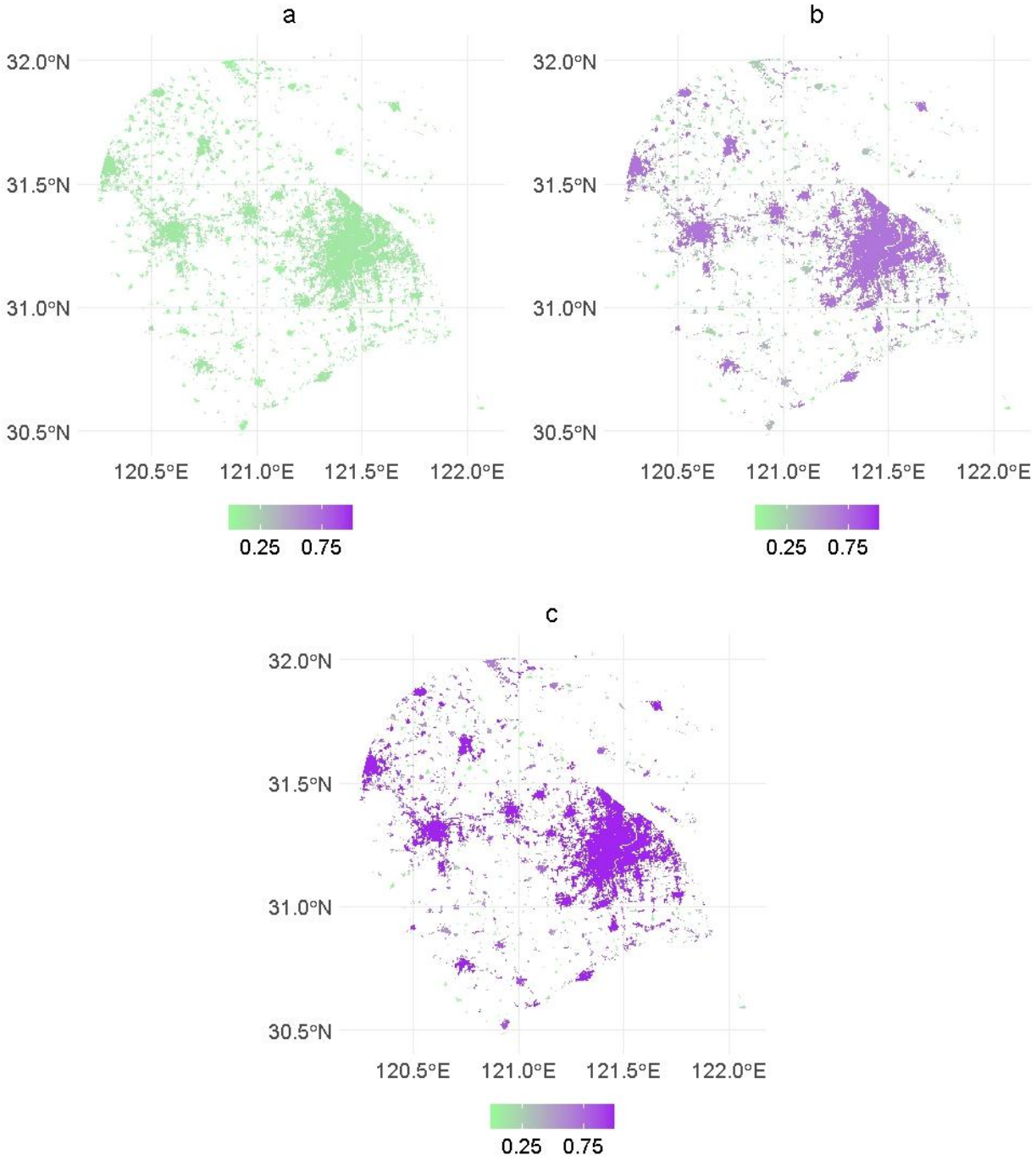

Figure 5.7 The posterior (a) lower, (b) mean and (c) upper limits of the 95% credible intervals of the predicted probability of coalescence in 2010.

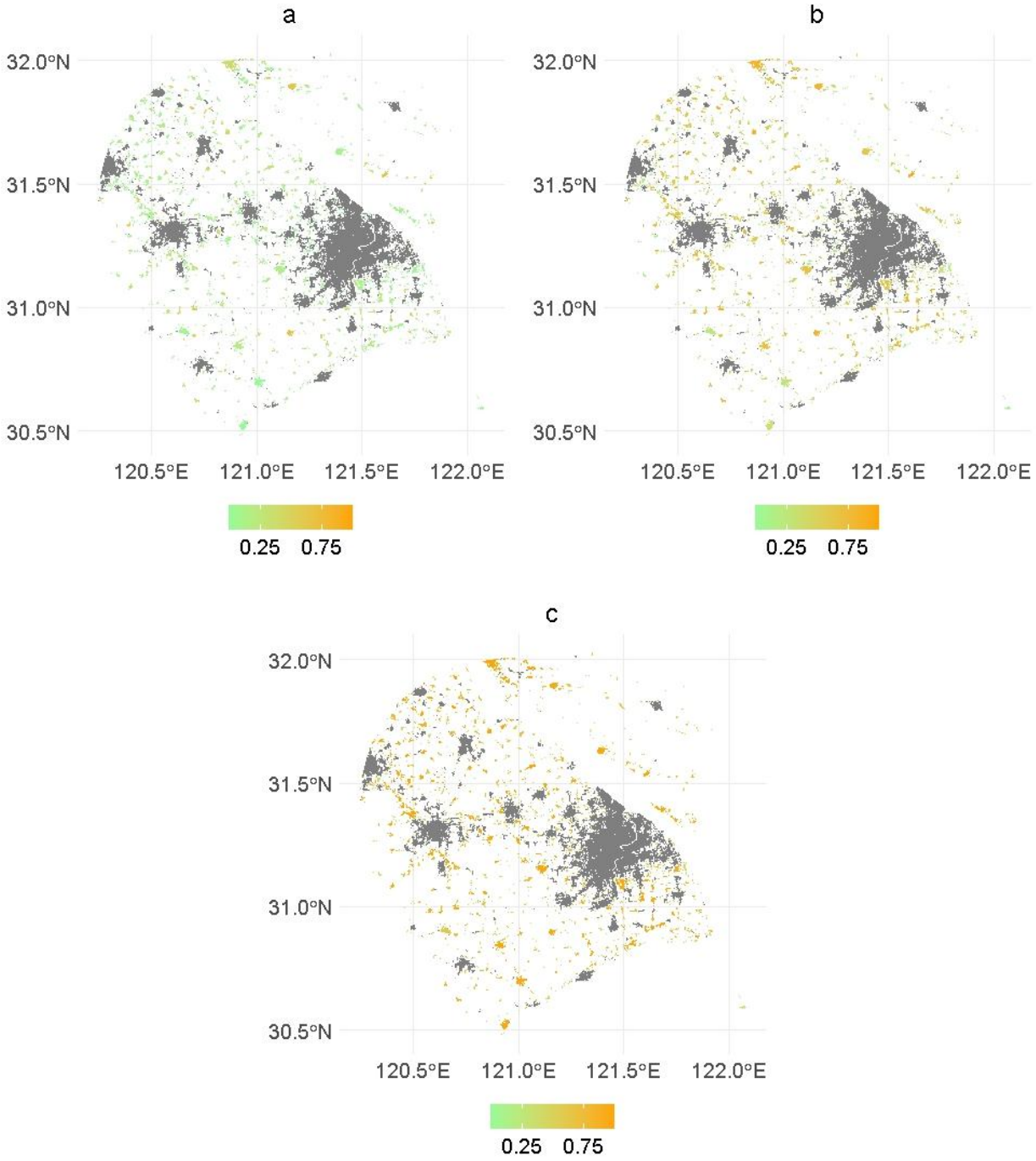

Figure 5.8 The posterior (a) lower, (b) mean and (c) upper limits of the 95% credible intervals of the predicted probability of growth in 2010.
The grey objects represent coalesced objects which are not included in the modelling.

5.4 Discussion

We proposed a novel object-based approach to explore the states of core urban spatial objects and their association with the dynamics of neighbouring urban objects. Utilizing

generalized linear mixed models, fitted in an approximate Bayesian inference framework via INLA, we were able to effectively model binary data and skewed data with a within-group structure. Our results demonstrate how changes in the states of neighbouring objects influence the state of urban objects. Specifically, the fitted models suggest that the coalescence state of urban objects is strongly affected by the *distance* to its nearest neighbouring object in the previous year. Intuitively, this makes sense, since coalescence requires proximate distance to collapse to zero. Additionally, the coalescence state is related to the states of the urban object itself and neighbouring objects located within a buffer around the core object, with a buffer width of the nearest distance from the core object to the neighbours plus 500 m.

The fitted models suggest that the growth state is related to the state of the core object itself as well as that of its *largest* neighbour in the previous year. Furthermore, it is also associated with the dynamics of local neighbours represented by the percentage of grown objects amongst its neighbours and the percentage of grown neighbours in a defined buffer. We found that the area of grown objects has a relation with the largest interaction between the core object and its neighbours which affects core objects of varying sizes in different ways.

For the coalescence state, an increase in the nearest distance from the core object to its neighbours significantly reduces the probability of coalescing. This is not surprising as for coalescence to occur, objects have to be close enough to be connected. However, when we analysed our findings further if the nearest distance is only 300 m (i.e., one

pixel side) while keeping the baseline probability and the other two covariates to 1, the probability of coalescence rises to 60.1%. While if the distance extends to 600 m (i.e., two-pixel sides), with other variables remaining unchanged, the probability decreases to 16.3%. At the same time, whether the nearest object changed in the previous year is insignificant. Taken together, these results suggest that the core does not necessarily coalesce with its closest object, but nevertheless is likely to coalesce with objects within a two-pixel plus the nearest distance radius around the core boundary, which corresponds to 600 m plus the nearest distance around the core object. This aligns with the observed significance of covariates nearest_500_changed_preyear and the insignificance of nearest_500_1000_changed_preyear.

For the growth model, our results indicate that the growth state of the core is significantly influenced by both the core itself in the previous year and its local dynamics in the previous year, represented by two relevant covariates (in percentage units). Similar to the coalescence model, the growth state does not correlate directly with the state of the nearest object; instead, it tends to be associated with the state of nearby neighbours. This implies a potential spatial autocorrelation in the growth state. In reality, a local space may share similar local growth drivers, causing objects within a neighbourhood to undergo similar changes. Furthermore, this could also explain why the state of the largest object has the second-largest effect: the largest object can act as a "source" and diffuse the "growth" outwards within a local space, thereby affecting the surrounding objects.

Both the coalescence and growth states were found to be related to the state of the core object itself in the previous year. However, it is important to note that when we incorporated an autoregressive correlation structure with order 1, namely the AR1 structure, into the growth model the estimated autocorrelation coefficient (rho) was minimal, with a mean value of 0.21 and a credible interval of [−0.163,0.568] as illustrated in Figure A2. This interval includes negative, positive and zero values, indicating that the temporal autocorrelation could be negative, positive and non-existent. This implies that although the growth state relates to its previous state, overall, it cannot be regarded simply through temporal autocorrelation. While most of the objects have a positive rho value, there remains the possibility of no temporal autocorrelation. This might be attributed to the complexity of urban systems that exhibit complex characteristics. It could also be due to local variation in the underlying processes. We included a random structure to allow for random deviation for each group (i.e., each continuous object with the same ID). However, there might be spatial heterogeneity that leads to non-consistent behaviour of urban objects and which cannot be captured fully by random deviation. Thus, the temporal relation appears to be complex for urban objects which requires further exploration, accounting for spatial variation.

For the area model, we focused mainly on the relationship between the area of the core object and its interaction with neighbouring objects. The findings indicate a positive relation between the size of the core and its largest interaction, with this relationship varying slightly depending on the size of the core object. Generally, smaller core objects exhibited a larger correlation with their neighbours, suggesting that the same interaction

could have a greater influence on smaller objects compared to larger ones. This observation aligns with our original hypothesis that the interaction could have different effects on different-sized objects. When rethinking the relationship between objects from a network perspective, where objects are treated as nodes and interactions as link weights in the network, larger nodes tend to have greater centrality and connectivity, thereby influencing the dynamics of surrounding nodes. In contrast, smaller nodes are more susceptible to being influenced by others. We examined this relationship at the patch level, and other studies have shown that it applies on a larger scale. For example, within an urban region, small cities are likely to be influenced by the core city that serves as a regional centre through flows and interactions occurring between them. Due to the limitations of our data, we were unable to check whether this relationship (larger objects tend to exhibit more coalescence and a shorter continuous period of existence) remains true for objects larger than 9 km^2, although the general behaviour is clearly driven by underlying geometrical laws. This could be investigated in future for the specific case of China through the collection of more data across different cities. Lastly, it is also worth mentioning that since the area model modelled only the area of grown objects which could not be continuous over time, we were not able to include an AR1 structure to examine the temporal autocorrelation in the model.

Models fitted using a Bayesian inference framework have been applied in various fields, including epidemiology, environmental science and crime geography (Cai and Dunson, 2006; Aguilera et al., 2011, 2011; Smith et al., 2017; Zheng et al., 2024), due to their ability to handle complex structures and spatial-temporal processes. To the best of our

knowledge, this is the first study to combine a mixed model fitted in an approximate Bayesian inference framework with an object-based approach to explicitly model the relationship between urban spatial objects and their neighbours. The fitted models handled efficiently the complex binary skewed data with a random structure. They reveal that the state of the urban spatial objects is associated with both their states in the previous year and the dynamics within a local neighbour in the previous year. The package used for approximate Bayesian inference, INLA, offers several spatial autocorrelation structures such as the commonly used ICAR (Intrinsic Conditional Autoregressive) and SPDE (Stochastic Partial Differential Equation) terms. However, since our goal extends beyond merely predicting the state of objects, to explicitly exploring how the dynamics of neighbouring objects affect the states of core urban objects we did not include a spatial autocorrelation structure in our model. While the need for such autocorrelation terms is diminished by the good fit of our models and the resulting small residuals, this could be explored further in future research alongside our findings. We also used a weakly informative prior in the Bayesian fitting. When applying the proposed models to other cities in the future, the information gained here from analysing the megacity of Shanghai could serve to provide more informative priors.

Our models predicted the state of coalescence with high accuracy. Amongst the predicted coalescence states, 93.1% were real coalescence events. 89.4% of all actual coalescence events were predicted as coalescence. In contrast, the growth model displayed greater uncertainty, with 67.9% of predicted growth events being actual

growth events and 61.3% of actual growth events being identified by the model. This lower accuracy can be partially explained by the fact that the growth model is applied only to non-coalescence data and 91.1% of the predicted non-coalescence objects are actual non-coalescence objects. Therefore, taking these two results together (non-coalescence and growth) the result can be seen as acceptable overall. The uncertainty may also be attributed to the complexities of the growth process. As discussed earlier the temporal autocorrelation in growth is complicated. Additionally, there may be social, economic and other activities not incorporated in the model apart from the inherent characteristics of urban objects. The underlying assumption of this model is that urban growth is systematic and exhibits simple characteristics, but temporal or spatial variation in the underlying processes could increase uncertainty in the models. Therefore, future research could include other types of data representing underlying processes and more complex spatial-temporal structures to increase model accuracy.

Our models generated a probability map for coalescence and growth, along with a predicted state map (Figures 5.7 and 5.8). Taking 2010 as an example, as can be seen from Figure 5.7, most large objects are predicted to coalesce and exhibit a high coalescence probability in 2010. From a network perspective, the changing state of these objects suggests these key nodes experience changes in their weights and connectivity, which subsequently influence the dynamics of the entire network. Consequently, identifying the states of these objects is important for understanding the dynamics of the entire network. Our labelling process does not directly label continuous coalescing objects, but our data suggest that larger objects, particularly those larger than

20 km², tend to show continuous coalescence. This can also be explained by our model, in which coalescence in the previous year, classified as changed, increases their probability of coalescing in the present year.

The selected region covered Suzhou, represented as the second largest object on the map, to the west of Shanghai which is the largest object (Figures 5.6-5.8). From the given example map, it could be seen that around the close neighbours of the largest core urban objects in Shanghai and Suzhou, objects tend to exhibit a greater probability of coalescence and growth. This implies changes of states in close neighbours around large objects, which further increases their probability of coalescence or growth in subsequent years. Interestingly a few urban objects around such large objects have a low estimated coalescence or growth probability. The potential reasons based on the fitted model could be (i) the object did not undergo any changes in the previous year, which would lower the probability of coalescence since the state of the core itself has an important role in its state in the following year, (ii) the network generated does not fully capture changes in the neighbours around these objects and (iii) as discussed earlier, the growth state is complicated and exhibits greater uncertainty. Identifying these low-probability objects located amongst neighbouring objects that are rich with changing states could help to increase model performance in the future.

Compared to traditional raster-based methods, our object-based approach provides insights into the explicit relationships among objects, as well as a framework for modelling the states of urban objects over time. First, commensurate with an increasing

focus on network studies in urban science, such as networks of cities, human activities and urban transportation, our research provides a way to build a spatial-temporal network of urban objects at the patch level (Cvetojevic and Hochmair, 2021; Mussone and Notari, 2021; Gu and Wang, 2022; Marin et al., 2022). Rather than concentrating solely on transitions in the objects themselves, we studied the dynamics of these urban objects from a relationship perspective. In the real world, urban objects evolve through growth and coalescence and interact with each other through the various activities located in objects, which leads to the dynamics of urban objects. We establish graph-based spatial-temporal connections amongst urban objects to represent, at an abstract level, their real-world evolution and interactions allowing us to study urban dynamics directly. Furthermore, this node-link perspective contributes to the study of patterns and processes in the evolution of urban systems. A central issue in studying urban growth is to link the spatial-temporal data gathered with relevant processes to uncover the underlying processes, and how they affect the dynamics of patterns. Our method incorporates interactions into the study of urban growth, which represent key processes that influence the dynamics of urban objects. This approach offers a novel perspective in urban growth studies that could integrate other real-world processes with urban object change.

This research can be extended in future by considering the following. First, we built graph-based links amongst urban objects based solely on proximity through a triangular irregular network (TIN) and, thus, modelled directly only the relationships with close neighbouring objects. However, within the network, some important nodes might

influence more distant nodes through direct links. Specifically, the impact of large urban objects on other objects may not be fully represented in the model. Second, our analysis focused on the dynamics of the objects themselves. Our implicit assumption was that urban growth is a systemic phenomenon and, thus, it can be modelled as a function of the inherent characteristics of the urban objects themselves. However, there exist many complex interactions in reality, such as population and transportation flows, occurring within and between the urban objects which may influence urban object dynamics. These exogenous and ingenuous drivers are not included in the present model, but integrating different types of data could help to extend the scope of this research in future. Third, in this research, we focused solely on the relations between the core urban object and its neighbouring objects. However, the constructed network structure allows the exploration of more dimensions, such as how the network structure evolves, including how its connectivity, node attributes and fractal dimensions change over time. Recently, networks have gained significant attention within urban studies due to the increasing availability of diverse data types and advances in network analysis methods. Nevertheless, many of them focus on the city level or the micro level of specific activities within a city (Castells, 2010; Esch et al., 2014; Inostroza, 2021; Jia et al., 2021). Patch-level study of objects in urban dynamics is still limited. Future research could, thus, explore the dynamics of urban object networks from spatial-temporal perspectives. Finally, this research examined only the linear relationships between the core urban object and neighbouring objects. Their relationships might be nonlinear which remains to be further explored.

5.5 Conclusion

In this research, we built spatial links amongst urban spatial objects and integrated them with the states of objects to model the states of urban objects and how they relate to the dynamics of other objects. Our method essentially creates spatial-temporal links among urban spatial objects which allows further exploration of the spatial-temporal relationships among objects. The fitted Bayesian linear mixed-effects model suggests that the coalescence state is related to the previous state of the object itself, the nearest distance to other objects and the state of neighbouring objects within a specified close buffer. The model suggests that the growth state is related to the previous state of the object itself, the state of the largest neighbouring object and the states of objects within a close buffer. The area of growth objects is affected by the largest interaction between the core object and its neighbours, with this effect varying for different-sized objects. The key contribution of our research is not merely to predict the states of urban objects but more importantly, to build spatial-temporal links among objects to explicitly model their relationships, which could help to a better understand urban dynamics and its associated processes. The research provides valuable insights into the evolution of spatial-temporal networks of urban objects and presents a novel perspective within urban growth studies.

6 Discussion

Chapters 3 to 5 analysed urban growth based on a comprehensive object-based method emphasizing different aspects including growth characteristics, growth processes, and the relationships between urban objects. This research suggests that an object-based approach is suitable as a means to capture the spatial-temporal pattern of urban growth across megacities, depict urban processes both at the patch level and the city level and explicitly represent the relationships between urban objects. Collectively, the research provides a new perspective with which to model and understand the patterns and interactions of urbanization both spatially and temporally.

6.1 Research Findings and Contribution

Chapter 3 analysed urban growth trajectories from an object-based perspective. It highlighted the unprecedented urban expansion in China from 1992 to 2014, driven by national reform policies, economic development and population migration. This expansion also exhibited disparities across China, with coastal regions experiencing faster and earlier growth due to policy benefits. By comparing the growth trends in different spatial buffers, urban growth characteristics at different levels were further explored. This provided insights into the relationships between core cities and their surrounding cities within megacity areas, and how the relationships differ across regions.

The results also identified synchronous growth trends across regions during certain periods, suggesting that national policies influenced overall urban growth dynamics. However, asynchronous patterns were also exhibited, which suggests the role of local factors such as geographic constraints and regional governance strategies in shaping urban growth trajectories. The general growth trends and disparities in the growth patterns of different regions imply that China's urban growth trajectory is the result of the interaction between national policies, local governance and geographic constraints. Understanding the influence of national and regional policies on urban growth trends and regional patterns could help design future development strategies as well as maintain future sustainability.

The inherent definition of urban objects determines that the object-based method provides a temporally-continuous measurement of urban growth. Therefore, it can directly reveal the evolution of urban objects that is difficult to achieve through other methods. The results suggests that the object-based method is highly effective at capturing spatial and temporal urban dynamics. It is scale-independent and, thus, is comparable across space and time, which makes it particularly useful for inferring underlying urban growth processes.

Chapter 4 focused on characterizing different urban growth events including dispersal, establishment and coalescence, representing different growth phases in the defined zones in four megacities. It provides a framework to measure urban growth events at the per-object level as well as the city level, which could further infer how

urban objects emerge, stabilize and merge, and how cities grow over time. Ideally, dispersal, establishment and coalescence should change at a stable rate if the underlying growth process remains constant. However, the results show variation in the growth rate of events for four cities, revealing the influence of "disturbances" such as the effects and interactions of spatial, economic and policy factors on urban growth.

By accumulating the occurrence of different events in different defined zones, synchronous trends in the events within the core areas and buffer zones were observed, which suggests that urban growth drivers have similar effects on the dynamics of the different events and, therefore, lead to similar behaviours of these events at the population level. Previous studies suggest that urban growth would follow a typical sequence of dispersal, establishment and coalescence. At the patch level, the proposed sequence is observed. However, varying sequences of dispersal, establishment and coalescence were observed across four cities at the population level. This suggests that the states are concurrent, with a dominant state arising alternately through time. The concurrent and varying sequences of the dominant events indicate that urban systems are complex and dynamic, influenced by various factors.

Object-based measurement enables us to track directly the evolution of each urban object for the first time. Through building temporal links, different states which correspond to different growth processes are assigned to urban objects. It then reveals

the urban growth process at the per-object level. When accumulating at the city level, the overall urban growth process could be further analysed. Through building temporal links among urban objects, the research findings contribute a comprehensive understanding of urban growth events at both the patch level and city level by quantifying changes in different events, which provide valuable insights into the underlying micro urban growth process and the overall evolution of urban systems.

Chapter 5 introduced a novel object-based approach to modelling urban growth with an emphasis on the interactions between urban objects. Using Bayesian linear mixed effects models and building spatial-temporal links between objects, the research examined how the states of coalescence, growth and 'unchanged' are related to the dynamics of urban objects and how the area of grown objects is related to the interaction between objects.

The coalescence state is influenced by the previous state of the objects, the state of objects in a defined close buffer and the nearest distance between the object in focus and other objects. Among these, the nearest distance plays a significant role with the probability of coalescence decreasing significantly as the nearest distance increases. According to the results, the urban object does not have to coalesce with the nearest object, but it is likely to coalesce with objects within a buffer of 'two-pixel radius plus the nearest distance between the core and neighbouring objects around the core boundary'. Since coalescence changes the overall urban pattern structure and urban

land connectivity, this suggests that the spatial proximity of objects plays a pivotal role in influencing urban growth patterns.

The growth state is heavily influenced by the previous state of the object in focus as well as the dynamics of its neighbouring objects. The temporal autocorrelation of the growth state is non-consistent, but the results imply an underlying spatial autocorrelation. The changes in the objects located in a defined neighbourhood contribute to increasing the probability of growth of the core urban object, which indicates that dynamic neighbours are potentially related to the growth of the core object. This highlights the importance of understanding local interactions in studying urban growth, as these micro-level dynamics can be accumulated to affect regional urban growth.

For the model predicting the area of objects that have grown, the result suggests varying relationships between the size of urban objects and their interactions with neighbouring objects depending on their size. In general, smaller objects have a greater relationship with the interaction terms especially for objects smaller than 9 km^2.

Combining the coalescence and growth models, an overall state of urban objects was calculated with high accuracy for the coalescence state and moderate accuracy for the growth state. In general, this suggests that the coalescence and growth states of urban objects can be predicted from their previous states and the dynamics of their defined neighbours. Taking the results of the three models together imply that smaller objects are more susceptible to object interactions while larger ones tend to affect the states of

their neighbours, especially for the growth state and their corresponding areas. This aligns with network theories, where larger nodes have greater influence within a system. In general, the results provide a novel framework with which to analyse the dynamics of urban objects and their relationships through the spatial-temporal links between objects.

Based on the temporal links between urban objects, additional spatial-temporal links are created. This approach is novel, demonstrating how the dynamics of urban objects can be viewed in the form of a spatial-temporal network. In this generated network, interactions between objects are represented as links and objects are treated as nodes. This means that the dynamics of urban objects can be modelled to analyse how they are influenced by the attributes of urban objects (nodes) and interactions between objects.

Chapters 3 to 5 demonstrate that urban land can be represented as urban objects which can be further analysed to study urban growth dynamics. These objects can be used to characterise urban growth continuously. This research is novel because it builds links between objects which allows their evolution and their potential interaction with other objects to be tracked. Through building temporal links between urban objects, urban growth processes are measured directly at both the patch level and population level, providing valuable insights into urban growth theory. The generation of spatial-temporal links between urban objects provides a way to model urban dynamics through the perspective of spatial-temporal network of urban objects. The results suggest that urban objects could be treated as an evolving system and the dynamics of objects could

be modelled by its inherent attributes.

Overall, the results suggest that the object-based method performs well at capturing urban growth processes at both patch-level and city-level. The key advantage of the object-based method is that it can represent urban entities directly and, therefore, analyse explicitly the relationships and interactions between urban entities. In contrast, in the raster-based method, the relationships between urban land are usually measured at the pixel level and such relationships are *inferred* from the analysis of raster data. The object-based method makes it possible to build spatial-temporal links of urban objects, which facilitates modelling their relationships directly, which is hard to achieve using a raster-based method. The temporal link provides an approach to tracking the dynamics of each urban object to study its evolution characteristics. The spatial link mirrors the interaction between objects. It not only allows for explicit modelling of the relationships between objects, but also provides a new perspective for studying the interplay between urban objects and the underlying processes.

6.2 Limitations and Future Research

While this research provides valuable insights into urban growth, several limitations should be noted. First, the measurement of urban growth focuses on spatial expansion, while urban entities are 3D in reality. Thus, the intensification of urban land use and vertical expansion should be considered as an important aspect when evaluating urban growth (Lin et al., 2014; Xia et al., 2020; Yang and Zhao, 2022; Yang et al., 2022). In future research, such vertical height data could be incorporated along with the land

cover data as a factor representing intensity to fully characterize urban growth. Also, the land use data used to represent cities necessitates that urban objects can only expand or be unchanged. However, although much less common, in the real world cities can also experience a decreasing area, for example, commensurate with a decrease in the population or economy (Mallach et al., 2017; Vinci et al., 2023). How to represent this phenomenon remains a further consideration. Another issue is that although the ESA data generally has a very high accuracy of land cover classification and this was evaluated through various means in this thesis. Nevertheless, some uncertainty remains, especially for specific outcomes such as the very high rates of growth reported synchronously across China in some years. Ideally, possible errors in the data and the classification process should be further examined through additional validation procedures. Moreover, the developed object-based methods should be applied to other data or the combination of multiple data in future research.

When building spatial links amongst urban objects to study their relationships, only the intrinsic attributes of the objects themselves are included, such as the area and the state of objects to represent their potential connections. In reality, the relationships between objects could be defined in multiple dimensions, and described by different types of activities, such as population flows, economic interactions and wireless connections (Sultana and Weber, 2014; Gibbons et al., 2018; Yang et al., 2022). These activities also contribute to the dynamics of urban growth patterns. In this research, the underlying processes are inferred through the analysis of the dynamics of urban objects. Some studies focused solely on the interactions of activities *within* cities, but how to integrate

these activities with the dynamics of urban spatial objects to study urban growth remains an open question for further investigation. Linking such data to urban objects could provide a more comprehensive understanding of the interactions between the related processes and urban growth patterns.

Although urban land is represented as objects in this research, the object data are extracted from raster data. The object-based method is scale-independent, but whether changing the spatial resolution of the raw data would affect the results of the analysis remains a topic for further research. For example, in the coalescence model, the results suggest that coalescence is likely to occur with objects located two pixels (i.e., 600 m) outwards from the core. Whether changing the spatial resolution of the raw data would influence the result should be further explored to evaluate the sensitivity of the model to such scale effects.

A key feature of the geographical phenomenon is spatial heterogeneity (Balaguer-Beser et al., 2013; Brelsford et al., 2017; Reia et al., 2022). Spatial heterogeneity is the fundamental basis of geographical models, but it also presents challenges in generalizing model results and applying models across different regions. The models in Chapter 5 focus on a specific city while whether the findings can be applied to other cities with differing contexts should be further examined to confirm the model's generalizability and robustness. Application to other cities could also reveal similarities and disparities among cities. Another issue with spatial heterogeneity is that it could also occur at the within-city level which increases the uncertainty of the models. The

model used implies a similar relationship between objects while there could be spatial variation in the relationships in practice. Local effects and geographical constraints could lead to differences in the interactions between objects. Future research could examine the spatial-temporal heterogeneity to obtain a deeper understanding of urban dynamics.

Last but not least, since there is limited research on exploring the relationships between objects, this research uses simple linear models that serve as a starting point for future research. Linear models are relatively straightforward to interpret which could provide general insights into the relationships to further exploration. However, the interactions between objects could be more complicated and non-linear. More advanced and sophisticated methods should be applied to acquire a deeper understanding of these complex relationships and more accurate predictions. Similarly in the area model, the temporal effect is simplified as a linear effect. It is modelled that time has a fixed linear effect on the area of urban objects suggesting that the growth rate is the same over time, but there could be short-term fluctuations in the growth of the area. In this research, we mainly focused on the interaction term, and more complicated structures could be included to increase model performance.

In this research, a set of spatial-temporal links between objects is constructed which generates a spatial-temporal network. The network of objects suggests a variety of aspects that could be further studied, such as the attributes of important nodes, the flow in the network and network evolution (Castells, 2010; Agryzkov et al., 2019; Maduako

and Wachowicz, 2019; Mussone and Notari, 2021). Some network studies have been applied at the city level to study the dynamics of cities at the regional level. Such methods could also be applied at the patch level to study inter-city dynamics. For example, some research defines city clusters through urban networks (Yu et al., 2014; Jia et al., 2021). This could also be applied at the patch level to identify inter-city structures.

The application of rank-size, fractal dimension and scaling law have been studied intensively in urban growth research, especially at the city level (Batty, 2012, 2023; Huang et al., 2015). These studies help to understand city evolution from a hierarchical perspective, and based on the morphology and spatial complexity of urban patterns. Based on object-based methods, these approaches could also be applied at the patch level to reveal the dynamics of objects over time from a unique perspective.

7 Conclusion

This thesis utilized a novel object-based method to characterize urban growth trajectories and infer the potential processes underlying them; propose urban growth events based on temporal links between objects and examine how these events differ spatial-temporally to rethink urban growth theories; explicitly model the relationships between urban objects through the spatial-temporal links and predict the states of objects based on model results. The main conclusions are as follows:

1. The object-based method captured the significant growth rate of megacities across China which each comprise individual cities and urban areas of various sizes. Synchronized growth behaviour of the majority of cities was observed in the early 2000s and these were shown to be correlated with national policy interventions. The regional differences across the selected megacities implied the effects of regional policies and local governance. At the regional level, different morphological trends were identified. The results provide insights into how policies could affect urban growth trends across different regions and cities of different sizes.

2. The results of the analysis of object events demonstrated that the establishment, dispersal and coalescence growth events can be measured directly at the per-object level. At the population (or landscape) level they exhibited concurrence, but with varying dominance over time, rather than following a specific logical sequence (e.g., introduction then growth then coalescence). The research

quantifies the dynamics of urban growth events and provides new insights into urban growth processes. A general synchronous trend of growth was observed in buffer zones where other states exhibit more dynamics.

3. The developed spatial-temporal network model of urban objects facilitated exploration of the dependence of the state of an urban object on its previous state and the previous states of its close neighbours. Coalescence was found to be related to the object's previous state and the distance to its nearest neighbour and neighbouring states in the previous year, and likely to occur with other objects within a buffer of 'two-pixel radius plus the nearest distance between the core and neighbouring objects around the core boundary'. The growth state was found to be related to the previous state and the dynamics of objects in a defined close neighbourhood and exhibited greater uncertainty. The area of objects that had grown was related to the largest interaction between the core object and its neighbours which varied for different-sized objects.

Overall, this research advances the understanding of urban growth patterns and processes, offering new insights into urban growth, especially for megacities that comprise 100s of individual urban cities and other urban areas. The results highlight the importance of spatial-temporal links in urban growth dynamics. This new approach should be further explored to better understand the dynamics of urban systems and promote resilient urban and environmental systems.

Appendix

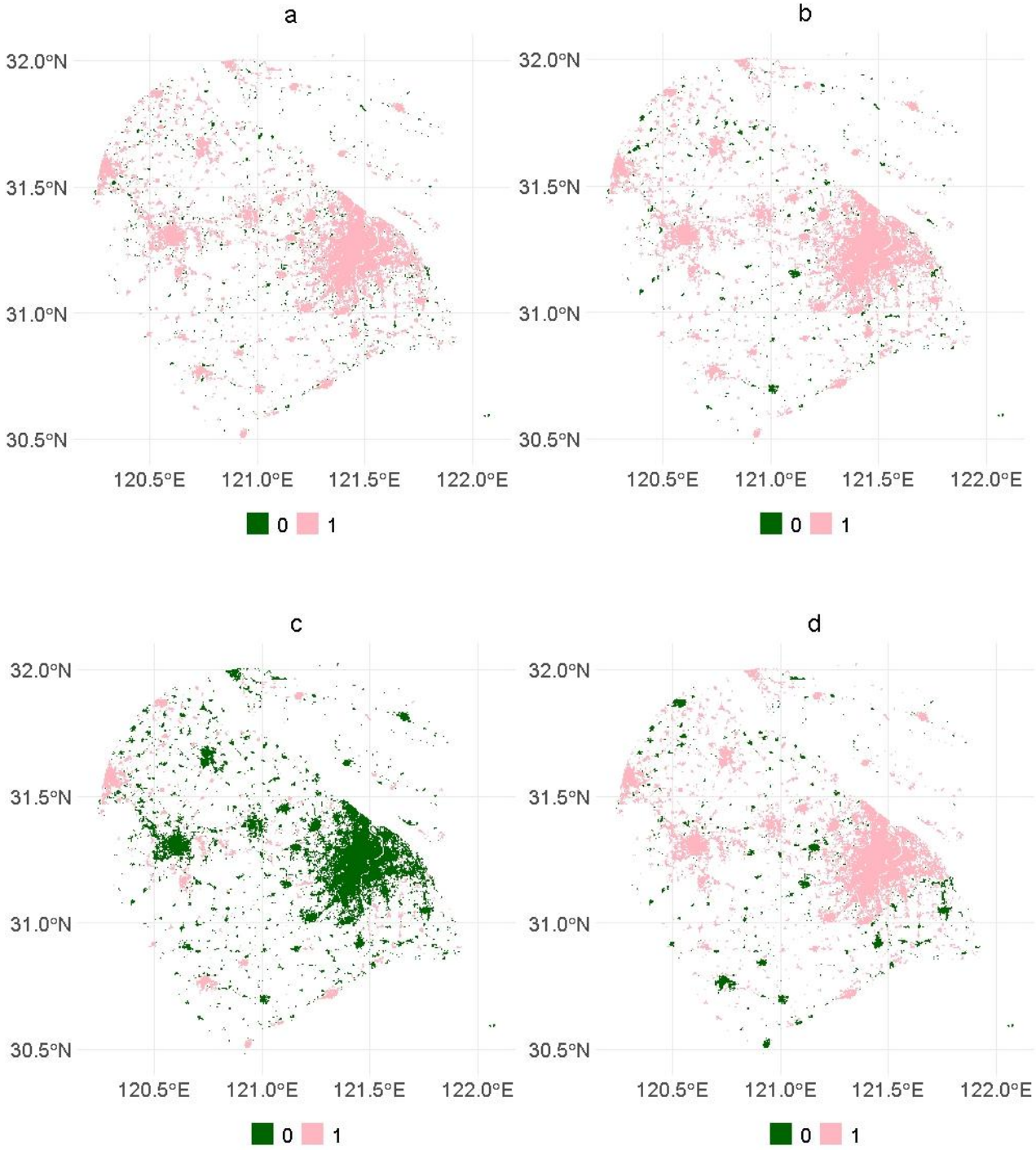

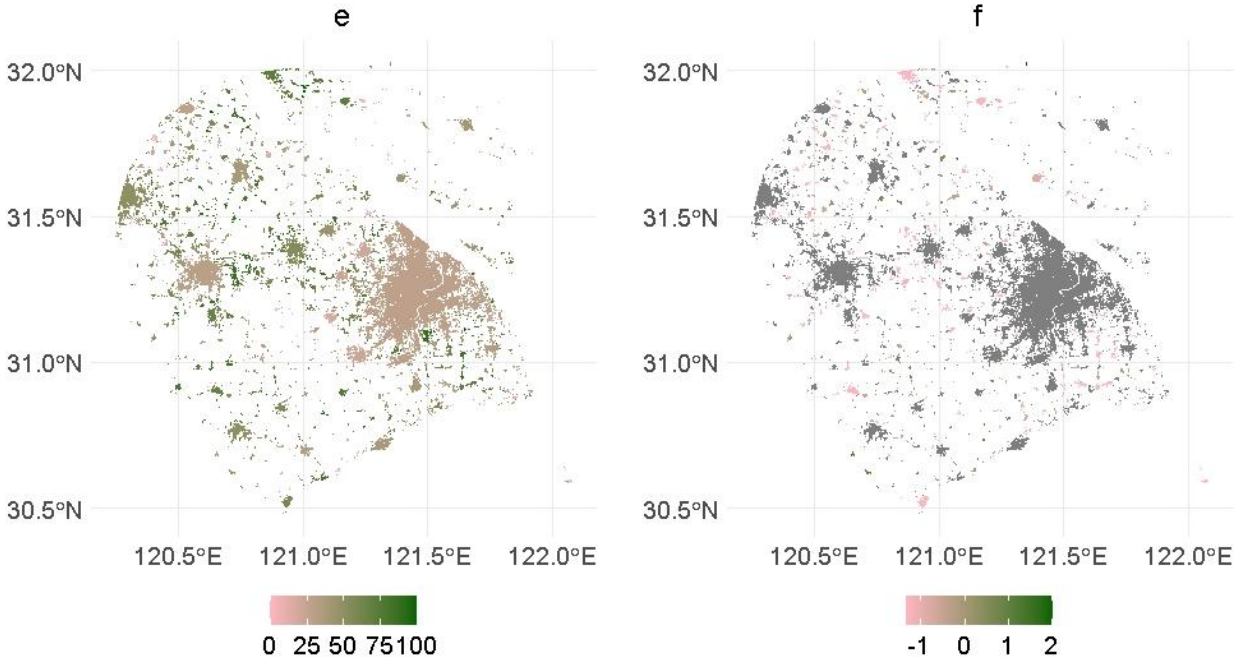

Figure A.9 The spatial distribution of core_changed_preyear (a), nearest_500_changed_preyear (b), nearest_500_1000_changed_preyear (c), largest_change_preyear (d), percentage_changed_preyear (e) and log(nearest_distance_preyear) (f) in 2010.

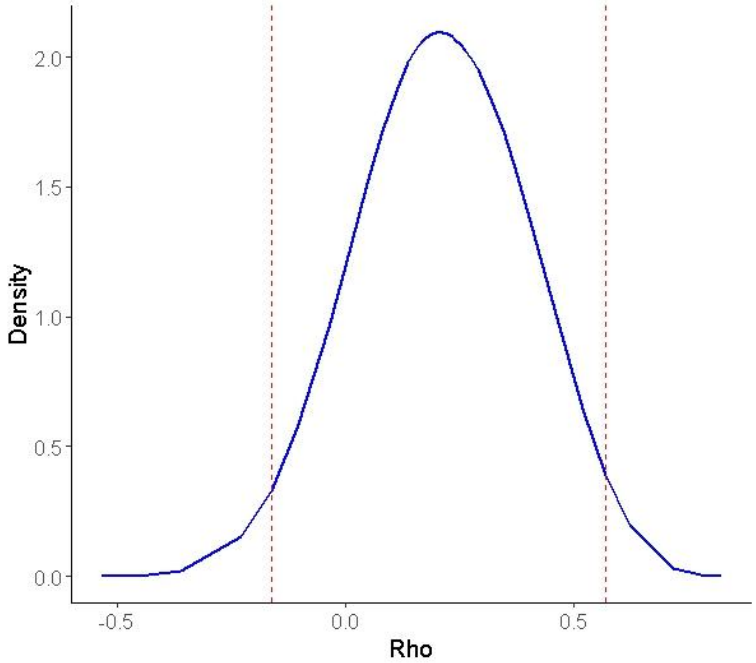

Figure A.10 The posterior distribution of Rho in the growth model includes an AR1 structure.

References:

Abolhasani, S., Taleai, M., Karimi, M., & Rezaee Node, A. (2016). Simulating urban growth under planning policies through parcel-based cellular automata (ParCA) model. *International Journal of Geographical Information Science*, *30*(11), 2276–2301. https://doi.org/10.1080/13658816.2016.1184271

Abramson, D. B. (2006). Urban planning in China: Continuity and change. *Journal of the American Planning Association*, *72*(2), 197–215. https://doi.org/10.1080/01944360608976739

Acuto, M., Parnell, S., & Seto, K. C. (2018). Building a global urban science. *Nature Sustainability*, *1*(1), 2–4

Agryzkov, T., Tortosa, L., Vicent, J. F., & Wilson, R. (2019). A centrality measure for urban networks based on the eigenvector centrality concept. *Environment and Planning B: Urban Analytics and City Science*, *46*(4), 668–689. https://doi.org/10.1177/2399808317724444

Aguilera, F., Valenzuela, L. M., & Botequilha-Leitão, A. (2011). Landscape metrics in the analysis of urban land use patterns: A case study in a Spanish metropolitan area. *Landscape and Urban Planning*, *99*(3), 226–238. https://doi.org/10.1016/j.landurbplan.2010.10.004

Aguilera, P. A., Fernández, A., Fernández, R., Rumí, R., & Salmerón, A. (2011). Bayesian networks in environmental modelling. *Environmental Modelling & Software*, *26*(12), 1376–1388. https://doi.org/10.1016/j.envsoft.2011.06.004

Aguilera-Benavente, F., Botequilha-Leitão, A., & Díaz-Varela, E. (2014). Detecting

multi-scale urban growth patterns and processes in the Algarve region (Southern Portugal). *Applied Geography*, *53*, 234–245. https://doi.org/10.1016/j.apgeog.2014.06.019

Alberti, M. (2005). The Effects of Urban Patterns on Ecosystem Function. *International Regional Science Review*, *28*(2), 168–192. https://doi.org/10.1177/0160017605275160

An, L., Linderman, M., Qi, J., Shortridge, A., & Liu, J. (2005). in a Human-Environment Exploring Complexity An Agent-Based Model for System: Spatial and Multiscale Integration Multidisciplinary. *Annals of the Association of American Geographers*, *95*(1), 54–79. https://doi.org/10.1111/j.1467-8306.2005.00450.x

An, L., Zvoleff, A., Liu, J., & Axinn, W. (2014). Agent-Based Modeling in Coupled Human and Natural Systems (CHANS): Lessons from a Comparative Analysis. *Annals of the Association of American Geographers*, *104*(4), 723–745. https://doi.org/10.1080/00045608.2014.910085

Anderson, G., & Ge, Y. (2004). Do Economic Reforms Accelerate Urban Growth? The Case of China. *Urban Studies*, *41*(11), 2197–2210. https://doi.org/10.1080/0042098042000268410

Anderson, J. R., Hardy, E. E., Roach, J. T., & Witmer, R. E. (1976). A Land Use and Land Cover Classification System for Use with Remote Sensor Data. *United States Geological Survey Professional Paper*, *964*.

Angel, S., Lamson-Hall, P., Blei, A., Shingade, S., & Kumar, S. (2021). Densify and

Expand: A Global Analysis of Recent Urban Growth. *Sustainability*, *13*(7), Article 7. https://doi.org/10.3390/su13073835

Angel, S., Parent, J., & Civco, D. L. (2012). The fragmentation of urban landscapes: Global evidence of a key attribute of the spatial structure of cities, 1990–2000. *Environment and Urbanization*, *24*(1), 249–283. https://doi.org/10.1177/0956247811433536

Anselin, L. (1995). Local indicators of spatial association—LISA. *Geographical Analysis*, *27*(2), 93–115.

Appleby, S. (1996). Multifractal characterization of the distribution pattern of the human population. *Geographical Analysis*, *28*(2), 147–160.

Arcaute, E., Hatna, E., Ferguson, P., Youn, H., Johansson, A., & Batty, M. (2015). Constructing cities, deconstructing scaling laws. *Journal of The Royal Society Interface*, *12*(102), 20140745. https://doi.org/10.1098/rsif.2014.0745

Arcaute, E., Molinero, C., Hatna, E., Murcio, R., Vargas-Ruiz, C., Masucci, A. P., & Batty, M. (2016). Cities and Regions in Britain through hierarchical percolation. *Royal Society Open Science*, *3*(4), 150691. https://doi.org/10.1098/rsos.150691

Arribas-Bel, D., Nijkamp, P., & Scholten, H. (2011). Multidimensional urban sprawl in Europe: A self-organizing map approach. *Computers, Environment and Urban Systems*, *35*(4), 263–275. https://doi.org/10.1016/j.compenvurbsys.2010.10.002

Aspinall, R. (2004). Modelling land use change with generalized linear models—A multi-model analysis of change between 1860 and 2000 in Gallatin Valley,

Montana. *Journal of Environmental Management*, *72*(1–2), 91–103. https://doi.org/10.1016/j.jenvman.2004.02.009

Atkinson, P. M. (1999). Spatial statistics. In *Spatial statistics for remote sensing* (pp. 57–81). Springer.

Atkinson, P. M., & Lewis, P. (2000). Geostatistical classification for remote sensing: An introduction. *Computers & Geosciences*, *26*(4), 361–371.

Atkinson, P. M., & Tate, N. J. (2000). Spatial Scale Problems and Geostatical Solutions: A Review. *Professional Geographer*, *52*(4), 607.

Balaguer-Beser, A., Ruiz, L. A., Hermosilla, T., & Recio, J. A. (2013). Using semivariogram indices to analyse heterogeneity in spatial patterns in remotely sensed images. *Computers and Geosciences*, *50*, 115–127. https://doi.org/10.1016/j.cageo.2012.08.001

Batty, M. (1986). Laboratories for Visualizing Urban Form. *Fractal Cities*.

Batty, M. (2008). The Size, Scale, and Shape of Cities. *Science*, *319*(5864), 769–771. https://doi.org/10.1126/science.1151419

Batty, M. (2012). Building a science of cities. *Cities*, *29*(SUPPL. 1), 9–16. https://doi.org/10.1016/j.cities.2011.11.008

Batty, M. (2013a). Big data, smart cities and city planning. *Dialogues in Human Geography*, *3*(3), 274–279. https://doi.org/10.1177/2043820613513390

Batty, M. (2013b). *The new science of cities*. Mit Press.

Batty, M. (2020). Defining City Size and Growth. In *Urban Empires*. Routledge.

Batty, M. (2023). Scaling in city size distributions. *Environment and Planning B: Urban*

Analytics and City Science, 239980832311557. https://doi.org/10.1177/23998083231155725

Batty, M., & Longley, P. (1994). The Shape of Cities: Geometry, Morphology, Complexity and Form. *Fractal Cities: A Geometry of Form and Function*, 7–57.

Batty, M., & Longley, P. A. (1988). The Morphology of Urban Land-Use. *Environment and Planning B-Planning & Design*, *15*(4), 461–488. https://doi.org/10.1068/b150461

Benenson, I., & Torrens, P. M. (2004). Geosimulation: Object-based modeling of urban phenomena. *Computers, Environment and Urban Systems*, *28*(1–2), 1–8. https://doi.org/10.1016/S0198-9715(02)00067-4

Benguigui, L., & Czamanski, D. (2004). Simulation Analysis of the Fractality of Cities. *Geographical Analysis*, *36*(1), 69–84. https://doi.org/10.1111/j.1538-4632.2004.tb01124.x

Benguigui, L., Czamanski, D., Marinov, M., & Portugali, Y. (2000). When and where is a city fractal? *Environment and Planning B: Planning and Design*, *27*(4), 507–519.

Berberoglu, S., Curran, P. J., Lloyd, C. D., & Atkinson, P. M. (2007). Texture classification of Mediterranean land cover. *International Journal of Applied Earth Observation and Geoinformation*, *9*(3), 322–334.

Berling-Wolff, S., & Wu, J. (2004a). Modeling Urban Landscape Dynamics: A Case Study in Phoenix, USA. *Urban Ecosystems*, *7*, 215–240.

https://doi.org/10.1023/B:UECO.0000044037.23965.45

Berling-Wolff, S., & Wu, J. (2004b). Modeling urban landscape dynamics: A review. *Ecological Research*, *19*(1), 119–129. https://doi.org/10.1111/j.1440-1703.2003.00611.x

Berry, B. J. L. (1961). City size distributions and economic development. *Economic Development and Cultural Change*, *9*(4, Part 1), 573–588.

Bettencourt, L. M. A., Lobo, J., Helbing, D., Kuhnert, C., & West, G. B. (2007). Growth, innovation, scaling, and the pace of life in cities. *Proceedings of the National Academy of Sciences*, *104*(17), 7301–7306. https://doi.org/10.1073/pnas.0610172104

Bitter, C., Mulligan, G. F., & Dall'erba, S. (2007). Incorporating spatial variation in housing attribute prices: A comparison of geographically weighted regression and the spatial expansion method. *Journal of Geographical Systems*, *9*(1), 7–27.

Bloom, D. E., Canning, D., & Fink, G. (2008). Urbanization and the Wealth of Nations. *Science*, *319*(5864), 772–775. https://doi.org/10.1126/science.1153057

Blumenfeld, H. (1954). The tidal wave of metropolitan expansion. *Journal of the American Planning Association*, *20*(1), 3–14.

Bosch, M., Jaligot, R., & Chenal, J. (2020). Spatiotemporal patterns of urbanization in three Swiss urban agglomerations: Insights from landscape metrics, growth modes and fractal analysis. *Landscape Ecology*, *35*(4), 879–891. https://doi.org/10.1007/s10980-020-00985-y

Brakman, S., Garretsen, H., Van Marrewijk, C., & Van Den Berg, M. (1999). The return

of Zipf: Towards a further understanding of the rank-size distribution. *Journal of Regional Science*, *39*(1), 183–213.

Brelsford, C., Lobo, J., Hand, J., & Bettencourt, L. M. A. (2017). Heterogeneity and scale of sustainable development in cities. *Proceedings of the National Academy of Sciences*, *114*(34), 8963–8968. https://doi.org/10.1073/pnas.1606033114

Bren d'Amour, C., Reitsma, F., Baiocchi, G., Barthel, S., Güneralp, B., Erb, K.-H., Haberl, H., Creutzig, F., & Seto, K. C. (2017). Future urban land expansion and implications for global croplands. *Proceedings of the National Academy of Sciences*, *114*(34), 8939–8944. https://doi.org/10.1073/pnas.1606036114

Brown, D. G., & Robinson, D. T. (2006). Effects of heterogeneity in residential preferences on an agent-based model of urban sprawl. *Ecology and Society*, *11*(1). https://doi.org/10.2337/dc11-1153

Brunsdon, C., Fotheringham, A. S., & Charlton, M. E. (1996). Geographically weighted regression: A method for exploring spatial nonstationarity. *Geographical Analysis*, *28*(4), 281–298.

Burger, M., & Meijers, E. (2012). Form Follows Function? Linking Morphological and Functional Polycentricity. *Urban Studies*, *49*(5), 1127–1149. https://doi.org/10.1177/0042098011407095

Burghardt, K., Uhl, J. H., Lerman, K., & Leyk, S. (2022). Road network evolution in the urban and rural United States since 1900. *Computers, Environment and Urban Systems*, *95*, 101803. https://doi.org/10.1016/j.compenvurbsys.2022.101803

Cai, B., & Dunson, D. B. (2006). Bayesian Covariance Selection in Generalized Linear Mixed Models. *Biometrics*, *62*(2), 446–457. https://doi.org/10.1111/j.1541-0420.2005.00499.x

Cantwell, M. D., & Forman, R. T. (1993). Landscape graphs: Ecological modeling with graph theory to detect configurations common to diverse landscapes. *Landscape Ecology*, *8*(4), 239–255. https://doi.org/10.1007/BF00125131

Capello, R., & Camagni, R. (2000). Beyond Optimal City Size: An Evaluation of Alternative Urban Growth Patterns. *Urban Studies*, *37*(9), 1479–1496. https://doi.org/10.1080/00420980020080221

Caruso, G., Hilal, M., & Thomas, I. (2017). Measuring urban forms from inter-building distances: Combining MST graphs with a Local Index of Spatial Association. *Landscape and Urban Planning*, *163*, 80–89. https://doi.org/10.1016/j.landurbplan.2017.03.003

Castells, M. (2010). Globalisation, Networking, Urbanisation: Reflections on the Spatial Dynamics of the Information Age. *Urban Studies*, *47*(13), 2737–2745. https://doi.org/10.1177/0042098010377365

Chan, K. W. (1992). Economic growth strategy and urbanization policies in China, 1949–1982. *International Journal of Urban and Regional Research*, *16*(2), 275–305.

Chan, K. W. (1994). Urbanization and Rural-Urban Migration in China since 1982: A New Baseline. *Modern China*, *20*(3), 243–281. https://doi.org/10.1177/009770049402000301

Chen, J., Gao, J., & Yuan, F. (2016). Growth Type and Functional Trajectories: An Empirical Study of Urban Expansion in Nanjing, China. *PLOS ONE*, *11*(2), e0148389. https://doi.org/10.1371/journal.pone.0148389

Chen, J., Guo, F., & Wu, Y. (2011). One decade of urban housing reform in China: Urban housing price dynamics and the role of migration and urbanization, 1995–2005. *Habitat International*, *35*(1), 1–8.

Chen, L., Zhao, L., Xiao, Y., & Lu, Y. (2022). Investigating the spatiotemporal pattern between the built environment and urban vibrancy using big data in Shenzhen, China. *Computers, Environment and Urban Systems*, *95*, 101827. https://doi.org/10.1016/j.compenvurbsys.2022.101827

Chen, W., Chen, X., Cheng, L., Liu, X., & Chen, J. (2022). Delineating borders of urban activity zones with free-floating bike sharing spatial interaction network. *Journal of Transport Geography*, *104*, 103442. https://doi.org/10.1016/j.jtrangeo.2022.103442

Chen, Y. (2010). Exploring the fractal parameters of urban growth and form with wave-spectrum analysis. *Discrete Dynamics in Nature and Society*, *2010*, 10–20. https://doi.org/10.1155/2010/974917

Chen, Y. (2013). Fractal analytical approach of urban form based on spatial correlation function. *Chaos, Solitons & Fractals*, *49*, 47–60. https://doi.org/10.1016/j.chaos.2013.02.006

Chen, Y., Li, X., Liu, X., & Ai, B. (2014). Modeling urban land-use dynamics in a fast developing city using the modified logistic cellular automaton with a patch-

based simulation strategy. *International Journal of Geographical Information Science*, *28*(2), 234–255. https://doi.org/10.1080/13658816.2013.831868

Chen, Y., & Wang, J. (2013). Multifractal characterization of urban form and growth: The case of Beijing. *Environment and Planning B: Planning and Design*, *40*(5), 884–904. https://doi.org/10.1068/b36155

Chen, Y., & Zhou, Y. (2004). Multi-fractal measures of city-size distributions based on the three-parameter Zipf model. *Chaos, Solitons & Fractals*, *22*(4), 793–805.

Cheng, J., & Masser, I. (2003a). Modelling Urban Growth Patterns: A Multiscale Perspective. *Environment and Planning A: Economy and Space*, *35*(4), 679–704. https://doi.org/10.1068/a35118

Cheng, J., & Masser, I. (2003b). Urban growth pattern modeling: A case study of Wuhan city, PR China. *Landscape and Urban Planning*, *62*(4), 199–217. https://doi.org/10.1016/S0169-2046(02)00150-0

Cheng, T., & Selden, M. (1994). The Origins and Social Consequences of China ' s Hukou System. *The China Quarterly*, *139*(139), 644–668.

Cheung, A. K. L., O'sullivan, D., & Brierley, G. (2015). Graph-assisted landscape monitoring. *International Journal of Geographical Information Science*, *29*(4), 580–605. https://doi.org/10.1080/13658816.2014.989856

ChristallerW, 1933 Die zentralen Orte in Su«ddeutschland (Jena); republished 1966 as Central Places in Southern Germany. (1933). *Die zentralen Orte in Su«ddeutschland (Jena); republished 1966 as Central Places in Southern Germanye*.

Clark, C. (1951). Urban population densities. *Journal of the Royal Statistical Society*, *114*(4), 490–496.

Clarke, K. C., & Gaydos, L. J. (1998). Loose-coupling a cellular automaton model and GIS: Long-term urban growth prediction for San Francisco and Washington/Baltimore. *International Journal of Geographical Information Science*, *12*(7), 699–714. https://doi.org/10.1080/136588198241617

Clemente, R. D. (2021). Urbanization and economic complexity. *Scientific Reports*.

Cottineau, C., Finance, O., Hatna, E., Arcaute, E., & Batty, M. (2018). Defining urban clusters to detect agglomeration economies. *Environment and Planning B: Urban Analytics and City Science*. https://doi.org/10.1177/2399808318755146

Crooks, A., Castle, C., & Batty, M. (2008). Key challenges in agent-based modelling for geo-spatial simulation. *Computers, Environment and Urban Systems*, *32*(6), 417–430. https://doi.org/10.1016/j.compenvurbsys.2008.09.004

Curran, P. J. (1988). The semivariogram in remote sensing: An introduction. *Remote Sensing of Environment*, *24*(3), 493–507.

Cvetojevic, S., & Hochmair, H. H. (2021). Modeling interurban mentioning relationships in the U.S. Twitter network using geo-hashtags. *Computers, Environment and Urban Systems*, *87*, 101621. https://doi.org/10.1016/j.compenvurbsys.2021.101621

Dahal, K. R., Benner, S., & Lindquist, E. (2017). Urban hypotheses and spatiotemporal characterization of urban growth in the Treasure Valley of Idaho, USA. *Applied Geography*, *79*, 11–25. https://doi.org/10.1016/j.apgeog.2016.12.002

Dai, E., Wang, Y., Ma, L., Yin, L., & Wu, Z. (2018). 'Urban-Rural' Gradient Analysis of Landscape Changes around Cities in Mountainous Regions: A Case Study of the Hengduan Mountain Region in Southwest China. *Sustainability*, *10*(4), 1019. https://doi.org/10.3390/su10041019

de Almeida, C. M., Batty, M., Monteiro, A. M. V., Câmara, G., Soares-Filho, B. S., Cerqueira, G. C., & Pennachin, C. L. (2003). Stochastic cellular automata modeling of urban land use dynamics: Empirical development and estimation. *Computers, Environment and Urban Systems*, *27*(5), 481–509.

De Cola, L. (2010). A Network Representation of Raster Land-Cover Patches. *Photogrammetric Engineering & Remote Sensing*, *76*(1), 61–72. https://doi.org/10.14358/PERS.76.1.61

de la Barra, F., Alignier, A., Reyes-Paecke, S., Duane, A., & Miranda, M. D. (2022). Selecting Graph Metrics with Ecological Significance for Deepening Landscape Characterization: Review and Applications. *Land*, *11*(3), 338. https://doi.org/10.3390/land11030338

Decker, E. H., Kerkhoff, A. J., & Moses, M. E. (2007). Global patterns of city size distributions and their fundamental drivers. *PLoS ONE*, *2*(9), 2–7. https://doi.org/10.1371/journal.pone.0000934

Defourny, P., Lamarche, C., Brockmann, C., Boettcher, M., Bontemps, S., De Maet, T., Duveiller, G. L., Harper, K., Hartley, A., & Kirches, G. (2023). *Observed annual global land-use change from 1992 to 2020 three times more dynamic than reported by inventory-based statistics*. preparation.

DeFries, R. S., Rudel, T., Uriarte, M., & Hansen, M. (2010). Deforestation driven by urban population growth and agricultural trade in the twenty-first century. *Nature Geoscience*, *3*(3), 178–181. https://doi.org/10.1038/ngeo756

Deng, X., Huang, J., Rozelle, S., & Uchida, E. (2010). Economic Growth and the Expansion of Urban Land in China. *Urban Studies*, *47*(4), 813–843. https://doi.org/10.1177/0042098009349770

Derudder, B., Timberlake, M., & Witlox, F. (2010). Introduction: Mapping Changes in Urban Systems. *Urban Studies*, *47*(9), 1835–1841. https://doi.org/10.1177/0042098010373504

Di Gregorio, A. (2005). *Land cover classification system. Classification concepts and user manual. Software version 2*.

Dibble, J., Prelorendjos, A., Romice, O., Zanella, M., Strano, E., Pagel, M., & Porta, S. (2017). On the origin of spaces: Morphometric foundations of urban form evolution. *Environment and Planning B: Urban Analytics and City Science*. https://doi.org/10.1177/2399808317725075

Dietzel, C., Herold, M., Hemphill, J. J., & Clarke, K. C. (2005a). Spatio-temporal dynamics in California's Central Valley: Empirical links to urban theory. *International Journal of Geographical Information Science*, *19*(2), 175–195. https://doi.org/10.1080/13658810410001713407

Dietzel, C., Oguz, H., Hemphill, J. J., Clarke, K. C., & Gazulis, N. (2005b). Diffusion and coalescence of the Houston Metropolitan Area: Evidence supporting a new urban theory. *Environment and Planning B: Planning and Design*, *32*(2), 231–

246. https://doi.org/10.1068/b31148

Ding, C. (2003). Land policy reform in China: Assessment and prospects. *Land Use Policy*, *20*(2), 109–120.

Ding, C. (2004). Urban Spatial Development in the Land Policy Reform Era: Evidence from Beijing. *Urban Studies*, *41*(10), 1889–1907. https://doi.org/10.1080/0042098042000256305

Ding, C., & Li, Z. (2019). Size and urban growth of Chinese cities during the era of transformation toward a market economy. *Environment and Planning B: Urban Analytics and City Science*, *46*(1), 27–46. https://doi.org/10.1177/2399808317696072

Dong, L., Duarte, F., Duranton, G., Santi, P., Barthelemy, M., Batty, M., Bettencourt, L., Goodchild, M., Hack, G., Liu, Y., Pumain, D., Shi, W., Verbavatz, V., West, G. B., Yeh, A. G. O., & Ratti, C. (2024). Defining a city—Delineating urban areas using cell-phone data. *Nature Cities*, *1*(2), 117–125. https://doi.org/10.1038/s44284-023-00019-z

Doxsey-Whitfield, E., MacManus, K., Adamo, S. B., Pistolesi, L., Squires, J., Borkovska, O., & Baptista, S. R. (2015). Taking Advantage of the Improved Availability of Census Data: A First Look at the Gridded Population of the World, Version 4. *Papers in Applied Geography*, *1*(3), 226–234. https://doi.org/10.1080/23754931.2015.1014272

Eaton, J., & Eckstein, Z. (1997). Cities and growth: Theory and evidence from France and Japan. *Regional Science and Urban Economics*, *27*(4–5), 443–474.

https://doi.org/10.1016/S0166-0462(97)80005-1

Entwisle, B., Rindfuss, R. R., Walsh, S. J., & Page, P. H. (2008). Population growth and its spatial distribution as factors in the deforestation of Nang Rong, Thailand. *Geoforum*, *39*(2), 879–897. https://doi.org/10.1016/j.geoforum.2006.09.008

ESA. Land Cover CCI Product User Guide Version 2. Tech. Rep. (2017). Available at: maps.elie.ucl.ac.be/CCI/viewer/download/ESACCI-LC-Ph2-PUGv2_2.0.pdf

Esch, T., Marconcini, M., Marmanis, D., Zeidler, J., Elsayed, S., Metz, A., Müller, A., & Dech, S. (2014). Dimensioning urbanization – An advanced procedure for characterizing human settlement properties and patterns using spatial network analysis. *Applied Geography*, *55*, 212–228. https://doi.org/10.1016/j.apgeog.2014.09.009

Falconer, K. J. (1986). *The geometry of fractal sets* (Vol. 85). Cambridge university press.

Fall, A., Fortin, M.-J., Manseau, M., & O'Brien, D. (2007). Spatial graphs: Principles and applications for habitat connectivity. *Ecosystems*, *10*, 448–461. https://doi.org/10.1007/s10021-007-9038-7

Fan, C., & Myint, S. (2014). A comparison of spatial autocorrelation indices and landscape metrics in measuring urban landscape fragmentation. *Landscape and Urban Planning*, *121*, 117–128. https://doi.org/10.1016/j.landurbplan.2013.10.002

Fan, X., Blackburn, G. A., Whyatt, J. D., & Atkinson, P. M. (2024). The Geographical Analysis of Megacities Through Changes in Their Individual Urban Objects.

Geographical Analysis. https://doi.org/10.1111/gean.12386

Fang, C., & Yu, D. (2017). Urban agglomeration: An evolving concept of an emerging phenomenon. *Landscape and Urban Planning*, *162*, 126–136. https://doi.org/10.1016/j.landurbplan.2017.02.014

Fang, S., Gertner, G. Z., Sun, Z., & Anderson, A. A. (2005). The impact of interactions in spatial simulation of the dynamics of urban sprawl. *Landscape and Urban Planning*, *73*(4), 294–306. https://doi.org/10.1016/j.landurbplan.2004.08.006

Favaro, J. M., & Pumain, D. (2011). Gibrat revisited: An urban growth model incorporating spatial interaction and innovation cycles. *Geographical Analysis*, *43*(3), 261–286. https://doi.org/10.1111/j.1538-4632.2011.00819.x

Fei, W., & Zhao, S. (2019). Urban land expansion in China's six megacities from 1978 to 2015. *Science of The Total Environment*, *664*, 60–71. https://doi.org/10.1016/j.scitotenv.2019.02.008

Feng, Y., Kugler, J., & Zak, P. J. (2002). Population Growth, Urbanisation and the Role of Government in China: A Political Economic Model of Demographic Change. *Urban Studies*, *39*(12), 2329–2343. https://doi.org/10.1080/0042098022000033908

Filatova, T., Verburg, P. H., Parker, D. C., & Stannard, C. A. (2013). Spatial agent-based models for socio-ecological systems: Challenges and prospects. *Environmental Modelling and Software*, *45*, 1–7. https://doi.org/10.1016/j.envsoft.2013.03.017

Fleischmann, M., Feliciotti, A., & Kerr, W. (2022). Evolution of Urban Patterns: Urban Morphology as an Open Reproducible Data Science. *Geographical Analysis*,

54(3), 536–558. https://doi.org/10.1111/gean.12302

Fragkias, M., & Seto, K. C. (2009). Evolving rank-size distributions of intra-metropolitan urban clusters in South China. *Computers, Environment and Urban Systems*, *33*(3), 189–199. https://doi.org/10.1016/j.compenvurbsys.2008.08.005

Frankhauser, P. (2009). The Fractal Approach. A New Tool for the Spatial Analysis of Urban Agglomerations Author (s): Pierre Frankhauser Source: Population: An English Selection , Vol. 10 , No. 1 , New Methodological Approaches in the Social Sciences (1998), pp. 205-24. *Social Sciences*, *10*(1), 205–240.

Fu, Z., & Hao, L. (2018). Agent-based modeling of China's rural–urban migration and social network structure. *Physica A: Statistical Mechanics and Its Applications*, *490*(Supplement C), 1061–1075. https://doi.org/10.1016/j.physa.2017.08.145

Fujita, M. (1976). Spatial patterns of urban growth: Optimum and market. *Journal of Urban Economics*, *3*(3), 209–241. https://doi.org/10.1016/0094-1190(76)90041-3

Gabaix, X. (1999). Zipf's Law and the Growth of Cities. *The American Economic Review*, *89*(2), 129–132.

Galea, S., & Vlahov, D. (2005). Urban health: Evidence, challenges, and directions. *Annual Review of Public Health*, *26*(1), 341–365. https://doi.org/10.1146/annurev.publhealth.26.021304.144708

Gao, B., Huang, Q., He, C., Sun, Z., & Zhang, D. (2016). How does sprawl differ across cities in China? A multi-scale investigation using nighttime light and census

data. *Landscape and Urban Planning*, *148*, 89–98. https://doi.org/10.1016/j.landurbplan.2015.12.006

Garrigues, S., Allard, D., & Baret, F. (2007). Using first-and second-order variograms for characterizing landscape spatial structures from remote sensing imagery. *IEEE Transactions on Geoscience and Remote Sensing*, *45*(6), 1823–1834.

Gaubatz, P. (1999). China's Urban Transformation: Patterns and Processes of Morphological change in Beijing, Shanghai and Guangzhou.pdf. *Urban Studies*, *36*(9), 1495–1521.

Gaughan, A. E., Stevens, F. R., Huang, Z., Nieves, J. J., Sorichetta, A., Lai, S., Ye, X., Linard, C., Hornby, G. M., Hay, S. I., Yu, H., & Tatem, A. J. (2016). Spatiotemporal patterns of population in mainland China, 1990 to 2010. *Scientific Data*, *3*, 160005. https://doi.org/10.1038/sdata.2016.5

Geertman, S., Hagoort, M., & Ottens, H. (2007). Spatial-temporal specific neighbourhood rules for cellular automata land-use modelling. *International Journal of Geographical Information Science*, *21*(5), 547–568. https://doi.org/10.1080/13658810601064892

Gibbons, J., Nara, A., & Appleyard, B. (2018). Exploring the imprint of social media networks on neighborhood community through the lens of gentrification. *Environment and Planning B: Urban Analytics and City Science*, *45*(3), 470–488. https://doi.org/10.1177/2399808317728289

Gielen, E., Riutort-Mayol, G., Miralles i Garcia, J. L., & Palencia Jiménez, J. S. (2021). Cost assessment of urban sprawl on municipal services using hierarchical

regression. *Environment and Planning B: Urban Analytics and City Science*, *48*(2), 280–297. https://doi.org/10.1177/2399808319869345

Glockmann, M., Li, Y., Lakes, T., Kropp, J. P., & Rybski, D. (2022). Quantitative evidence for leapfrogging in urban growth. *Environment and Planning B: Urban Analytics and City Science*, *49*(1), 352–367. https://doi.org/10.1177/2399808321998713

González-Val, R. (2023). Parametric, semiparametric and nonparametric models of urban growth. *Cities*, *132*, 104079. https://doi.org/10.1016/j.cities.2022.104079

Goodkind, D., & West, L. A. (2002). China's Floating Population: Definitions, Data and Recent Findings. *Urban Studies*, *39*(12), 2237–2250. https://doi.org/10.1080/0042098022000033845

Grimm, N. B., Faeth, S. H., Golubiewski, N. E., Redman, C. L., Wu, J., Bai, X., & Briggs, J. M. (2008). Global change and the ecology of cities. *Science*, *319*(5864), 756–760. https://doi.org/10.1126/science.1150195

Gu, Y., & Wang, Y. (2022). Using weighted multilayer networks to uncover scaling of public transport system. *Environment and Planning B: Urban Analytics and City Science*, *49*(6), 1631–1645. https://doi.org/10.1177/23998083211062905

Guan, D., Li, H., Inohae, T., Su, W., Nagaie, T., & Hokao, K. (2011). Modeling urban land use change by the integration of cellular automaton and Markov model. *Ecological Modelling*, *222*(20), 3761–3772. https://doi.org/10.1016/j.ecolmodel.2011.09.009

Guan, X., Xing, W., Li, J., & Wu, H. (2023). HGAT-VCA: Integrating high-order graph

attention network with vector cellular automata for urban growth simulation. *Computers, Environment and Urban Systems*, *99*, 101900. https://doi.org/10.1016/j.compenvurbsys.2022.101900

Guérin-Pace, F. (1995). Rank-size distribution and the process of urban growth. *Urban Studies*, *32*(3), 551–562.

Güneralp, B., Reilly, M. K., & Seto, K. C. (2012). Capturing multiscalar feedbacks in urban land change: A coupled system dynamics spatial logistic approach. *Environment and Planning B: Planning and Design*, *39*(5), 858–879.

Haag, G. (1994). The rank-size distribution of settlements as a dynamic multifractal phenomenon. *Chaos, Solitons & Fractals*, *4*(4), 519–534.

Hagoort, M., Geertman, S., & Ottens, H. (2008). Spatial externalities, neighbourhood rules and CA land-use modelling. *Annals of Regional Science*, *42*(1), 39–56. https://doi.org/10.1007/s00168-007-0140-8

Han, J., Hayashi, Y., Cao, X., & Imura, H. (2009). Application of an integrated system dynamics and cellular automata model for urban growth assessment: A case study of Shanghai, China. *Landscape and Urban Planning*, *91*(3), 133–141. https://doi.org/10.1016/j.landurbplan.2008.12.002

Hatab, A. A., Cavinato, M. E. R., Lindemer, A., & Lagerkvist, C.-J. (2019). Urban sprawl, food security and agricultural systems in developing countries: A systematic review of the literature. *Cities*, *94*, 129–142. https://doi.org/10.1016/j.cities.2019.06.001

He, C., Okada, N., Zhang, Q., Shi, P., & Li, J. (2008). Modelling dynamic urban

expansion processes incorporating a potential model with cellular automata. *Landscape and Urban Planning*, *86*(1), 79–91. https://doi.org/10.1016/j.landurbplan.2007.12.010

He, J., Wei, Y., & Yu, B. (2023). Geographically weighted regression based on a network weight matrix: A case study using urbanization driving force data in China. *International Journal of Geographical Information Science*, *37*(6), 1209–1235. https://doi.org/10.1080/13658816.2023.2192122

He, Q., Song, Y., Liu, Y., & Yin, C. (2017). Diffusion or coalescence? Urban growth pattern and change in 363 Chinese cities from 1995 to 2015. *Sustainable Cities and Society*, *35*, 729–739. https://doi.org/10.1016/j.scs.2017.08.033

He, X., & Zhou, Y. (2024). Urban spatial growth and driving mechanisms under different urban morphologies: An empirical analysis of 287 Chinese cities. *Landscape and Urban Planning*, *248*, 105096. https://doi.org/10.1016/j.landurbplan.2024.105096

Hernando, A., Hernando, R., & Plastino, A. (2013). Space-time correlations in urban sprawl. *Journal of The Royal Society Interface*, *11*(91), 20130930–20130930. https://doi.org/10.1098/rsif.2013.0930

Herold, M., Goldstein, N. C., & Clarke, K. C. (2003). The spatiotemporal form of urban growth: Measurement, analysis and modeling. *Remote Sensing of Environment*, *86*(3), 286–302. https://doi.org/10.1016/S0034-4257(03)00075-0

Hoffhine Wilson, E., Hurd, J. D., Civco, D. L., Prisloe, M. P., & Arnold, C. (2003). Development of a geospatial model to quantify, describe and map urban growth.

Remote Sensing of Environment, *86*(3), 275–285. https://doi.org/10.1016/S0034-4257(03)00074-9

Hsu, M.-L. (1996). China's urban development: A case study of Luoyang and Guiyang. *Urban Studies*, *33*(6), 895–910.

Hu, H., Shen, J., Gu, H., & Zhang, J. (2024). Identifying the spatio-temporal dynamics of mega city region range and hinterland: A perspective of inter-city flows. *Computers, Environment and Urban Systems*, *112*, 102146. https://doi.org/10.1016/j.compenvurbsys.2024.102146

Huang, L., Yan, L., & Wu, J. (2016). Assessing urban sustainability of Chinese megacities: 35 years after the economic reform and open-door policy. *Landscape and Urban Planning*, *145*, 57–70. https://doi.org/10.1016/j.landurbplan.2015.09.005

Huang, Q., He, C., Gao, B., Yang, Y., Liu, Z., Zhao, Y., & Dou, Y. (2015). Detecting the 20 year city-size dynamics in China with a rank clock approach and DMSP/OLS nighttime data. *Landscape and Urban Planning*, *137*, 138–148. https://doi.org/10.1016/j.landurbplan.2015.01.004

Huang, Q., & Wong, D. W. S. (2016). Activity patterns, socioeconomic status and urban spatial structure: What can social media data tell us? *International Journal of Geographical Information Science*, *30*(9), 1873–1898. https://doi.org/10.1080/13658816.2016.1145225

Huang, Z., Wei, Y. D., He, C., & Li, H. (2015). Urban land expansion under economic transition in China: A multi-level modeling analysis. *Habitat International*, *47*,

69–82. https://doi.org/10.1016/j.habitatint.2015.01.007

Inostroza, L. (2021). *The metabolic urban network: Urbanisation as hierarchically ordered space of flows*. https://doi.org/10.1016/j.cities.2020.103029

Irwin, E. G., Jayaprakash, C., & Munroe, D. K. (2009). Towards a comprehensive framework for modeling urban spatial dynamics. *Landscape Ecology*, *24*(9), 1223–1236. https://doi.org/10.1007/s10980-009-9353-9

Jenerette, G. D., & Potere, D. (2010). Global analysis and simulation of land-use change associated with urbanization. *Landscape Ecology*, *25*(5), 657–670. https://doi.org/10.1007/s10980-010-9457-2

Jia, T., Luo, X., & Li, X. (2021). Delineating a hierarchical organization of ranked urban clusters using a spatial interaction network. *Computers, Environment and Urban Systems*, *87*, 101617. https://doi.org/10.1016/j.compenvurbsys.2021.101617

Jiao, L. (2015). Urban land density function: A new method to characterize urban expansion. *Landscape and Urban Planning*, *139*, 26–39. https://doi.org/10.1016/j.landurbplan.2015.02.017

Jiao, L., Liu, J., Xu, G., Dong, T., Gu, Y., Zhang, B., Liu, Y., & Liu, X. (2018). Proximity Expansion Index: An improved approach to characterize evolution process of urban expansion. *Computers, Environment and Urban Systems*, *70*, 102–112. https://doi.org/10.1016/j.compenvurbsys.2018.02.005

Jiao, L., Mao, L., & Liu, Y. (2015). Multi-order Landscape Expansion Index: Characterizing urban expansion dynamics. *Landscape and Urban Planning*,

137, 30–39. https://doi.org/10.1016/j.landurbplan.2014.10.023

Jonathan A. Foley, Ruth DeFries, Gregory P. Asner, Carol Barford, Gordon Bonan, S. R. C. (2005). Global Consequences of Land Use. *Science*, *309*(5734), 570–574.

Kalnay, E., & Cai, M. (2003). Impact of urbanization and land-use change on climate. *Nature*, *423*(6939), 528–531. https://doi.org/10.1038/nature01675

Kam Wing Chan. (1994). Urbanization and Rural-Urban Migration in China since 1982: A New Baseline. *Modern China*, *20*(3), 243–281.

Kelley, H., & Evans, T. (2011). The relative influences of land-owner and landscape heterogeneity in an agent-based model of land-use. *Ecological Economics*, *70*(6), 1075–1087. https://doi.org/10.1016/j.ecolecon.2010.12.009

Kontgis, C., Schneider, A., Fox, J., Saksena, S., Spencer, J. H., & Castrence, M. (2014). Monitoring peri-urbanization in the greater Ho Chi Minh City metropolitan area. *Applied Geography*, *53*, 377–388. https://doi.org/10.1016/j.apgeog.2014.06.029

Krings, G., Calabrese, F., Ratti, C., & Blondel, V. D. (2009). Urban gravity: A model for inter-city telecommunication flows. *Journal of Statistical Mechanics: Theory and Experiment*, *2009*(7). https://doi.org/10.1088/1742-5468/2009/07/L07003

Kuang, W., Liu, J., Dong, J., Chi, W., & Zhang, C. (2016). The rapid and massive urban and industrial land expansions in China between 1990 and 2010: A CLUD-based analysis of their trajectories, patterns, and drivers. *Landscape and Urban Planning*, *145*, 21–33. https://doi.org/10.1016/j.landurbplan.2015.10.001

Lagarias, A., & Prastacos, P. (2020). Comparing the urban form of South European cities using fractal dimensions. *Environment and Planning B: Urban Analytics and City Science*, *47*(7), 1149–1166. https://doi.org/10.1177/2399808318820911

Lengyel, J., Alvanides, S., & Friedrich, J. (2023). Modelling the interdependence of spatial scales in urban systems. *Environment and Planning B: Urban Analytics and City Science*, *50*(1), 182–197. https://doi.org/10.1177/23998083221091569

Li, C., Li, J., & Wu, J. (2013). Quantifying the speed, growth modes, and landscape pattern changes of urbanization: A hierarchical patch dynamics approach. *Landscape Ecology*, *28*(10), 1875–1888. https://doi.org/10.1007/s10980-013-9933-6

Li, D., Newman, G. D., Wilson, B., Zhang, Y., & Brown, R. D. (2022). Modeling the relationships between historical redlining, urban heat, and heat-related emergency department visits: An examination of 11 Texas cities. *Environment and Planning B: Urban Analytics and City Science*, *49*(3), 933–952. https://doi.org/10.1177/23998083211039854

Li, H., Wei, Y. D., & Zhou, Y. (2017). Spatiotemporal analysis of land development in transitional China. *Habitat International*, *67*, 79–95. https://doi.org/10.1016/j.habitatint.2017.07.003

Li, J., Li, C., Zhu, F., Song, C., & Wu, J. (2013). Spatiotemporal pattern of urbanization in Shanghai, China between 1989 and 2005. *Landscape Ecology*, *28*(8), 1545–1565. https://doi.org/10.1007/s10980-013-9901-1

Li, X., Cai, Z., Li, W., Feng, Y., & Cao, S. (2023). The sustainability of urbanized land: Impacts of the growth of urbanized land in prefecture-level cities in China. *Ambio*, *52*(2), 465–475. https://doi.org/10.1007/s13280-022-01781-5

Li, X., Chen, Y., Liu, X., Xu, X., & Chen, G. (2017). Experiences and issues of using cellular automata for assisting urban and regional planning in China. *International Journal of Geographical Information Science*, *31*(8), 1606–1629. https://doi.org/10.1080/13658816.2017.1301457

Li, X., & Gong, P. (2016). Urban growth models: Progress and perspective. *Science Bulletin*, *61*(21), 1637–1650. https://doi.org/10.1007/s11434-016-1111-1

Li, X., & Yeh, A. G.-O. (2002). Neural-network-based cellular automata for simulating multiple land use changes using GIS. *International Journal of Geographical Information Science*, *16*(4), 323–343.

Li, Y., & Wu, F. (2018). Understanding city-regionalism in China: Regional cooperation in the Yangtze River Delta. *Regional Studies*, *52*(3), 313–324. https://doi.org/10.1080/00343404.2017.1307953

Lin, G. C. S. (2001). Metropolitan Development in a Transitional Socialist Economy: Spatial Restructuring in the Pearl River Delta, China. *Urban Studies*, *38*(3), 383–406.

Lin, G. C. S. (2002). The growth and structural change of Chinese cities: A contextual and geographic analysis. *Cities*, *19*(5), 299–316. https://doi.org/10.1016/S0264-2751(02)00039-2

Lin, J., Huang, B., Chen, M., & Huang, Z. (2014). Modeling urban vertical growth

using cellular automata—Guangzhou as a case study. *Applied Geography*, *53*, 172–186. https://doi.org/10.1016/j.apgeog.2014.06.007

Lin, J., Li, X., Wen, Y., & He, P. (2023). Modeling urban land-use changes using a landscape-driven patch-based cellular automaton (LP-CA). *Cities*, *132*, 103906. https://doi.org/10.1016/j.cities.2022.103906

Liu, J., & Diamond, J. (2005). China's environment in a globalizing world. *Nature*, *435*(7046), 1179–1186.

Liu, X., Li, X., Chen, Y., Tan, Z., Li, S., & Ai, B. (2010). A new landscape index for quantifying urban expansion using multi-temporal remotely sensed data. *Landscape Ecology*, *25*(5), 671–682. https://doi.org/10.1007/s10980-010-9454-5

Liu, X., Li, X., Shi, X., Wu, S., & Liu, T. (2008). Simulating complex urban development using kernel-based non-linear cellular automata. *Ecological Modelling*, *211*(1–2), 169–181. https://doi.org/10.1016/j.ecolmodel.2007.08.024

Liu, X., Li, X., Shi, X., Zhang, X., & Chen, Y. (2010b). Simulating land-use dynamics under planning policies by integrating artificial immune systems with cellular automata. *International Journal of Geographical Information Science*, *24*(5), 783–802. https://doi.org/10.1080/13658810903270551

Liu, X., Ma, L., Li, X., Ai, B., Li, S., & He, Z. (2014). Simulating urban growth by integrating landscape expansion index (LEI) and cellular automata. *International Journal of Geographical Information Science*, *28*(1), 148–163.

https://doi.org/10.1080/13658816.2013.831097

Liu, X., & Wang, M. (2016). How polycentric is urban China and why? A case study of 318 cities. *Landscape and Urban Planning*, *151*, 10–20. https://doi.org/10.1016/j.landurbplan.2016.03.007

Liu, Y., He, Q., Tan, R., Liu, Y., & Yin, C. (2016). Modeling different urban growth patterns based on the evolution of urban form: A case study from Huangpi, Central China. *Applied Geography*, *66*, 109–118. https://doi.org/10.1016/j.apgeog.2015.11.012

Liu, Y., Kong, X., Liu, Y., & Chen, Y. (2013). Simulating the conversion of rural settlements to town land based on multi-agent systems and cellular automata. *PLoS ONE*, *8*(11), 1–14. https://doi.org/10.1371/journal.pone.0079300

Liu, Y., Yin, G., & Ma, L. J. C. (2012). Local state and administrative urbanization in post-reform China: A case study of Hebi City, Henan Province. *Cities*, *29*(2), 107–117. https://doi.org/10.1016/j.cities.2011.08.003

Liu, Y., & Zhang, X. (2022). Does labor mobility follow the inter-regional transfer of labor-intensive manufacturing? The spatial choices of China's migrant workers. *Habitat International*, *124*, 102559.

Lloyd, C. T., Sorichetta, A., & Tatem, A. J. (2017). High resolution global gridded data for use in population studies. *Scientific Data*, *4*, 170001. https://doi.org/10.1038/sdata.2017.1

Lu, Y., & Tang, J. (2004). Fractal dimension of a transportation network and its relationship with urban growth: A study of the Dallas-Fort Worth area.

Environment and Planning B: Planning and Design, *31*(6), 895–911. https://doi.org/10.1068/b3163

Luan, H., & Fuller, D. (2022). Urban form in Canada at a small-area level: Quantifying "compactness" and "sprawl" with bayesian multivariate spatial factor analysis. *Environment and Planning B: Urban Analytics and City Science*, *49*(4), 1300–1313. https://doi.org/10.1177/23998083211062901

Luck, M., & Wu, J. (2002). A gradient analysis of urban landscape pattern: A case study from the Phoenix metropolitan region, Arizona, USA. *Landscape Ecology*, *17*(1925), 327–339. https://doi.org/10.1023/A:1020512723753

Luo, J., & Wei, Y. H. D. (2009). Modeling spatial variations of urban growth patterns in Chinese cities: The case of Nanjing. *Landscape and Urban Planning*, *91*(2), 51–64. https://doi.org/10.1016/j.landurbplan.2008.11.010

Maduako, I., & Wachowicz, M. (2019). A space-time varying graph for modelling places and events in a network. *International Journal of Geographical Information Science*, *33*(10), 1915–1935. https://doi.org/10.1080/13658816.2019.1603386

Magliocca, N., McConnell, V., & Walls, M. (2015). Exploring sprawl: Results from an economic agent-based model of land and housing markets. *Ecological Economics*, *113*, 114–125. https://doi.org/10.1016/j.ecolecon.2015.02.020

Magliocca, N. R., Brown, D. G., & Ellis, E. C. (2014). Cross-site comparison of land-use decision-making and its consequences across land systems with a generalized agent-based model. *PLoS ONE*, *9*(1).

https://doi.org/10.1371/journal.pone.0086179

Mahtta, R., Fragkias, M., Güneralp, B., Mahendra, A., Reba, M., Wentz, E. A., & Seto, K. C. (2022). Urban land expansion: The role of population and economic growth for 300+ cities. *Npj Urban Sustainability*, *2*(1), Article 1. https://doi.org/10.1038/s42949-022-00048-y

Makse, H. A., Andrade, J. S., Batty, M., Havlin, S., & Stanley, H. E. (1998). Modeling urban growth patterns with correlated percolation. *Physical Review E*, *58*(6), 7054–7062. https://doi.org/10.1103/PhysRevE.58.7054

Makse, H. A., Andrade Jr., J. S., Batty, M., Havlin, S., Eugene Stanley, H., Jr, S. A., Stanley, H. E., Batty, M., Havlin, S., Stanley, H. E., Makse, H. A., Andrade Jr., J. S., Batty, M., Havlin, S., Eugene Stanley, H., Jr, S. A., & Stanley, H. E. (1998). Modeling urban growth patterns with correlated percolation. *Physical Review E - Statistical Physics, Plasmas, Fluids, and Related Interdisciplinary Topics*, *58*(6 SUPPL. A), 7054–7062. https://doi.org/10.1103/PhysRevE.58.7054

Mallach, A., Haase, A., & Hattori, K. (2017). The shrinking city in comparative perspective: Contrasting dynamics and responses to urban shrinkage. *Cities*, *69*, 102–108. https://doi.org/10.1016/j.cities.2016.09.008

Marin, V., Molinero, C., & Arcaute, E. (2022). Uncovering structural diversity in commuting networks: Global and local entropy. *Scientific Reports*, *12*(1), Article 1. https://doi.org/10.1038/s41598-022-05556-6

Marshall, J. D. (2007). Urban Land Area and Population Growth: A New Scaling Relationship for Metropolitan Expansion. *Urban Studies*, *44*(10), 1889–1904.

https://doi.org/10.1080/00420980701471943

Martellozzo, F., & Clarke, K. C. (2011). Measuring urban sprawl, coalescence, and dispersal: A case study of Pordenone, Italy. *Environment and Planning B: Planning and Design*, *38*(6), 1085–1104. https://doi.org/10.1068/b36090

Matsumoto, H., Domae, K., & O'Connor, K. (2016). Business connectivity, air transport and the urban hierarchy: A case study in East Asia. *Journal of Transport Geography*, *54*, 132–139. https://doi.org/10.1016/j.jtrangeo.2016.05.005

Matthews, R. B., Gilbert, N. G., Roach, A., Polhill, J. G., & Gotts, N. M. (2007). Agent-based land-use models: A review of applications. *Landscape Ecology*, *22*(10), 1447–1459. https://doi.org/10.1007/s10980-007-9135-1

Medda, F., Nijkamp, P., & Rietveld, P. (1998). Recognition and classification of urban shapes. *Geographical Analysis*, *30*(4), 304–314. https://doi.org/10.1111/j.1538-4632.1998.tb00404.x

Meerow, S., Pajouhesh, P., & Miller, T. R. (2019). Social equity in urban resilience planning. *Local Environment*, *24*(9), 793–808. https://doi.org/10.1080/13549839.2019.1645103

Meng, X., Gregory, R., & Wang, Y. (2005). Poverty, inequality, and growth in urban China, 1986–2000. *Journal of Comparative Economics*, *33*(4), 710–729.

Meyfroidt, P., Lambin, E. F., & II, B. L. T. (2009). Forest Transition in Vietnam and Displacement of Deforestation Abroad. *Proceedings of the National Academy of Sciences of the United States of America*, *106*(38), 16139–16144.

Millward, A. A. (2011). Urbanisation viewed through a geostatistical lens applied to remote-sensing data. *Area*, *43*(1), 53–66.

Minor, E. S., & Urban, D. L. (2008). A Graph-Theory Framework for Evaluating Landscape Connectivity and Conservation Planning. *Conservation Biology*, *22*(2), 297–307. https://doi.org/10.1111/j.1523-1739.2007.00871.x

Mohajeri, N., Longley, P., & Batty, M. (2012). City Shape and the Fractality of Street Patterns. *Quaestiones Geographicae*, *31*(2). https://doi.org/10.2478/v10117-012-0016-6

Molinero, C., & Thurner, S. (2021). How the geometry of cities determines urban scaling laws. *Journal of The Royal Society Interface*, *18*(176), 20200705. https://doi.org/10.1098/rsif.2020.0705

Montero, G., Tannier, C., & Thomas, I. (2021). Delineation of cities based on scaling properties of urban patterns: A comparison of three methods. *International Journal of Geographical Information Science*, *35*(5), 919–947. https://doi.org/10.1080/13658816.2020.1817462

Mussone, L., & Notari, R. (2021). A comparative analysis of underground and bus transit networks through graph theory. *Environment and Planning B: Urban Analytics and City Science*, *48*(3), 574–591. https://doi.org/10.1177/2399808319879460

Nassar, A. K., Alan Blackburn, G., & Duncan Whyatt, J. (2014). Developing the desert: The pace and process of urban growth in Dubai. *Computers, Environment and Urban Systems*, *45*, 50–62.

https://doi.org/10.1016/j.compenvurbsys.2014.02.005

Nations, U. (2022). *World Population Prospects 2022*. United Nations. https://www.un-ilibrary.org/content/books/9789210014380

Overmars, K. P., de Koning, G. H. J., & Veldkamp, A. (2003). Spatial autocorrelation in multi-scale land use models. *Ecological Modelling*, *164*(2–3), 257–270. https://doi.org/10.1016/S0304-3800(03)00070-X

Parr, J. B. (2005). Perspectives on the city-region. *Regional Studies*, *39*(5), 555–566. https://doi.org/10.1080/00343400500151798

Parr, J. B. (2007). Spatial definitions of the City: Four perspectives. *Urban Studies*, *44*(2), 381–392. https://doi.org/10.1080/00420980601075059

Peris, A., Meijers, E., & van Ham, M. (2021). Information diffusion between Dutch cities: Revisiting Zipf and Pred using a computational social science approach. *Computers, Environment and Urban Systems*, *85*, 101565. https://doi.org/10.1016/j.compenvurbsys.2020.101565

Pijanowski, B. C., Brown, D. G., Shellito, B. A., & Manik, G. A. (2002). Using neural networks and GIS to forecast land use changes: A Land Transformation Model. *Computers, Environment and Urban Systems*, *26*(6), 553–575. https://doi.org/10.1016/S0198-9715(01)00015-1

Pijanowski, B. C., Tayyebi, A., Doucette, J., Pekin, B. K., Braun, D., & Plourde, J. (2014). A big data urban growth simulation at a national scale: Configuring the GIS and neural network based Land Transformation Model to run in a High Performance Computing (HPC) environment. *Environmental Modelling and*

Software, *51*, 250–268. https://doi.org/10.1016/j.envsoft.2013.09.015

Plan, F. (2014). Realizing China's urban dream. *Nature*, *509*(7499), 158–160. https://doi.org/10.1038/509158a

Power, A. (2018). Regional politics of an urban age: Can Europe's former industrial cities create a new industrial economy to combat climate change and social unravelling? *Palgrave Communications*, *4*(1), Article 1. https://doi.org/10.1057/s41599-018-0120-x

Reed, W. J. (2002). On the rank-size distribution for human settlements. *Journal of Regional Science*, *42*(1), 1–17.

Reia, S. M., Rao, P. S. C., & Ukkusuri, S. V. (2022). Modeling the dynamics and spatial heterogeneity of city growth. *Npj Urban Sustainability*, *2*(1), Article 1. https://doi.org/10.1038/s42949-022-00075-9

Riitters, K., Costanza, J. K., & Buma, B. (2017). Interpreting multiscale domains of tree cover disturbance patterns in North America. *Ecological Indicators*, *80*(May), 147–152. https://doi.org/10.1016/j.ecolind.2017.05.022

Riitters, K., Wickham, J., Costanza, J. K., & Vogt, P. (2016). A global evaluation of forest interior area dynamics using tree cover data from 2000 to 2012. *Landscape Ecology*, *31*(1), 137–148. https://doi.org/10.1007/s10980-015-0270-9

Robinson, D. T., Murray-Rust, D., Rieser, V., Milicic, V., & Rounsevell, M. (2012). Modelling the impacts of land system dynamics on human well-being: Using an agent-based approach to cope with data limitations in Koper, Slovenia.

Computers, Environment and Urban Systems, *36*(2), 164–176. https://doi.org/10.1016/j.compenvurbsys.2011.10.002

Rounsevell, M. D. A., Robinson, D. T., & Murray-Rust, D. (2012). From actors to agents in socio-ecological systems models. *Philosophical Transactions of the Royal Society B: Biological Sciences*, *367*(1586), 259–269. https://doi.org/10.1098/rstb.2011.0187

Sahana, M., Hong, H., & Sajjad, H. (2018). Analyzing urban spatial patterns and trend of urban growth using urban sprawl matrix: A study on Kolkata urban agglomeration, India. *Science of The Total Environment*, *628–629*, 1557–1566. https://doi.org/10.1016/j.scitotenv.2018.02.170

Salvati, L., & Serra, P. (2016). Estimating Rapidity of Change in Complex Urban Systems: A Multidimensional, Local-Scale Approach. *Geographical Analysis*, *48*(2), 132–156. https://doi.org/10.1111/gean.12093

Santé, I., García, A. M., Miranda, D., & Crecente, R. (2010). Cellular automata models for the simulation of real-world urban processes: A review and analysis. *Landscape and Urban Planning*, *96*(2), 108–122. https://doi.org/10.1016/j.landurbplan.2010.03.001

Sarkar, S., Wu, H., & Levinson, D. M. (2020). Measuring polycentricity via network flows, spatial interaction and percolation. *Urban Studies*, *57*(12), 2402–2422. https://doi.org/10.1177/0042098019832517

Schneider, a, & Mertes, C. M. (2014). Expansion and growth in Chinese cities, 1978–2010. *Environmental Research Letters*, *9*(2), 024008.

https://doi.org/10.1088/1748-9326/9/2/024008

Schneider, A. (2012). Monitoring land cover change in urban and peri-urban areas using dense time stacks of Landsat satellite data and a data mining approach. *Remote Sensing of Environment*, *124*, 689–704. https://doi.org/10.1016/j.rse.2012.06.006

Schneider, A., Chang, C., & Paulsen, K. (2015). The changing spatial form of cities in Western China. *Landscape and Urban Planning*, *135*, 40–61. https://doi.org/10.1016/j.landurbplan.2014.11.005

Schneider, A., Seto, K. C., & Webster, D. R. (2005). Urban growth in Chengdu, western China: Application of remote sensing to assess planning and policy outcomes. *Environment and Planning B: Planning and Design*, *32*(3), 323–345. https://doi.org/10.1068/b31142

Schneider, A., & Woodcock, C. E. (2008). Compact, Dispersed, Fragmented, Extensive? A Comparison of Urban Growth in Twenty-five Global Cities using Remotely Sensed Data, Pattern Metrics and Census Information. *Urban Studies*, *45*(3), 659–692. https://doi.org/10.1177/0042098007087340

Seto, K. C., & Fragkias, M. (2005). Quantifying Spatiotemporal Patterns of Urban Land-use Change in Four Cities of China with Time Series Landscape Metrics. *Landscape Ecology*, *20*(7), 871–888. https://doi.org/10.1007/s10980-005-5238-8

Seto, K. C., Güneralp, B., & Hutyra, L. R. (2012). Global forecasts of urban expansion to 2030 and direct impacts on biodiversity and carbon pools. *Proceedings of the*

National Academy of Sciences, *109*(40), 16083–16088.

Seto, K. C., & Kaufmann, R. K. (2003). Modeling the drivers of urban land use change in the Pearl River Delta, China: Integrating remote sensing with socioeconomic data. *Land Economics*, *79*(1), 106–121.

Seto, K. C., Reenberg, A., Boone, C. G., Fragkias, M., Haase, D., Langanke, T., Marcotullio, P., Munroe, D. K., Olah, B., & Simon, D. (2012). Urban land teleconnections and sustainability. *Proceedings of the National Academy of Sciences*, *109*(20), 7687–7692. https://doi.org/10.1073/pnas.1117622109

Seto, K. C., Sánchez-Rodríguez, R., & Fragkias, M. (2010). The New Geography of Contemporary Urbanization and the Environment. *Annual Review of Environment and Resources*, *35*(1), 167–194. https://doi.org/10.1146/annurev-environ-100809-125336

Sexton, J. O., Song, X. P., Huang, C., Channan, S., Baker, M. E., & Townshend, J. R. (2013). Urban growth of the Washington, D.C.-Baltimore, MD metropolitan region from 1984 to 2010 by annual, Landsat-based estimates of impervious cover. *Remote Sensing of Environment*, *129*, 42–53. https://doi.org/10.1016/j.rse.2012.10.025

Shafizadeh-Moghadam, H., Asghari, A., Tayyebi, A., & Taleai, M. (2017). Coupling machine learning, tree-based and statistical models with cellular automata to simulate urban growth. *Computers, Environment and Urban Systems*, *64*, 297–308. https://doi.org/10.1016/j.compenvurbsys.2017.04.002

Shen, G. (2002). Fractal dimension and fractal growth of urbanized areas. *International*

Journal of Geographical Information Science, *16*(5), 419–437. https://doi.org/10.1080/13658810210137013

SShi, Y., Sun, X., Zhu, X., Li, Y., & Mei, L. (2012). Characterizing growth types and analyzing growth density distribution in response to urban growth patterns in peri-urban areas of Lianyungang City. *Landscape and Urban Planning*, *105*(4), 425–433. https://doi.org/10.1016/j.landurbplan.2012.01.017

Silva, R. A., West, J. J., Zhang, Y., Anenberg, S. C., Lamarque, J.-F., Shindell, D. T., Collins, W. J., Dalsoren, S., Faluvegi, G., & Folberth, G. (2013). Global premature mortality due to anthropogenic outdoor air pollution and the contribution of past climate change. *Environmental Research Letters*, *8*(3), 034005.

Smith, J. W., Smart, L. S., Dorning, M. A., Dupéy, L. N., Méley, A., & Meentemeyer, R. K. (2017). Bayesian methods to estimate urban growth potential. *Landscape and Urban Planning*, *163*, 1–16. https://doi.org/10.1016/j.landurbplan.2017.03.004

Stefanov, W. L. (2001). Monitoring urban land cover change: An expert system approach to land cover classification of semiarid to urban centers. *Remote Sensing of Environment*, *77*, 173–185. https://doi.org/10.1016/S0034-4257(01)00204-8

Stein, A. (1999). Some basic elements of statistics. In *Spatial statistics for remote sensing* (pp. 9–25). Springer.

Stoebner, T. J., & Lant, C. L. (2014). Geographic determinants of rural land covers and

the agricultural margin in the Central United States. *Applied Geography*, *55*, 138–154. https://doi.org/10.1016/j.apgeog.2014.09.008

Suel, E., Polak, J. W., Bennett, J. E., & Ezzati, M. (2019). Measuring social, environmental and health inequalities using deep learning and street imagery. *Scientific Reports*, *9*(1), 6229. https://doi.org/10.1038/s41598-019-42036-w

Sultana, S., & Weber, J. (2014). The Nature of Urban Growth and the Commuting Transition: Endless Sprawl or a Growth Wave? *Urban Studies*, *51*(3, SI), 544–576. https://doi.org/10.1177/0042098013498284

Syphard, A. D., Clarke, K. C., & Franklin, J. (2005). Using a cellular automaton model to forecast the effects of urban growth on habitat pattern in southern California. *Ecological Complexity*, *2*(2 SPEC. ISS.), 185–203. https://doi.org/10.1016/j.ecocom.2004.11.003

Tan, X., Huang, B., Batty, M., & Li, J. (2021). Urban Spatial Organization, Multifractals, and Evolutionary Patterns in Large Cities. *Annals of the American Association of Geographers*, *111*(5), 1539–1558. https://doi.org/10.1080/24694452.2020.1823203

Tannier, C., & Thomas, I. (2013). Defining and characterizing urban boundaries: A fractal analysis of theoretical cities and Belgian cities. *Computers, Environment and Urban Systems*, *41*, 234–248. https://doi.org/10.1016/j.compenvurbsys.2013.07.003

Taubenböck, H., Standfuß, I., Wurm, M., Krehl, A., & Siedentop, S. (2017). Measuring morphological polycentricity—A comparative analysis of urban mass

concentrations using remote sensing data. *Computers, Environment and Urban Systems*, *64*, 42–56. https://doi.org/10.1016/j.compenvurbsys.2017.01.005

Thomas, I., Frankhauser, P., & Badariotti, D. (2012). Comparing the fractality of European urban neighbourhoods: Do national contexts matter? *Journal of Geographical Systems*, *14*(2), 189–208. https://doi.org/10.1007/s10109-010-0142-4

Tobler, W. R. (1979). Cellular Geography. *Philosophy in Geography*, 379–386. https://doi.org/10.1007/978-94-009-9394-5

Tong, L., Hu, S., Frazier, A. E., & Liu, Y. (2017). Multi-order urban development model and sprawl patterns: An analysis in China, 2000–2010. *Landscape and Urban Planning*, *167*, 386–398. https://doi.org/10.1016/j.landurbplan.2017.07.001

Torres, A., Jaeger, J. A. G., & Alonso, J. C. (2016). Multi-scale mismatches between urban sprawl and landscape fragmentation create windows of opportunity for conservation development. *Landscape Ecology*, *31*(10), 2291–2305. https://doi.org/10.1007/s10980-016-0400-z

Tu, Y., Chen, B., Yu, L., Song, Y., Wu, S., Li, M., Wei, H., Chen, T., Lang, W., Gong, P., & Xu, B. (2023). Raveling the nexus between urban expansion and cropland loss in China. *Landscape Ecology*, *38*(7), 1869–1884. https://doi.org/10.1007/s10980-023-01653-7

UNDESA. (2014). World Urbanization Prospects. In *Undesa*. https://doi.org/10.4054/DemRes.2005.12.9

Urban, D. L., Minor, E. S., Treml, E. A., & Schick, R. S. (2009). Graph models of

habitat mosaics. *Ecology Letters*, *12*(3), 260–273. https://doi.org/10.1111/j.1461-0248.2008.01271.x

Valbuena, D., Verburg, P. H., Bregt, A. K., & Ligtenberg, A. (2010). An agent-based approach to model land-use change at a regional scale. *Landscape Ecology*, *25*(2), 185–199. https://doi.org/10.1007/s10980-009-9380-6

van der Meer, F. (2012). Remote-sensing image analysis and geostatistics. *International Journal of Remote Sensing*, *33*(18), 5644–5676. https://doi.org/10.1080/01431161.2012.666363

Vasanen, A. (2012). Functional Polycentricity: Examining Metropolitan Spatial Structure through the Connectivity of Urban Sub-centres. *Urban Studies*, *49*(16), 3627–3644. https://doi.org/10.1177/0042098012447000

Vinci, S., Vardopoulos, I., & Salvati, L. (2023). A tale of a shrinking City? Exploring the complex interplay of socio-demographic dynamics in the recent development of Attica, Greece. *Cities*, *132*, 104089. https://doi.org/10.1016/j.cities.2022.104089

Von Der Dunk, A., Grêt-Regamey, A., Dalang, T., & Hersperger, A. M. (2011). Defining a typology of peri-urban land-use conflicts—A case study from Switzerland. *Landscape and Urban Planning*, *101*(2), 149–156. https://doi.org/10.1016/j.landurbplan.2011.02.007

von Thünen. (1826). *Die Isoliste Staat*.

Walsh, S. J., Malanson, G. P., Entwisle, B., Rindfuss, R. R., Mucha, P. J., Heumann, B. W., McDaniel, P. M., Frizzelle, B. G., Verdery, A. M., Williams, N. E., Yao, X.,

& Ding, D. (2013). Design of an agent-based model to examine population-environment interactions in Nang Rong District, Thailand. *Applied Geography*, *39*, 183–198. https://doi.org/10.1016/j.apgeog.2012.12.010

Walsh, S. J., Messina, J. P., Mena, C. F., Malanson, G. P., & Page, P. H. (2008). Complexity theory, spatial simulation models, and land use dynamics in the Northern Ecuadorian Amazon. *Geoforum*, *39*(2), 867–878. https://doi.org/10.1016/j.geoforum.2007.02.011

Wang, C., Liu, H., & Zhang, M. (2016). The influence of administrative boundary on the spatial expansion of urban land: A case study of Beijing-Tianjin-Hebei urban agglomeration. *Geographical Research*, *35*(1), 173–183.

Wang, C., Yu, B., Chen, Z., Liu, Y., Song, W., Li, X., Yang, C., Small, C., Shu, S., & Wu, J. (2022). Evolution of Urban Spatial Clusters in China: A Graph-Based Method Using Nighttime Light Data. *Annals of the American Association of Geographers*, *112*(1), 56–77. https://doi.org/10.1080/24694452.2021.1914538

Wang, X. S., Liu, J. Y., Zhuang, D. F., & Wang, L. (2005). Spatial-temporal changes of urban spatial morphology in China. *Acta Geographica Sinica*, *60*(3), 392–400.

Wang, Y., & Li, S. (2011). Simulating multiple class urban land-use/cover changes by RBFN-based CA model. *Computers & Geosciences*, *37*(2), 111–121. https://doi.org/10.1016/j.cageo.2010.07.006

Wang, Y., Lyu, J., Liang, X., Luo, C., Ma, X., Li, J., Li, Q., Zheng, L., & Guan, Q. (2024). Using Zipf's Law to Optimize Urban Spatial Layouts in an Urban Agglomeration Area. *Annals of the American Association of Geographers*,

114(6), 1342–1364. https://doi.org/10.1080/24694452.2024.2332647

Wang, Y., Sha, Z., Tan, X., Lan, H., Liu, X., & Rao, J. (2020). Modeling urban growth by coupling localized spatio-temporal association analysis and binary logistic regression. *Computers, Environment and Urban Systems*, *81*, 101482. https://doi.org/10.1016/j.compenvurbsys.2020.101482

Weiss, D. J., Nelson, A., Gibson, H. S., Temperley, W., Peedell, S., Lieber, A., Hancher, M., Poyart, E., Belchior, S., Fullman, N., Mappin, B., Dalrymple, U., Rozier, J., Lucas, T. C. D., Howes, R. E., Tusting, L. S., Kang, S. Y., Cameron, E., Bisanzio, D., … Gething, P. W. (2018). A global map of travel time to cities to assess inequalities in accessibility in 2015. *Nature*, *553*(7688), 333–336. https://doi.org/10.1038/nature25181

Wei, Y., & Zhao, M. (2009). Urban spill over vs. local urban sprawl: Entangling land-use regulations in the urban growth of China's megacities. *Land Use Policy*, *26*(4), 1031–1045. https://doi.org/10.1016/j.landusepol.2008.12.005

Wentz, E. A. (2000). A shape definition for geographic applications based on edge, elongation, and perforation. *Geographical Analysis*, *32*(2), 95–112. https://doi.org/10.1111/j.1538-4632.2000.tb00419.x

Wheeler, D., & Tiefelsdorf, M. (2005). Multicollinearity and correlation among local regression coefficients in geographically weighted regression. *Journal of Geographical Systems*, *7*(2), 161–187.

Wilson, E. H., Hurd, J. D., Civco, D. L., Prisloe, M. P., & Arnold, C. (2003). Development of a geospatial model to quantify, describe and map urban growth.

Remote Sensing of Environment, *86*(3), 275–285. https://doi.org/10.1016/S0034-4257(03)00074-9

Wolfram, S. (1984). Universality and complexity in cellular automata. *Physica D: Nonlinear Phenomena*, *10*(1–2), 1–35.

Wong, D. W. S., & Fotheringham, A. S. (1990). Urban systems as examples of bounded chaos: Exploring the relationship between fractal dimension, rank-size, and rural-to- urban migration. *Geografiska Annaler*, *72 B*(2–3), 89–99.

Woodcock, C. E., Strahler, A. H., & Jupp, D. L. B. (1988). The use of variograms in remote sensing: II. Real digital images. *Remote Sensing of Environment*, *25*(3), 349–379. https://doi.org/10.1016/0034-4257(88)90109-5

Wu, B., Yu, B., Shu, S., Wu, Q., Zhao, Y., & Wu, J. (2021). A spatiotemporal structural graph for characterizing land cover changes. *International Journal of Geographical Information Science*, *35*(2), 397–425. https://doi.org/10.1080/13658816.2020.1778706

Wu, B., Yu, B., Yao, S., Wu, Q., Chen, Z., & Wu, J. (2019). A surface network based method for studying urban hierarchies by night time light remote sensing data. *International Journal of Geographical Information Science*, *33*(7), 1377–1398. https://doi.org/10.1080/13658816.2019.1585540

Wu, F. (1998a). SimLand: A prototype to simulate land conversion through the integrated GIS and CA with AHP-derived transition rules. *International Journal of Geographical Information Science*, *12*(1), 63–82.

Wu, F. (1998b). Simulating urban encroachment on rural land with fuzzy-logic-

controlled cellular automata in a geographical information system. *Journal of Environmental Management*, *53*(4), 293–308.

Wu, F. (2002). China's changing urban governance in the transition towards a more market-oriented economy. *Urban Studies*, *39*(7), 1071–1093.

Wu, J., Jenerette, G. D., Buyantuyev, A., & Redman, C. L. (2011). Quantifying spatiotemporal patterns of urbanization: The case of the two fastest growing metropolitan regions in the United States. *Ecological Complexity*, *8*(1), 1–8. https://doi.org/10.1016/j.ecocom.2010.03.002

Wu, J., Wei-Ning Xiang, & Zhao, J. (2014). Urban ecology in China: Historical developments and future directions. *Landscape and Urban Planning*, *125*, 222–233. https://doi.org/10.1016/j.landurbplan.2014.02.010

Wu, W., Zhao, S., & Henebry, G. M. (2019). Drivers of urban expansion over the past three decades: A comparative study of Beijing, Tianjin, and Shijiazhuang. *Environmental Monitoring and Assessment*, *191*(1), 1–15. https://doi.org/10.1007/s10661-018-7151-z

Wu, W., Zhao, S., Zhu, C., & Jiang, J. (2015). Landscape and Urban Planning A comparative study of urban expansion in Beijing , Tianjin and Shijiazhuang over the past three decades. *Landscape and Urban Planning*, *134*, 93–106. https://doi.org/10.1016/j.landurbplan.2014.10.010

Wu, X., Hu, Y., He, H., Xi, F., & Bu, R. (2010). Study on forecast scenarios for simulation of future urban growth in Shenyang City based on SLEUTH model. *Geo-Spatial Information Science*, *13*(1), 32–39.

https://doi.org/10.1007/s11806-010-0155-7

Xia, C., Yeh, A. G.-O., & Zhang, A. (2020). Analyzing spatial relationships between urban land use intensity and urban vitality at street block level: A case study of five Chinese megacities. *Landscape and Urban Planning*, *193*, 103669. https://doi.org/10.1016/j.landurbplan.2019.103669

Xia, C., Zhang, A., Wang, H., Zhang, B., & Zhang, Y. (2019). Bidirectional urban flows in rapidly urbanizing metropolitan areas and their macro and micro impacts on urban growth: A case study of the Yangtze River middle reaches megalopolis, China. *Land Use Policy*, *82*, 158–168. https://doi.org/10.1016/j.landusepol.2018.12.007

Xing, L., Zhu, Y., & Wang, J. (2021). Spatial spillover effects of urbanization on ecosystem services value in Chinese cities. *Ecological Indicators*, *121*, 107028. https://doi.org/10.1016/j.ecolind.2020.107028

Xu, C., Liu, M., Zhang, C., An, S., Yu, W., & Chen, J. M. (2007). The spatiotemporal dynamics of rapid urban growth in the Nanjing metropolitan region of China. *Landscape Ecology*, *22*(6), 925–937.

Xu, F., Li, Y., Jin, D., Lu, J., & Song, C. (2021). Emergence of urban growth patterns from human mobility behavior. *Nature Computational Science*, *1*(12), 791–800. https://doi.org/10.1038/s43588-021-00160-6

Xu, G., Zhu, M., Chen, B., Salem, M., Xu, Z., Cobbinah, P. B., Li, X., Sumari, N. S., Zhang, X., Jiao, L., & Gong, P. (2025). Underlying rules of evolutionary urban systems in Africa. *Nature Cities*, *2*(4), 327–335.

https://doi.org/10.1038/s44284-025-00208-y

Xu, Y., Olmos, L. E., Mateo, D., Hernando, A., Yang, X., & González, M. C. (2023). Urban dynamics through the lens of human mobility. *Nature Computational Science*, *3*(7), 611–620. https://doi.org/10.1038/s43588-023-00484-5

Xu, Z., & Harriss, R. (2010). A Spatial and Temporal Autocorrelated Growth Model for City Rank—Size Distribution. *Urban Studies*, *47*(2), 321–335.

Yang, C., & Zhao, S. (2022). Urban vertical profiles of three most urbanized Chinese cities and the spatial coupling with horizontal urban expansion. *Land Use Policy*, *113*, 105919. https://doi.org/10.1016/j.landusepol.2021.105919

Yang, J., Tang, W., Gong, J., Shi, R., Zheng, M., & Dai, Y. (2023). Simulating urban expansion using cellular automata model with spatiotemporally explicit representation of urban demand. *Landscape and Urban Planning*, *231*, 104640. https://doi.org/10.1016/j.landurbplan.2022.104640

Yang, Q., Wang, L., Li, Y., Fan, Y., & Liu, C. (2022). Urban land development intensity: New evidence behind economic transition in the Yangtze River Delta, China. *Journal of Geographical Sciences*, *32*(12), 2453–2474. https://doi.org/10.1007/s11442-022-2056-8

Yao, Y., Jiang, Y., Sun, Z., Li, L., Chen, D., Xiong, K., Dong, A., Cheng, T., Zhang, H., Liang, X., & Guan, Q. (2024). Applicability and sensitivity analysis of vector cellular automata model for land cover change. *Computers, Environment and Urban Systems*, *109*, 102090. https://doi.org/10.1016/j.compenvurbsys.2024.102090

Yu, B., Shu, S., Liu, H., Song, W., Wu, J., Wang, L., & Chen, Z. (2014). Object-based spatial cluster analysis of urban landscape pattern using nighttime light satellite images: A case study of China. *International Journal of Geographical Information Science*, *28*(11), 2328–2355. https://doi.org/10.1080/13658816.2014.922186

Yu, D. L. (2006). Spatially varying development mechanisms in the Greater Beijing Area: A geographically weighted regression investigation. *Annals of Regional Science*, *40*(1), 173–190. https://doi.org/10.1007/s00168-005-0038-2

Yu, X. J., & Ng, C. N. (2007). Spatial and temporal dynamics of urban sprawl along two urban–rural transects: A case study of Guangzhou, China. *Landscape and Urban Planning*, *79*(1), 96–109.

Yu, Y., Feng, K., & Hubacek, K. (2013). Tele-connecting local consumption to global land use. *Global Environmental Change*, *23*(5), 1178–1186. https://doi.org/10.1016/j.gloenvcha.2013.04.006

Yue, W., Liu, Y., & Fan, P. (2013). Land Use Policy Measuring urban sprawl and its drivers in large Chinese cities: The case of Hangzhou. *Land Use Policy*, *31*, 358–370. https://doi.org/10.1016/j.landusepol.2012.07.018

Zhai, Y., Yao, Y., Guan, Q., Liang, X., Li, X., Pan, Y., Yue, H., Yuan, Z., & Zhou, J. (2020). Simulating urban land use change by integrating a convolutional neural network with vector-based cellular automata. *International Journal of Geographical Information Science*, *34*(7), 1475–1499. https://doi.org/10.1080/13658816.2020.1711915

Zhang, H., Lan, T., & Li, Z. (2020). Advances in Fractal Cities: A Shift from Morphology to Network. *Journal of Geo-Information Science*, *22*(4), 827–841. https://doi.org/10.12082/dqxxkx.2020.200160

Zhang, Q., Ban, Y., Liu, J., & Hu, Y. (2011). Simulation and analysis of urban growth scenarios for the Greater Shanghai Area, China. *Computers, Environment and Urban Systems*, *35*(2), 126–139. https://doi.org/10.1016/j.compenvurbsys.2010.12.002

Zhang, Y. (2001). Texture-integrated classification of urban treed areas in high-resolution color-infrared imagery. *Photogrammetric Engineering & Remote Sensing*, *67*(12), 1359–1365.

Zhang, Y., Kwan, M.-P., & Yang, J. (2023). A user-friendly assessment of six commonly used urban growth models. *Computers, Environment and Urban Systems*, *104*, 102004. https://doi.org/10.1016/j.compenvurbsys.2023.102004

Zhao, C., Jensen, J., & Zhan, B. (2017). A comparison of urban growth and their influencing factors of two border cities: Laredo in the US and Nuevo Laredo in Mexico. *Applied Geography*, *79*, 223–234. https://doi.org/10.1016/j.apgeog.2016.12.017

Zheng, H., Liu, D., Wang, Y., & Yue, X. (2024). Bayesian analysis of urban theft crime in 674 Chinese cities. *Scientific Reports*, *14*(1), 26447.

Zhou, D., Zhao, S., Zhang, L., Sun, G., & Liu, Y. (2015). The footprint of urban heat island effect in China. *Scientific Reports*, *5*(1), 11160.

Zhou, Y., Smith, S. J., Zhao, K., Imhoff, M., Thomson, A., Bond-Lamberty, B., Asrar,

G. R., Zhang, X., He, C., & Elvidge, C. D. (2015). A global map of urban extent from nightlights. *Environmental Research Letters*, *10*(5), 054011. https://doi.org/10.1088/1748-9326/10/5/054011

Zhu, W., & Yuan, C. (2023). Urban heat health risk assessment in Singapore to support resilient urban design—By integrating urban heat and the distribution of the elderly population. *Cities*, *132*, 104103. https://doi.org/10.1016/j.cities.2022.104103

Zou, X., Liu, X., Liu, M., Tian, L., Zhu, L., & Zhang, Q. (2023). Spatiotemporal graph-based analysis of land cover evolution using remote sensing time series data. *International Journal of Geographical Information Science*, *0*(0), 1–32. https://doi.org/10.1080/13658816.2023.2168006